# Reliability and Resilience Evaluation of Distribution Automation

Kieran Morris

A thesis presented for the degree of
Doctor of Philosophy
in
Electrical and Computer Engineering
at the
University of Canterbury,
Christchurch, New Zealand.

14 March 2019

# ABSTRACT

Modern distribution grid utilities are steadily adapting to the concepts of Smart Grids by augmenting distribution grids with Distribution Automation (DA) to enhance visibility and control for the purpose of enhanced system availability. Existing methods to place and evaluate DA overlook the important enhancement it provides to the resilience of a system. Resilience, a much-discussed but poorly defined measure for power systems, represents a system's ability to withstand and recover from High-Impact Low-Probability (HILP) events such as storms and earthquakes. This thesis argues that exisiting resilience quantification methods do not capture the direct contribution which DA can make to enhance system resilience. It develops a novel model and methodology to analyse distribution grid resilience using the formalisms of Reliability Graphs (RGs), and Stochastic Reward Nets (SRNs). These two models capture the different parts of the complex recovery process which distribution grids perform to recover from faults using DA.

There are three novel contributions in this thesis. Firstly, a three-tier hierarchical model which contains an RG is developed to assess the enhancement which DA equipment provides to load point and feeder availability and resilience. Next, and SRN is used to develop a load point (LP) model which incorporates the dependence of feeder assets during the fault isolation phase of the recovery process. Finally, the SRN model is augmented with a phased recovery model to represent the complex recovery process for distribution grids. Utilising these models, the placement of switch automation and fault indicators is evaluated, and the contribution they make to resilience demonstrated. Collectively, these models give a novel means of assessing the the availability, sensitivity and resilience of distribution grids which utilise DA.

# ACKNOWLEDGEMENTS

I was fortunate enough to have three academic supervisors to assist me throughout this research, Assc. Prof. Alan Wood, Dr. Graeme Woodward and Dr. Dong Seong Kim. Each of them provided me with a wealth of knowledge, criticism and support throughout. I am truly appreciative for the assistance that they have provided me as I completed this work.

Thanks also go to Dr. Clive Horn from Tait Communications who was my industry supervisor. I am thankful for his advice, guidance and encouragement. I would also like to thank Tait Communications and The Tait Foundation, who gave me the a scholarship which funded this research. I have gained a great deal of knowledge through the opportunities and experiences they have provided me.

A large portion of this work was undertaken at the Wireless Research Centre at the University of Canterbury. I would like to thank all of my colleagues there, each of whom gave me helpful advice and made the past few years entertaining.

Many thanks also go to my friends and family who have supported and encouraged me over the course of this work. I especially would like to thank my wonderful partner Karyn. Her help and support over these three years has been immeasurable and I am extremely grateful.

# CONTENTS

# ABBREVIATIONS

**AEC** Automation Enabling Communications.

**AENS** Average Energy Not Served.

**AR** analytical resilience.

**CAIDI** Customer Average Interruption Duration Index.

**CDF** Cumulative Density Function.

**CTMC** Continuous-Time Markov Chain.

**DA** Distribution Automation.

**DG** Distributed Generation.

**DT** down time.

**FAR** Fully Automated Reconfiguration.

**FI** Fault Indicator.

**GOF** Goodness of Fit.

**HILP** High-Impact Low-Probability.

**LP** load point.

**LV** low voltage.

**MLE** Maximum Likelihood Estimation.

**MTTF** Mean Time To Failure.

**MTTI** Mean Time To Isolation.

**MTTR** Mean Time To Recovery.

**PDF** Probability Density Function.

**PMU** Phasor Measurement Unit.

**RG** Reliability Graph.

**SAIDI** System Average Interruption Duration Index.

**SAIFI** System Average Interruption Frequency Index.

**SBR** simulation-based resilience.

**SD** standard deviation.

**SMP** Semi-Markov Process.

**SRN** Stochastic Reward Net.

**SSR** sum of squared residuals.

**TTF** Time To Failure.

**TTR** Time To Recovery.

**W&E** Weather and Environment.

# NOMENCLATURE

| | |
|---|---|
| $\lambda$ | Failure rate |
| $\mu$ | Recovery rate |
| $\sigma$ | Isolation rate |
| $\tau$ | Switch opening rate |
| $\tau 2$ | Switch closing rate |
| $\boldsymbol{\pi}(t)$ | CTMC State Probability Vector |
| $\boldsymbol{\pi}$ | Steady-state CTMC State Probability Vector |
| $R(t)$ | Reliability Function |
| $A(t)$ | Transient Availability Function |
| $F(t)$ | Survival Function |
| $A$ | Steady-state availability |
| $D$ | Down time |

# LIST OF FIGURES

# Chapter 1

# INTRODUCTION

## 1.1 RESEARCH MOTIVATION

Modern power systems are constantly evolving to better provide reliable and consistent power to their users. Part of this evolution is the enhancement of existing grids with communications and automation [2]. Traditionally, the grid has been designed and regulated from the perspective of reliability, the key objective being to maintain an adequate supply on a day-to-day basis [3]. Events such as Superstorm Sandy [4] in the Eastern parts of USA, 2012, or the earthquakes affecting Christchurch, New Zealand since the year 2010 [5] have demonstrated the shortfalls of this policy. The management strategies of utilities must be extended to better prepare for, and mitigate these High-Impact Low-Probability (HILP) events. These events all share the feature of not being predictable, and in most cases, not able to be effectively prepared for before they occur. They generally cause widespread failures and significantly reduce a power system's ability to supply power to its customers.

In the field of distribution reliability analysis, topics relating to smart grids are the overarching themes for the majority of the literature which has been published in the previous ten years [3]. There are a number of technologies which can aid in the enhancement of reliability, and many of these have been analysed rigorously. The following technologies are commonly addressed in current distribution grid reliability literature:

- Distribution Automation (DA) - Deploying communications and remote sensing technology to enhance grid visibility and allow the grid to be managed and reconfigured remotely.
- Microgrids - Intentional islanding of sections of a feeder of an low voltage (LV) network using distributed generation and by using automation of reconfiguration and protection equipment.
- Energy Storage and Electric Vehicles - Utilising grid-connected storage to provide power to the grid, or to microgrids, in the event of an outage.

- Demand Response - Controlling the grid demand in the event of an outage can enhance reliability by allowing critical loads to have priority access to storage and Distributed Generation (DG).

Resilience is a characterisation of how capable a system is to withstand HILP events. Often it is confused with the concept of reliability, or related concepts such as fault tolerance [6]. The primary difference between reliability and resilience is that resilience goes beyond the representation of the impact of day-to-day failures. It represents how well a system and its controlling utility can prepare for, mitigate, recover from and learn from HILP events when they occur [7].

DA aids in the recovery of distribution grids when outages occur. It does this by improving the visibility and control of an existing distribution grid by means of communications infrastructure. Distribution grids are maintained in a mesh structure, but operated radially using sectionalising switches. This means that there is only a single connected path from source to load. When an outage occurs, faults can be isolated by reconfiguring the distribution grid. DA provides a means of automating this isolation process. It is an alternative to hardening or replacing existing power system equipment and lines because the existing grid infrastructure is not removed or replaced, but augmented. DA is a blanket term for technology such as sensors, actuators and communications. These are utilised to enable remote and automatic detection and location of faults, and remote reconfiguration after an outage has occurred.

A prominent advantage of DA is a reduction in the time required to find the location of a fault when an outage occurs. A Fault Indicator (FI) is a type of sensor which, when coupled with communications, transmits a notification if it detects an electrical current which can be attributed to a fault. By utilising this example of DA technology, it is possible to significantly reduce the search area during an outage and increase the overall availability of the system.

DA communications also enable the remote control of switches on distribution grids. Sectionalising switches are used to reduce the geographical size of an outage by restricting the number of assets and lines connected to a fault. They can also be used to connect offline sections of the grid to alternate supplies or DG in order to provide power to a subset of offline load points (LPs) while a fault is being repaired. DA enhances the operation of these switches by enabling them to be controlled remotely, reducing the time required to reconfigure the grid during an outage.

The benefits of DA are not restricted to just enhancing day-to-day performance. Resilience can also be improved by utilising DA technology [8]. HILP events cause a large number of outages to occur in a short period of time and DA enables the location of faults and reconfiguration of the grid to be significantly faster in these situations. Furthermore, during a severe storm or related HILP event, it is often unsafe for utilities to deploy operators into the field to reconfigure the grid or locate and repair faults. DA

enables the recovery process to begin quickly and remotely, reducing the impact of such events on the overall grid performance.

Despite the contribution which DA can make to the resilience of distribution grids, the methods used to evaluate DA contribution often overlook it. There is a significant amount of research available which demonstrates the optimal placement of DA technology for the purpose of reducing customer downtime. Placement of both FIs (also known as fault current indicators (FCIs)) [9–12] and sectionalising switches [13–16] utilise the same approach to evaluate the downtime improvement attributed to the placement. These methods make the assumption that the cost of each individual outage on the system is constant, regardless of other lines' states. The downtime of assets after a failure in these models is a fixed duration, and independent of other failures. Therefore they do not consider cases with multiple outages. In most cases this is a valid assumption for day-to-day analysis, but not when destructive HILP events occur.

Specific analysis of the contribution of these technologies to resilience is much less common. The general approach for resiliency analysis is based on investigating the severity of a potential event with a probabilistic approach. Typical distribution grid resiliency analysis methods assign fragility curves [17] or other probabilistic models to the failure of assets, and then simulate a specific event for a system. There is significant merit in this approach, because it gives a system-wide representation of the impact of an event on a system [1]. For the evaluation of specific DA devices, and their contribution to system resilience, this method is less appropriate. This will be explained in Section 1.2.

In summary, there currently exists no effective means of evaluation the contribution which DA can make to enhancing distribution grid resilience. This thesis will develop such a tool, and demonstrate it is capable of fulfilling this need.

## 1.2 RESILIENCY ANALYSIS

### 1.2.1 Introduction

Resilience is a topic which has become of interest to distribution grids with the concept of smart grids. Its definition often varies, depending on the field of engineering in which it is defined. From a general engineering perspective, a widely referenced definition for resilience is: "How well a system can handle disruptions and variations that fall outside of the base mechanisms/model for being adaptive as defined in that system" [18]. From the perspective of this work, 'disruptions and variations' will be considered HILP events. Despite this general consensus of the meaning of system resilience, there are several different specific definitions and means of quantifying it specific to the field of distribution grid analysis. This section will review existing methods to calculate and quantify resilience, and choose one which will be used in this thesis for evaluation of distribution grid resilience.

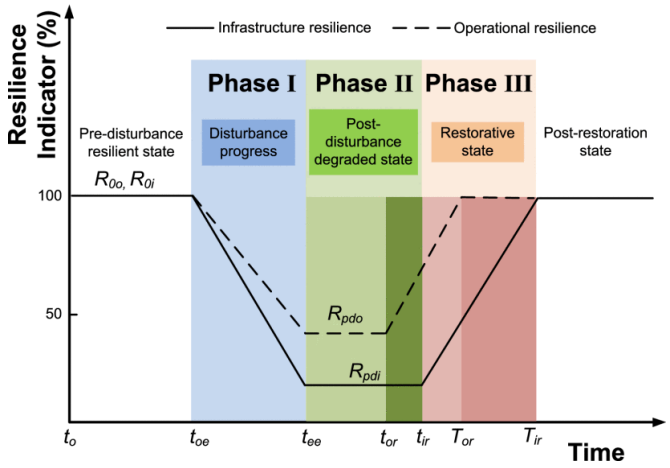


**Figure 1.1** Resilience trapezoid for operational and infrastructure resilience. Taken directly from [1].

The key overlying purpose of resilience planning in a disaster or catastrophe context, is to enhance a population's ability survive with a minimum loss of life and property [19]. From a large-scale perspective, there are many indeterminate factors which influence the resilience of distribution grids, as well as the people and communities which they serve. An all-encompassing planned resilience framework must therefore consider beyond that of a distribution grid itself. This is because the infrastructure which supports distribution grids also influences its resilience. For example, a utility will be less capable of repair and recovery if transport infrastructure is burdened by evacuation or damage. Another important example is the communications network which supports modern smart grid technology, both wired and wireless. If this is damaged or is overloaded with traffic after an event, the ability of a distribution utility to monitor and control their grid will be reduced.

Just as distribution grid resilience is affected by the resilience of the infrastructure it surrounds, distribution grid resilience also has significant effect on communities and neighbourhoods which it supplies [20]. Distribution grid resilience plays an important role in supporting overall community resilience and its operation is crucial for modern society to recovery from disaster. Enhancing the resilience of a distribution grid therefore enhances the overall resilience of the society it supports.

The work described in this thesis aims to develop a means of evaluating the contribution from deploying automation technology onto a distribution grid to that grid's resilience. A resiliency analysis methodology which can assess the contribution of individual assets on the system resiliency is therefore required. A review of different methodologies for resiliency analysis will be performed and one will be chosen which meets this requirement.

### 1.2.2 Discussion of Existing Methodolgies

A prominent contribution to resiliency analysis discussion in recent years is in reference [21]. This work presents resilience quantification as an analysis of the performance of the system before, during and after an outage sequence in the form of a *resilience trapezoid*. Later research by the same author in reference [1] proposed that there are three primary phases which occur during a HILP event. During the first phase of an HILP event such as a severe storm, the output load of a system will drop as lines and other assets fail. During the second phase, the utility assesses the damage and plans repairs. The third phase is when repairs begin, and the system will gradually return to normal during this phase. These phases can be represented in the form of a trapezoid, depicted in Figure 1.1. Time is on the x-axis, and a resilience indicator such as the percentage of load supplied, or the percentage of assets remaining operational, is on the y-axis. Quantification of a systems resilience to a specific event can be assessed by observing the shape of this trapezoid. Further explanation of this quantification follows, but the overall concept is that a smaller area trapezoid indicates a more resilient system.

There are secondary phases which could be considered for resilience, specifically the prior planning and retrospective analysis phases. During the prior planning phase, which has a duration depending on the event type, the utility prepares the system for the event. During the retrospective analysis phase, the utility analyses the response taken during the three primary phases of the HILP event.

There is a distinction made between operational resilience (e.g. amount of load supplied by the system) and infrastructure resilience (e.g. percentage of lines/assets which are functioning). Operational resilience is of interest for the case of DA, because DA specifically enhances operational resilience by utilising existing infrastructure to restore service in the case of failed assets.

Reference [22] builds upon this concept to develop a resiliency quantification framework for transmission grids called $\Phi\Lambda E\Pi$ .[1] This quantifies resilience with four key parameters; each of which represents a different part of a systems response to an outage. The four parameters are:

- $\Phi$ - How *fast* the system performance drops
- $\Lambda$ - How *low* the system performance drops.
- $E$ - How *extensive* the post-disturbance degradation is.
- $\Pi$ - How *promptly* the system recovers.

These parameters are defined for both operational and infrastructural resilience. They are able to collectively summarise the decline and recovery of a system in each

[1] Pronouced 'flep'

stage of the HILP event. This methodology can assess a system with both simulation, and retrospective analysis of resilience.

Reference [23] explains that resilient operation requires both high absorbing potential and high recovery potential. It states that resilience is more concerned with the impact (in terms of severity and duration) of a fault, rather than its likelihood. Based on this, many resilience quantification techniques utilise fragility curves to model the effect of severe weather on each asset in a system. These are specific functions which present the probability of failure of an asset based on an input event severity [1]. This input can be any representation of an event's intensity, such as wind speed. The methodology was demonstrated for a transmission grid, but it can be applied to distribution grids [22].

The $\Phi\Lambda E\Pi$ methodology is able to summarise the resilience of a distribution grid, but it does contain limitations for the purposes of this research. Whilst being able to model the relaibility of each asset using fragility curves, the overall analysis requires the execution of simulation methods such as Monte Carlo simulations. This work aims to evaluate the effect of deploying technology to improve resilience on distribution grids. A simulation-based analysis to perform this evaluation would be computationally expensive, especially if an analytical alternative is available which has a direct solution, making it less computationally expensive [3]. For later reference, this form of resiliency analysis will be referred to as simulation-based resilience (SBR).

Other methods have been developed to assess distribution grid infrastructure resilience. [24] presents a methodology which assesses resilience by retrospectively analysing the costs that resulted from a specific event. This provides an intuitive means of deconstructing the performance of a distribution grid at a system level, but does not specifically allow for the analysis of the effect which each asset has on overall system resilience.

Outside of the field of power systems, there are well-established network resilience evaluation and quantification methods in the field of distributed computing. A point made in [25], as well as [26], is that due to the protection systems on a distribution grid essentially being a distributed network, resilience analysis techniques from the field of distributed computing are applicable to resilience analysis of an automated distribution grid. [27] details a methodology for resilience quantification which is usable for both non-state-space and state-space analytical system models. This means it can be applied to distribution grids. This can be done by utilising their reliability and availability models, such as the reliability graph model developed in Chapter 3.

This method is based on the definition of resilience given in [28]. This states that resilience is: "The persistence of service delivery that can justifiably be trusted, when facing *changes*". Reference [27] uses this notion of changes for resiliency quantification and analysis. These changes are classified as ones which are outside of a system's designed fault tolerance. This means system structure and parameter changes which

are outside of their intended design values, and thus what can be considered well-outside normal, day-to-day ranges. These are classed as either parametric or structural. Parametric changes are changes in system parameters, but not the systems assets themselves or their interconnections. Structural changes involve changes in assets or interconnections

The work of this thesis will use parametric changes to represent the performance changes when HILP events occur. For example, a severe storm is a HILP event which can be represented by a significant reduction in the Mean Time To Failure (MTTF) of overhead lines. This will have an impact on overall system reliability and availability. The magnitude of the change in these system metrics conveys the resilience of the system to the introduced parametric change. For later reference, this form of resiliency analysis will be referred to as analytical resilience (AR).

It is important to contrast and compare SBR with AR. Both of these compute resilience based on system level metrics such as energy or customers served. For a distribution grid, SBR demonstrates operational resilience in the form of energy served. This is derived from the availability of each LP in a feeder; similar to System Average Interruption Duration Index (SAIDI), but with a weighting on lost load instead of customers not served. This point is drawn here because AR assesses resilience based on output system metrics, and so the two methods present resilience in similar ways.

Though the two are similar, the core difference between the SBR and AR is how the effects of HILP events are presented to individual assets. The SBR method replaces existing failure rate parameters for all assets within a system with failure probabilities derived from a fragility curve. A simulation is then performed based on these applied probabilities, and the systems response given. This simulation is run multiple times with a Monte Carlo approach. Put in the form of a question, this could be summarised as: *"What will happen to the system when an HILP event of a specific magnitude occurs?"* Alternatively, analysis with the AR method assesses assets by dramatically altering their failure rate parameters significantly to a value which is outside of normal, day-to-day range. The change in system-wide performance (e.g. availability, down time (DT) or SAIDI) due to this change represents the resilience. Put in the form of a question, this could be summarised as: *"What will happen to the system if a specific asset becomes extremely unreliable due to an HILP event?"*

The overall point of this comparison is that the two forms of resiliency analysis complement each other. Analysis using the AR method demonstrates the resilience of a system to failures in a specific asset, rather than of the whole system. This is useful for the purpose of assessing the contribution of DA technology to distribution grid resilience. By modifying recovery parameters of the system attributed to enhancements due to DA, the improvement in resilience of the system can be demonstrated. Furthermore, this method is not simulation-based, so it only requires a single calculation of the

system performance using a developed model. This means that this method is less computationally expensive.

A new method based on the principles of AR will be developed in this thesis. It will be used to analyse the contribution of DA technology to the resilience of a system to parametric changes in its assets during HILP events.

## 1.3 BACKGROUND AND FUNDAMENTALS

This section will outline the fundamentals required for understanding the later content of this thesis. First, Section 1.3.1 will introduce the reliability metrics and distributions used in this thesis. Sections 1.3.2 1.3.3, 1.3.4 and 1.3.5 will then outline the modelling techniques of Continuous-Time Markov Chains (CTMCs), Semi-Markov Processs (SMPs), Stochastic Reward Nets (SRNs) and Reliability Graphs (RGs), respectively.

### 1.3.1 Relevant Reliability Measures and Distributions

This thesis contains metrics from several different engineering fields. This section will define all the measures of interest in this thesis, and briefly discuss what these values represent.

#### 1.3.1.1 Reliability, Availability and Down Time

The reliability function, also known as the survival function, is a function which represents the likelihood that a system will have operated without failure after a period of time. If $X$ is the time at which a system fails, the reliability function, $R(t)$ is defined as

$$R(t) = P(X > t) = 1 - F(t). \tag{1.1}$$

Put in words, reliability is the probability that a system is still operational at time $t$. The failure or unreliability function, $F(t)$, [29] is the probability that a system has failed at time $t$. This value is a measure of the expected time a system will exist without a failure. It is purely defined based on the failure rate of a system. For example, if the time to failure is exponentially distributed with failure rate $\lambda$, then,

$$R(t) = 1 - e^{-\lambda t} \tag{1.2}$$

Availability is a representation of the portion of a time which a system spends online, or live. It can have a transient or steady-state value, depending on how it is defined. Transient availability, $A(t)$, represents the portion of time which a system has been online, at time $t$. Steady-state availability is defined as $A = \lim_{t\to\infty} A(t)$. This thesis will only calculate and discuss the steady-state availability, and will not refer to transient availability beyond this point.

Availability is calculated in different ways. For a system with states online and offline, availability represents the probability that the system is in the online state. See Section 1.3.2.2 for further definition of availability for CTMCs. For the case of SRNs availability will be calculated using reward functions.

Finally, DT is a measure based on the availability. It is defined as,

$$D = (1 - A) \times 8760, \tag{1.3}$$

where $A$ is the availability and 8760 is the number of hours in a year. $A$ is unit-less so $D$ has units of hours per year. $D$ represents the number of hours per year that a system is offline. It will be used throughout this thesis because it is more intuitive than availability when grid enhancements are implemented. Availability is a probability value and is thus bound to range $A \in [0, 1]$. This value is often extremely close to 1.0, as it should be to be considered adequate for a system. As such, an improvement to this is not as obvious as it would be for DT.

In some literature [30, 31] DT is known as *unavailability*, with symbol $U$. This is easily confused with availability in this thesis and thus this terminology will not be used.

#### 1.3.1.2 System Indices SAIDI and SAIFI

Two important measures for analysis and regulation of distribution grids are System Average Interruption Duration Index (SAIDI) and System Average Interruption Frequency Index (SAIFI). They are each used to represent the performance of a distribution grid from the perspective of the customer. As such, they are each a customer-weighted aggregation of each feeders LP metrics.

System Average Interruption Frequency Index (SAIFI) is a customer-weighted representation of the reliability of a feeder. It is purely based on the failure rate of each LP and therefore does not consider the recovery process. It is a mean of how many *sustained* interruptions an average customer will experience over the course of a year. Sustained interruptions are ones which last over a utility-specific or country-specific duration. In most cases outages must be longer than a few minutes [32] to be classed as sustained. *Momentary* outages are ones which do not meet this threshold. This thesis will only consider sustained outages unless specified. SAIFI can be calculated empirically ($SAIFI_{emp}$), by the following formula [33],

$$SAIFI_{emp} = \frac{\text{Total number of customer interruptions}}{\text{Total number of customers}}. \tag{1.4}$$

SAIFI can also be defined analytically ($SAIFI_{ana}$) using the failure rate, $\lambda_i$, of each

LP, $i$.

$$SAIFI_{ana} = \frac{\sum_i N_i \lambda_i}{N_T}, \tag{1.5}$$

where $N_i$ is the number of customers served by LP $i$, and $N_t = \sum N_i$ is the total number of customers served [31].

SAIDI is a customer-weighted representation of the availability of a feeder. It is a measure of the DT which the average customer experience on a yearly basis. Again, SAIDI only considers sustained outages. It is calculated empirically ($SAIDI_{emp}$) by the formula [30],

$$SAIDI_{emp} = \frac{\sum \text{Customer interruption durations}}{\text{Total number of customers}}. \tag{1.6}$$

SAIDI can be calculated analytically ($SAIDI_{ana}$) by the formula [31],

$$SAIDI_{ana} = \frac{\sum D_i N_i}{N_T}. \tag{1.7}$$

The two indices SAIDI and SAIFI are commonly used by utilities to evaluate the performance of distribution grids. Often power distribution grid regulators set SAIDI and SAIFI targets for utilities. These are a significant motivator for utilities to ensure that their customers receive a consistent and rarely interrupted supply of power. Because of the interest which utilities have in these indices, they will be used for feeder-level representation of reliability and availability throughout this thesis. It should also be noted that the majority of feeder-level results in this thesis are presented using just SAIDI. This is because the results are generated for the purpose of evaluating grid recovery.

The methods developed within this work can be used to derive system-wide indices, including ones not discussed in this chapter such as Average Energy Not Served (AENS) and Customer Average Interruption Duration Index (CAIDI). Though not directly relevant to the works of this thesis, these metrics can be calculated using the failure rate and availability outputs of the models in the same way as SAIDI and SAIFI.

#### 1.3.1.3 Probability Distributions

This section will outline relevant probability distributions which are used in this thesis. They play an important role in the representation of timing data, particularly in the case of parameterisation. This section will introduce their parameters, and the maximum likelihood estimators for them for each them.

**Exponential Distribution** The exponential distribution is commonly used to model component Time To Failure (TTF). It is represented by a single parameter, $\lambda$, making it straightforward to estimate and giving it some useful properties which are often

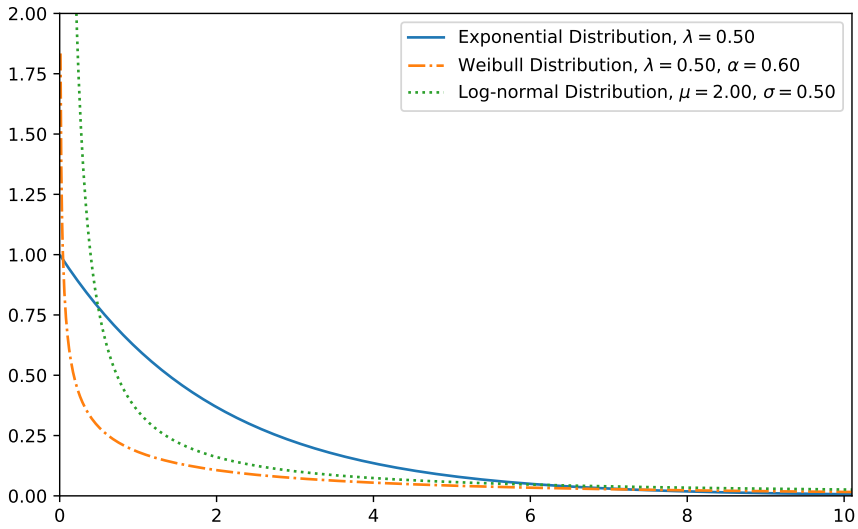


**Figure 1.2** PDF of the exponential, log-normal and Weibull distributions.

utilised in reliability engineering. The Probability Density Function (PDF), $f(t)$, of the exponential distribution is shown in Figure 1.2 and defined as [30]

$$f(t) = \begin{cases} \lambda e^{-\lambda t}, & if\ t > 0 \\ 0, & otherwise. \end{cases} \tag{1.8}$$

The Cumulative Density Function (CDF), $F(t)$, is defined as

$$F(t) = \begin{cases} 1 - e^{-\lambda t}, & if\ 0 \leq t \leq \infty \\ 0, & otherwise. \end{cases} \tag{1.9}$$

Finally, $\hat{\lambda}$ is the maximum likelihood estimator for $\lambda$. It can be defined as

$$\hat{\lambda} = \frac{1}{\bar{x}} = \frac{n}{\sum_i x_i}, \tag{1.10}$$

where $\bar{x} = \frac{\sum_i x_i}{n}$ is the sample mean, for $n$ samples. $x_i$ denotes a failure time sample.

Thus the exponential distribution is fit purely based on the sample mean, making its estimation very straightforward, because it is a closed-form solution. Though there are many advantages to this, it does make the distribution very simplistic. The exponential is a widely-used distribution, largely due to its memoryless property. This property means that component age does not affect the likelihood of failure.

**Log-normal Distribution** The log-normal distribution is closely related to the normal distribution, however its skewed shape causes its peak to always be less than the mean [34].

The PDF of the log-normal distribution, $f(t)$, is shown in Figure 1.2 and defined as

$$f(t) = \frac{1}{t}\frac{1}{\sigma\sqrt{2\pi}}\ \exp\left(-\frac{\ln(t)-\mu)^2}{2\sigma^2}\right), \tag{1.11}$$

and its CDF as

$$F(t) = \frac{1}{2} + \frac{1}{2}erf\left[\frac{\ln(t)-\mu}{\sqrt{2}\sigma}\right], \tag{1.12}$$

where *erf* is the error function. $\mu$ and $\sigma$ are the mean and standard deviation of the distribution, respectively. They are the two parameters used to define a log-normal distribution.

The maximum likelihood estimators for $\mu$ and $\sigma$, $\hat{\mu}$ and $\hat{\sigma}$ are both closed-form. For $i$ samples they are defined as,

$$\hat{\mu} = \frac{\sum_i \ln(x_i)}{n}, \tag{1.13}$$

and,

$$\hat{\sigma}^2 = \frac{\sum_i (\ln(x_i)-\hat{\mu})^2}{n}. \tag{1.14}$$

The log-normal distribution is commonly used to model Time To Recovery (TTR) because it has closed form solutions for its parameters, and [30].

**Weibull Distribution** The Weibull distribution is a commonly used two-parameter model in reliability engineering. Depending on its shape parameter, $\alpha$, it can model increasing, decreasing and constant failure rate. This definition and notation, are borrowed from [29].

The PDF of the Weibull distribution, $f(t)$, is shown in Figure 1.2 and defined as

$$f(t) = \lambda\alpha t^{\alpha-1}e^{-\lambda t^{\alpha}}, \tag{1.15}$$

and the CDF, $F(t)$, is defined as,

$$F(t) = 1 - e^{-\lambda t^{\alpha}}. \tag{1.16}$$

Unlike the previous distributions, the Weibull distribution has no closed-form maximum likelihood estimators, except in special circumstances [30]. The parameters must be estimated iteratively. Methodology for this is available in several text books, including reference [35].

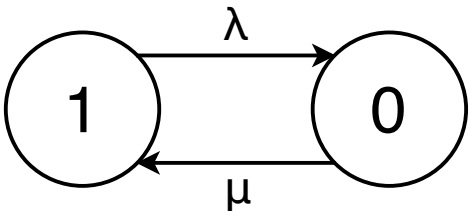


**Figure 1.3** Basic two-state CTMC of transmission line.

### 1.3.2 Continuous-Time Markov Chains

#### 1.3.2.1 Introduction

This section will detail the basic functionality and purpose of a homogeneous Continuous-Time Markov Chain (CTMC). CTMCs are a tool commonly use to model systems or components. They are based on the idea that for a system, there exists a set of states which represent all of the behavior of that system. If all of the possible states of system are known, and probability of shifting between each state is known, then the probability of a system being in any of its defined states can be calculated. The specific case of *continuous*-time Markov chains have the transitions from state-to-state defined as rates in time. Furthermore, to be defined as *Markovian* the mean time to transition between two states is modelled with an exponential distribution. The single parameter for this distribution is the rate of transition.

The basic concept of CTMCs can be demonstrated with a simple example. The CTMC for a power transmission line can be seen in Figure 1.3. This CTMC has two states, 1 and 0. When the line is in state 1, it can be considered online, and likewise it can be considered offline when in state 0. There are two parameters defined for this CTMC, $\lambda$, the *failure rate* and $\mu$, the *recovery rate*.[2] Based on these specified states, and the transition rates between them, it is possible to determine the probability of the system being in either states. This can be calculated as a function of time, or a steady-state case can be evaluated. For this thesis, the steady-state probabilities will always be used and defined, unless explicitly stated.

#### 1.3.2.2 CTMC State Probabilities and Availability

Each CTMC has a state probability vector $\boldsymbol{\pi}(t)$ which defines the probability that a modelled system is in each state at any time $t$. This probability vector is defined as,

$$\boldsymbol{\pi}(t) = [\pi_0(t), \pi_1(t), \cdots, \pi_n(t)], \tag{1.17}$$

[2]It will be seen in later chapters that recovery rate should not be confused with repair rate. The reasoning for this will be demonstrated when the point becomes relevant.

where $\pi_j(t)$ is the probability of being in state $i$ at time $t$. This vector has length $n$, where $n$ is the number of states in the state-space system. Clearly the probability vector $\boldsymbol{\pi}(t)$ must satisfy the conditions:

$$\sum_j \pi_i(t) = 1 \ \forall i, \ \pi_i(t) \geq 0 \ \forall i,$$

where $i = 1, 2, \ldots, n$ is the index of all elements in $\boldsymbol{\pi}(t)$ [36].

The probability that a state-space system is in some state, $j$, at time $t_1$; *given* that it was in state $i$ at time $t_0$, is called the *transition probability* [36]. The transition probability from state $i$ to $j$ can be defined as:

$$\pi_{ij}(t_1 - t_0) = Pr[X(t_1) = j | X(t_0) = i], \tag{1.18}$$

where $X(t)$ is the system state at time $t$ [37].

It is possible to find the *steady-state* values of $\boldsymbol{\pi}(t)$, $\boldsymbol{\pi}$. The elements of $\boldsymbol{\pi}$ are defined as

$$\pi_j = \lim_{t \to \infty} \pi_j(t) = \lim_{t \to \infty} Pr[X(t) = j] \tag{1.19}$$

We next define a matrix, known as a *generator matrix*, $Q$. $Q$ has the following properties:

$$\begin{array}{ll} (i) & 0 \leq -q_{ii} < \infty \ \forall \ i \\ (ii) & q_{ij} \geq 0 \ \forall \ i \neq j \\ (iii) & \sum_j q_{ij} = 0 \ \forall \ i \end{array}$$

This means that all non-diagonal terms in $Q$ for some system are the transitions between states in the system. The diagonal elements are set to be

$$q_{ii} = -\sum_j q_{ij} \ \forall \ j \neq i \tag{1.20}$$

Using this definition of $Q$, the *Kolmogorov differential equation* is defined as,

$$\frac{d\boldsymbol{\pi}(t)}{dt} = \boldsymbol{\pi}(t)Q \tag{1.21}$$

The Kolmogorov differential equation is used to solve the transient state probabilities of a CTMC.

It is shown in [38, 39] that the generator matrix, $Q$, is sufficient to calculate the steady-state probabilities, $\boldsymbol{\pi}$ of a system because the left-side derivative term in Equation 1.21 will be zero at steady-state. The values of $\boldsymbol{\pi}$ can be calculated with the

following two equations.

$$\boldsymbol{\pi} Q = \bar{0} \tag{1.22}$$

$$\sum_{j} \pi_j = 1 \tag{1.23}$$

The derivations of Equations 1.22 and 1.23 can be found in [37].

Once the steady-state state probabilities of a CTMC have been calculated for a state-space system, it is straightforward to calculate values for availability, downtime and failure frequency.

Availability is the proportion of time (and equivalent to the probability) the component is in a functional state [40]. To calculate availability, each state must be defined as an *up* or *down* state. When all up states, $U$, and down states, $D$, have been defined, the availability, $A$, of a system can be calculated as [31]

$$A = \sum_{k \in U} \pi_i = 1 - \sum_{k \in D} \pi_i \tag{1.24}$$

For a two-state CTMC such as the one in Figure 1.3, it can be shown that the availability is

$$A = \frac{\mu}{\lambda + \mu} \tag{1.25}$$

The downtime of a system can then be calculated by multiplying $1 - A$ (the unavailability) by the number of hours in a year, as is shown in Equation 1.3.

#### 1.3.2.3 CTMCs for System Modelling

Multiple assets and their interdependencies can be modelled using CTMCs. For a CTMC with multiple assets, each state in the state diagram must represent all assets. For example, for a CTMC with two assets $a_1$ and $a_2$, the following states will be contained in the state diagram:

- (1,1) - $a_1$ and $a_2$ in online state.
- (0,1) - Asset $a_1$ in offline state, asset $a_2$ in online state.
- (1,0) - Asset $a_1$ in online state, asset $a_2$ in offline state.
- (0,0) - Both assets $a_1$ and $a_2$ in offline state.

The size of CTMCs grows rapidly as they model more assets. For a system with $n$ two-state assets, there will be $2^n$ states. This feature quickly becomes problematic for large systems because the state-space of a CTMC can be too large to solve in a feasible timeframe. This issue is known as state explosion. Despite the state explosion issue,

modelling multiple components with CTMCs can be useful because the dependence between assets can be modelled. For example, the opening of a sectionalising switch in order to isolate a failed line will change asset dependencies.

### 1.3.3 Semi-Markov Processes

A SMP is a generalisation of a Markov model which does not have the time-homogeneous requirement. Thus, the time a model spends in a given state is not exponentially distributed. This means that a number of the assumptions and features required for CTMCs do not apply to SMPs. The most relevant example of this is that the rate of departure from a given state (for example the failure rate, or other transition rate) is dependent on the time which the system spent in that state [29]. Transition rates are no longer constant in time.

Note that the method presented in this section is somewhat simplified, because it evaluates a two-state model. Despite this, it is possible to model more complex procedures, such as maintenance, using this methodology. Further examples can be found in [29].

To manage the rates which are no longer constant in time, a SMP bases its functionality on models of the time spent in a given state, known as the *sojourn time*. These times are built by evaluating the models of the transitions which depart from a given state. A vector of sojourn times, $\boldsymbol{H}(t)$, is used with a matrix of state transition probabilities (known as a *kernel matrix*), $P$, to calculate the state probabilities, i.e. the probability of a system being in a given state. Using these state probabilities, availability and other related metrics can be calculated. The kernel matrix is a constructed from Discrete Time Markov Chains (DTMCs), and the vector $\boldsymbol{H}(t)$ makes the model continuous in time.

#### 1.3.3.1 Semi-Markov Process Availability

An arbitrary overhead line model contains two states, 1, and 0. State 1 represents the line being online, while 0 represents the line being in a failed state. The transitions between these two states are semi-Markov processes. The transition rate to the failure state, 0, is modelled with a Weibull distribution, and the transition to the online state, 1, is modelled with a log-normal distribution. A diagram of this two state model can be seen in Figure 1.4

The kernel matrix is constructed by observing all of the transitions leaving each state, and evaluating the probability of each transition. For example, if there are two transitions leaving a given state with sojourn time $T$, one modelled by some distribution $X$, and the other by some distribution $Y$, then we are interested in $P(X > Y)$ and vice

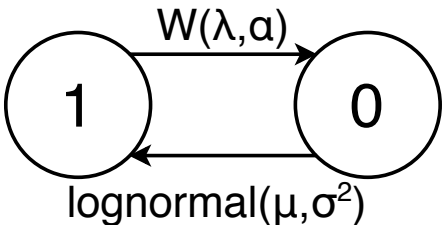


**Figure 1.4** 2-state SMP for overhead lines, with failure transition modelled with Weibull distribution, and the recovery transition modelled with log-normal distribution.

versa. These are given as

$$P(X > Y) = \int_0^T P(X > t) f_Y(t) dt. \tag{1.26}$$

This is a two-state model and so the kernel matrix is the identity matrix because each of the two states only has a single departing transition.

For any given DTMC kernel matrix, there exists an eigenvector, $\boldsymbol{v}$, with eigenvalue 1. Thus, the vector can be solved using using standard means of solving DTMCs with following two equations:

$$\boldsymbol{v} = \boldsymbol{v}P \tag{1.27}$$

$$\sum \boldsymbol{v} = 1 \tag{1.28}$$

The sojourn time of state 1, $H_1(t)$, corresponds to a single transition for a 2-state model, thus its sojourn time function is solely distributed by the model of that transition, in this case, a Weibull distribution. The same applies to $H_0(t)$ and the log-normal distribution. Refer to Section 1.3.1.3 for the CDF of these two distributions. Thus we can define the two terms of the $\boldsymbol{H}(t)$ vector as,

$$H_1(t) = 1 - e^{-\lambda t^\alpha} \tag{1.29}$$

and

$$H_0(t) = \frac{1}{2} + \frac{1}{2} erf\left[\frac{ln(t) - \mu}{\sqrt{2}\sigma}\right] \tag{1.30}$$

where *erf* is the error function.

The state probabilities are calculated based on the mean time the model remains in a state, i.e. the mean sojourn time. For a state, $i$, the mean sojourn time is calculated as,

$$h_i = \int_0^\infty [1 - H_i(t)] dt. \tag{1.31}$$

For this system we have,

$$h_1 = \int_0^\infty 1 - e^{\lambda t^\alpha} dt = \left(\frac{1}{\lambda}\right)^{\frac{1}{\alpha}} \Gamma\left(1 + \frac{1}{\alpha}\right), \tag{1.32}$$

where $\Gamma$ is the Gamma function, and,

$$h_0 = \int_0^\infty \frac{1}{2} - \frac{1}{2} erf\left[\frac{ln(t) - \mu}{\sqrt{2}\sigma}\right] dt = 1 - e^{\mu + \frac{\sigma^2}{2}}. \tag{1.33}$$

Finally, the state probability vector, $\boldsymbol{\pi}$, is defined based on the $\boldsymbol{v}$ and $\boldsymbol{\pi}$ vectors, for each state $\pi_i$ [29],

$$\pi_i = \frac{v_i h_i}{\Sigma_j v_j h_j}. \tag{1.34}$$

Thus we have the two state probabilities, $\pi_1$ and $\pi_0$, which can be defined as,

$$\pi_1 = \frac{v_1 h_1}{v_1 h_1 + v_0 h_0} \tag{1.35}$$

and

$$\pi_0 = \frac{v_0 h_0}{v_1 h_1 + v_0 h_0}. \tag{1.36}$$

Because this is a 2-state model, and therefore each state has only a single departing and single arriving transition, the mean time spent in a state is the same as the mean time to each transition. Thus, we can conclude with,

$$\pi_1 = \frac{MTTF}{MTTF + MTTR} \tag{1.37}$$

and

$$\pi_0 = \frac{MTTR}{MTTF + MTTR}. \tag{1.38}$$

Availability, $A$ is calculated based on the probability of the system being in an up state. This has been introduced in Section 1.3.2. For this two-state mode, this is the probability of being in state $\pi_1$.

To conclude this section: it is possible to use SMPs in place of CTMCs using the methodology described above. An important constraint is that the solution to SMPs must be calculated using numerical methods because an analytical solution is not available for any but the two-state case.

### 1.3.4 Stochastic Reward Nets

#### 1.3.4.1 Introduction

This section will present the methodology for constructing a Stochastic Reward Net (SRN), and then the core methods will be demonstrated with an example in Sec-

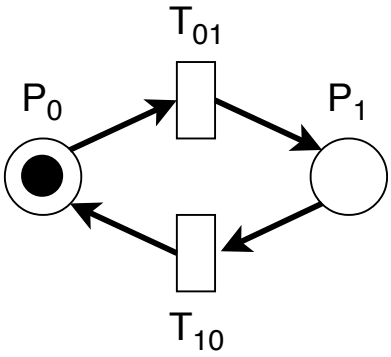


**Figure 1.5** Basic two-place SRN containing one token.

tion 1.3.4.2. Concepts not covered by the basic example, but that are used in later chapters, will be briefly described in Section 1.3.4.3.

The procedure for utilising CTMCs for analysis of availability and system performance requires first abstracting a system to a basic definition, constructing a series of linear equations and then solving these equations using various methods. For large systems, the process of even defining the equations for a system before solving them can be error-prone and tedious [29]. Additionally, if a number of subsystems are to be modelled using CTMCs, the resulting model is likely to be far-removed from the system it represents as strong dependencies are treated with the same status as weak dependencies. The fundamental purpose of SRNs and related formalisms is to automate the generation of such models.

An SRN is a directed graph which contains two types of node, *places* and *transitions*. Places are represented as a hollow circle, labeled $\mathrm{P}_x$ where $x$ is a description of the state which the place represents. Transitions are a hollow oblong, labeled $\mathrm{T}_x$ where $x$ is a description of what occurs when the transition *fires*. The edges connecting these two types of node are called *arcs* [37]. An example SRN can be seen in Figure 1.5. An SRN can comprise of a number of subsystems. Each of these will have one or more *tokens*, seen as the black dot in the diagram. Tokens move between places when transitions *fire*. The rate at which a transition fires is specified in a similar way to how state-to-state transitions are specified for CTMCs. For the applications of this thesis, each SRN subsystem will contain only one token, however for other applications, there is no limit. There are no arcs connecting each subsystem, so each subsystem is independent.

#### 1.3.4.2 Example SRN

The overall construction of SRNs will be demonstrated with a simple two asset example system. A SRN for the system is presented in Figure 1.6. This SRN contains two subsystems, each of which is a two-place model representing lines L1 and L2, respectively. This model is able to simultaneously model the two separate assets, but define them separately.

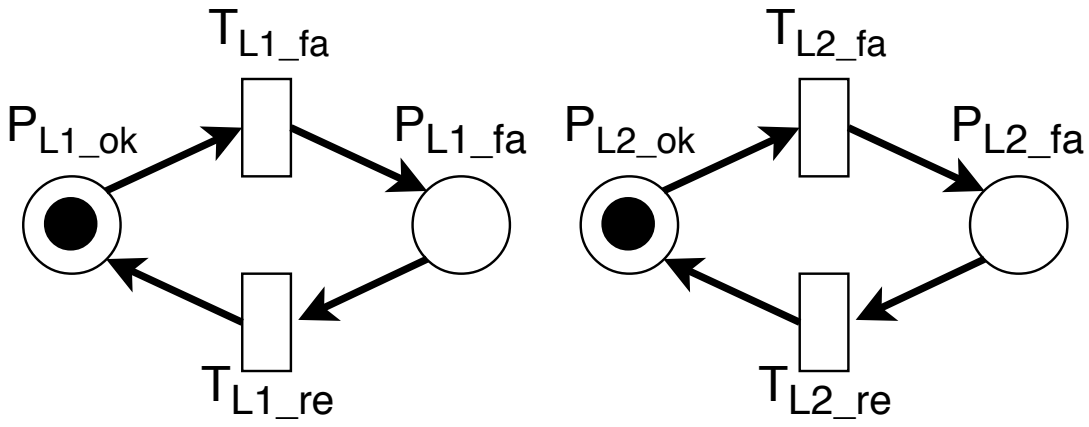


(a) L1 subsystem (b) L2 subsystem

**Figure 1.6** SRN for system containing lines L1 and L2, with a two-place subsystem for each.

| **Name** | **Attached Transition** | **Description** | **Assigned Value** |
|---|---|---|---|
| $\lambda_{L1}$ | $T_{L1\_fa}$ | Failure rate of L1 | 0.01 $yr^{-1}$ |
| $\lambda_{L2}$ | $T_{L2\_fa}$ | Failure rate of L2 | 0.01 $yr^{-1}$ |
| $\mu_{L1}$ | $T_{L1\_re}$ | Recovery rate of L1 | 8760 $yr^{-1}$ |
| $\mu_{L2}$ | $T_{L2\_re}$ | Recovery rate of L2 | 8760 $yr^{-1}$ |

**Table 1.1** Parameter definitions and values for example SRN model

Each of the two subsystems of the example SRN contains a place $P_{Lx\_ok}$ representing the line Lx being online, and a place, $P_{Lx\_fa}$ representing the line Lx having failed (i.e. offline). There is a transition, $T_{Lx\_fa}$ from $P_{Lx\_ok}$ to $P_{Lx\_fa}$ which represents the failure of line Lx. Similarly, there is a transition, $T_{Lx\_re}$ from $P_{Lx\_fa}$ to $P_{Lx\_ok}$ which represents the recovery. Table 1.1 contains the assigned values for the example SRN. The values for firing rates are arbitrary, but this table is a demonstration of how the parameters will be given in later examples throughout this thesis. For analysis of a real system, these parameters would be estimated using the methods introduced in Chapter 2. The failure rates $\lambda_{L1}$ and $\lambda_{L2}$ are rates of 0.01 $yr^{-1}$, and the recovery rates $\mu_{L1}$ and $\mu_{L2}$ are 8760 $yr^{-1}$. The number 8760 will be regularly seen throughout this thesis, as it is the number of hours in a year, and so $\mu_{L1}$ and $\mu_{L1}$ correspond to a mean recovery time of $1hr$, as they are exponentially distributed.

The process used to calculate the steady-state solution of a SRN involves first constructing a *reachability graph*. This is done by defining a $N$-tuple, where $N$ is the total number of places in the SRN. This is an aggregation of all of the subsystems. For this example this will be a four-tuple, and the structure will be ($\#P_{L1\_ok}$,$\#P_{L1\_fa}$,$\#P_{L2\_ok}$,$\#P_{L2\_fa}$), where $\#P_x$ is the quantity of tokens in place $P_x$. The models in this thesis each have a value for $\#P_x$ of 0 or 1, because each subsystem has a single token. Using this four-tuple,

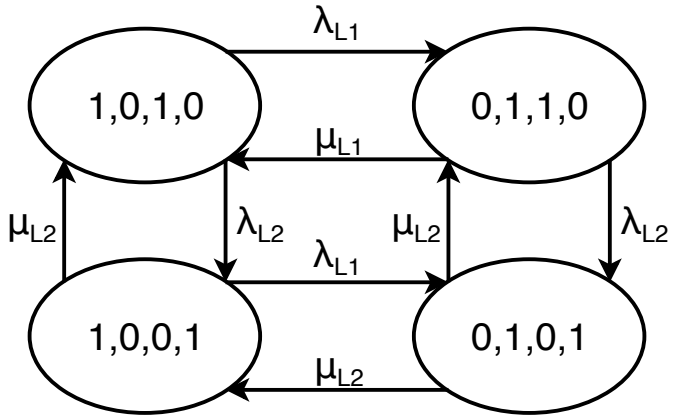


**Figure 1.7** CTMC of the reachability graph of SRN given in Figure 1.6.

a reachability graph is constructed. A reachability graph represents all the different *reachable* forms of the four-tuples. The CTMC for this is given in Figure 1.7.

Reachability graphs are a complete description of all possible states of a system modelled with a SRN. This complete reachability graph is a CTMC, with transitions defined by the firing rate of the transitions in the SRN. For an SRN with $M$ subsystems, each of size $N_m$, the total number of states, $N_R$, on the reachability graph can be calculated as

$$N_R = \prod_{m \in M} N_m$$

For a SRN with a number of subsystems, the underlying reachability graph will have many more states than the SRN will have places. This is a clear advantage of a SRNs when compared to CTMCs, because a CTMC requires the same number of states as a SRN's reachability graph to represent the same system. It can be seen that the transitions of states of individual assets in a reachability graph are defined a number of times. For example in Figure 1.7, $\lambda_{L1}$ is defined as the transition rate for (1,0,1,0) to (0,1,1,0), and also for (1,0,0,1) to (0,1,0,1). A transition which only occurs in a single subsystem of an SRN, is defined multiple times for a corresponding CTMC.

This SRN is sufficiently defined to calculate the probabilities of the token of each subsystem being in each state. These probability values are used in a defined *reward function*, to evaluate a system. Reward functions can be used to calculate metrics such as availability and DT. An explanation of the reward function is given in Section 1.3.4.3. The system can be solved by hand to find the aforementioned probabilities, using methods which will now be demonstrated. Alternatively, there are a number of software packages availability which can be used, including SHARPE [41], and SPNP [42].

#### 1.3.4.3 Advanced Functionality of SRNs

SRNs contain several features which make them better able to represent systems and assets. There are three features of interest, reward functions, guard functions and immediate transitions. These will now be explained.

Reward functions map SRNs to a Markov reward model [29]. This means that values can be assigned to each place. For the purposes of this thesis, defining a reward value to specific places means that a system's dependence on specific configurations can be analysed and the availability and related parameters can be modelled. By observing the probability that a token is in a specific subsystem, it is possible to analyse the availability of an LP by assessing the probability that it is in a specific configuration. Reward functions are further discussed in Section 4.3.2.

Guard functions are similar to reward functions, in that they observe the positions of tokens in a subsystem. Their purpose however, is to prevent a transition from firing and moving tokens from place to place, unless specific conditions are met. A common example of a system which would utilise them is one which contains subsystems for switches with associated transition times for opening and closing. Switches only open or close when assets such as lines are in an offline (or failed) state. Guard functions in this application would restrict a switch's subsystem from transitioning unless a certain asset is offline. Guard functions are utilised in the extended switch model which is developed in Section 4.5.

The final feature of SRNs which will be used is immediate transitions. These are transitions which have no associated rate, and so if they are enabled then they fire immediately, transitioning a token from place to place. For the model within this thesis, these are utilised with guard functions. The purpose of them is to allow certain transitions to be modelled based on the state of other subsystems, better representing one subsystems dependence on another.

### 1.3.5 Reliability Graphs

#### 1.3.5.1 Introduction

This section will discuss and introduce the basic concepts of a Reliability Graph (RG). RGs are a formalism represented by a set of nodes and directed edges. Edges represent assets, and nodes represent the interconnections between them. A single RG has one node, called a source, which has no arriving edges; and one node, called a sink, which has no departing edges. Systems modelled by RGs fail when there is no connected path from source to sink. Each of the edges in an RG is assigned a failure rate, or an availability. A basic example of an RG is given in Figure 1.8. RGs are analysed using factoring algorithms.

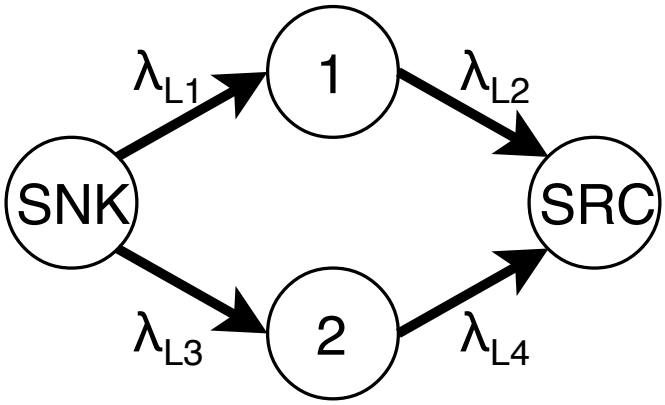


**Figure 1.8** Basic reliability graph. SRC denotes the source node, and SNK denotes the sink node.

The reliability, MTTF, and availability of a LP is analytically calculated using RGs that are based on the set of connected assets which make it up. The reliability of a RG can be calculated by factorising each assets' reliability with the following formula [37]:

$$R(t) = 1 - \begin{cases} 1 - \prod_{i=1}^{N} R_i(t), & \text{for series subsystem} \\ \prod_{i=1}^{N} [1 - R_i(t)], & \text{for parallel subsystem} \end{cases} \tag{1.39}$$

where N is the total number of $i$ subsystems, each with reliability $R_i(t)$. Similarly, if the edges of an RG are assigned availability values, the availability for an RG with series-parallel components is calculated as,

$$A = \begin{cases} \prod_{i=1}^{N} A_i, & \text{for series subsystem} \\ 1 - \prod_{i=1}^{N} [1 - A_i], & \text{for parallel subsystem} \end{cases}. \tag{1.40}$$

The final output, MTTF, can be calculated based on the reliability function. It is defined as,

$$MTTF = \int_0^\infty R(t)dt. \tag{1.41}$$

Example analysis of RGs will be demonstrated when they are employed in Section 3.3.5.

## 1.4 SCOPE AND GOALS OF THESIS

A top-down approach will be taken to construct a model for distribution grid availability and resiliency analysis. The thesis will start by demonstrating the analysis of outage data from a real system to obtain model parameters, and investigate resilience based on just this outage data. From this point, several models are developed to assess availability and resilience. First, an RG model is developed to investigate the benefits of Fully Automated Reconfiguration (FAR) after an outage, and the resilience contribution which

it provides. After this, a novel SRN model is constructed which models a feeder and its reconfiguration process. This model is analysed and extended to assess the placement of Automation Enabling Communications (AEC) onto the existing sectionalising switches, reducing their operation time. Finally, a model is developed to model the outage recovery process, by augmenting the developed SRN model. Collectively, these models provide a set of tools to analyse the contribution of DA onto distribution grids. The contributions and developments of this thesis will be separated and presented in four chapters.

Chapter 2 presents the methodology to process a generalised distribution utility's outage database. Failure modes will be established through this to gain knowledge of the causes of failure within a system. Additionally, it presents techniques to analyse an outage database to obtain failure and recovery parameters which can be used to represent the system during later modelling. A study is presented based on analysis of an actual distribution grid.

Chapter 3 develops a hierarchical model to assess system and load point availability along with its sensitivity and resiliency using RGs. This model allows for the evaluation of the connected components in a system and their individual reliability or availability. It is used to evaluate and compare the benefit of fully automating the post-fault reconfiguration process. Furthermore, this RG model is structured such that it can utilise parameters estimated from outage data, such as is in Chapter 2. It will be used to analyse the resilience of distribution grid feeders, and compare with the resilience benefit of fully automating a feeder with DA. It is demonstrated in Chapter 3 that the developed hierarchical model is able to analyse availability and resilience of interconnected distribution grids, but it is unable to model the complex recovery process, a feature desired for this thesis.

Chapter 4 develops a model to assess system and load point availability and its sensitivity and resilience using SRNs. Unlike the RG hierarchical model of Chapter 3, this SRN is specifically designed to incorporate the complex recovery process which occurs after an outage on a distribution grid. This model is created to assess the customer DT reduction from increasing the speed of the recovery process and the reduction from enabling more redundant connections throughout a load point using logic-based rewards functions. The developed modelled is used to evaluate the contribution which automating the post-fault reconfiguration process has on the system. Both availability and resilience are analysed and quantified using this model.

It is revealed in Chapter 4 that to model the recovery process accurately and fully incorporate the affect of DA, an augmented model is required. Chapter 5 expands the analysis of recovery to assess the impact of differing amounts of fault location knowledge. The purpose of this is to remove some of the assumptions typically used to model distribution grids, in order to develop a model which can holistically model the

recovery process. This recovery model is used to augment the SRN of Chapter 4. The expansion adds the ability to assess the sensitivity of a modelled system to the time it takes to locate a failure on a feeder and then evaluate the contribution of placement of FIs. Doing so will underline the value that DA can provide to a system.

## 1.5 SUMMARY

There currently exists no effective methodology to analyse the contribution which DA provides to distribution grid resilience. This thesis will develop a methodology of evaluating the specific contribution of DA technology. The purpose of DA is almost exclusively to enhance the recover process. The placement of DA must be based on maximising its contribution to this recovery process. A model is developed which can assess the contribution provided from deploying switch automation and FIs for the purpose of improving LP and feeder availability. Furthermore, this model will be used to evaluate the contribution of these individual devices on the resilience of both LPs and feeders.

## 1.6 PUBLISHED WORKS

Two papers have been published that are related to the works presented in this thesis.

1. K. Morris, D. S. Kim, A. Wood, and G. Woodward, "Availability and resiliency analysis of modern distribution grids using stochastic reward nets," in *Innovative Smart Grid Technologies-Asia (ISGT-Asia), 2017 IEEE*, IEEE, 2017
2. K. Morris, D. S. Kim, A. Wood, and G. Woodward, "Reliability and resiliency analysis of modern distribution grids using reliability graphs," in *IEEE International Conference on Communications (ICC) Workshop 2018*, IEEE, 2018

The first paper contains works which are described in Chapter 4. The second contains works which are described in Chapter 3.

# Chapter 2

# OUTAGE DATA ANALYSIS AND PARAMETERISATION

## 2.1 INTRODUCTION

Distribution grids span large geographical areas, and serve power in many different climates and environments. The reliability of assets within distribution grids depends greatly on the environment they operate in, and this varies significantly from one system to another. As a result, establishing a single availability and resilience model for all distribution grids would produce one that is inaccurate and unrealistic. Due to the variation of conditions in each distribution grid, and even within a single distribution grid, it is important to establish failure and recovery parameters which are based on the conditions which different components and assets experience. Failure and recovery rates used to model assets must be dependent upon the assets and the environment they exist in. The purpose of this chapter of research is to establish methods which can produce parameters reflecting the unique environment of individual distribution grids.

All distribution grid utilities in New Zealand, and many other countries, collect data to monitor, store and report the status of their system. An important database for this research is the outage database, which contains a log of each outage, planned or unplanned, that has occurred over its duration. Each entry in this database contains details of the date and time of occurrence, date and time of recovery, type of asset which failed, and the cause of the outage. They also contain data expressing the feeder which contained the outage, and the number of customers affected. Outage databases provides utilities with a means to determine their regulated index values (System Average Interruption Duration Index (SAIDI), System Average Interruption Frequency Index (SAIFI)), and also allow retrospective analysis of performance, and maintenance of assets and the system as a whole. There is a large amount of information which can be extracted from this type of recorded data, but central to this work, which focuses on reliability and resilience analysis, is the rate at which outages occur, and how long recovery takes.

Existing methods of outage analysis for statistical inference and parameter estima-

tion are well established, for distribution grids and other systems. However there is significant variability between each distribution grid [45], so there is merit in conducting this analysis. The work in [46] demonstrates that there are several causes for this large variability. The most important of these are cause of outage, actions taken by crew to restore the system, protection devices activated to clear the fault, and weather conditions. With the deployment of smart grid technology, the amount of recorded data is increasing; including data related to outages [47]. Recently, [48] presented an analysis of data center failures, and the methods demonstrated are very applicable to distribution grid outage data, which is recorded in a similar way. The methodology of failure type and cause breakdown from this will be utilised here. Finally, [46] conducted an analysis of outage data and identified that the distribution grid recovery time has a high variance, due to the range of possible factors which affect the duration.

The existing data parameterisation methods will be used to extract failure and recovery parameters from the outage database and used to establish an accurate representation of the system they are recorded within. These results will provide the ability to accurately assess reliability, availability and resilience through an analytical model of the system. Additionally, because this data records all individual outages in the system, analysis will look at failure and recovery rates related to specific events and failure causes to observe how the failure and recovery rates vary from normal rates. Through this analysis, the performance of different sections of a system can be assessed and the performance of individual asset types can be analysed in different environments. This will provide initial insight into the resilience of the system, and enhance later modelling and optimisation.

Overall, the intended goal of this chapter of work is to analyse distribution outage databases to estimate recovery and failure parameters. The majority of this work will be presented by demonstrating the methods on a real system outage database, from a distribution grid utility in New Zealand. The contributions in this work are:

- Conduct failure cause breakdown analysis will be performed to provide assessment of asset failure frequency how proportions change in different environments. (Section 2.3)

- Deploy statistical inference methods will be used to estimate failure and recovery parameters, based on data taken from the outage database. This will provide estimates of the Mean Time To Recovery (MTTR) and Mean Time To Failure (MTTF), based on each of the probability models built from sampled data. (Section 2.4 and Section 2.5).

- Demonstrate methods developed to evaluate distribution grid resilience based on the outage database. This insight will provide a basis for later analytical resilience modelling. (Section 2.6).

Along with these works, Section 2.2 will describe the data used in this analysis, and Section 2.7 will discuss the results of this chapter, and fit them into the context of this thesis.

## 2.2 DESCRIPTION OF DATA

Each utility maintains an outage database for several reasons including asset tracking and retrospectively reviewing performance. They are used to calculate the SAIDI and SAIFI indices which are required annually as a regulatory requirement. These indices, which were introduced in the Section 1.3.1.2, make up an important part of the key performance indicators which regulators require distribution utilities to achieve.

The outage database contains a log of all outages, planned or unplanned, which have occurred over their duration. Each row represents an individual outage event, with a number of a different columns containing information about each event. It should be noted that in general, the columns and structure of each utility's recorded outage database are different. Despite this, there are a number of columns which are common to all, and these make up the primary sources of information which are needed for this analysis. This data allows for system-specific estimations of parameters and other information, increasing the accuracy and usability of later results. This will be discussed further in later sections. The columns of interest from the outage database are shown in Table 2.1.

| **Column** | **Description** |
|---|---|
| ID Reference | A unique value assigned to each outage |
| Date Off | The date which the outage occurred |
| Time Off | The time which the outage occurred |
| Date On | The date when all customers are restored |
| Time On | The time when all customers are restored |
| Substation And Feeder | The name of the substation and feeder which contained the outage |
| Asset Affected | Type of asset which was brought offline, selected from a list of options |
| Cause Of Failure | Cause attributed to the outage, selected from a list of options |
| Customers Affected | Total number of customers who lost power at any time due to the outage |
| Comments | Additional information about the failure. Usually contains details about the cause of a failure, and the procedure used to restore power. |

**Table 2.1** Columns expected in all outage databases

The source of the specific data which is used in this chapter is intended to be anonymous, however general details of the data follow. The data contains 12000

unplanned outages, 8000 of which are in areas considered rural. It spans 17 years, from 2000 to 2017. The data recorded for each outage is: when the outage occurred; when the recovery was complete; what caused the outage; what asset failed; and what was the impact on the customers who lost power. It will be demonstrated that this data is sufficient to estimate parameters for MTTR and MTTF for the assets within the system which has been recorded.

### 2.2.1 Note on Planned Outages

Outage databases collect records of planned outages, as well as unplanned. "Planned outage" is an all-encompassing term for outages which have been scheduled by the managing utility for reasons including maintaining or upgrading equipment. The overall purpose of this chapter is to evaluate the parameters for failure and recovery rate. These rates do have a small dependence on the maintenance schedule of the managing utility, for the following reasons:

- Planned maintenance extends the life of assets, thus reducing failure rate.
- Planned maintenance can affect the recovery process by removing potential reconfiguration options.
- Errors during maintenance can cause failures, or exacerbate them.

All of these cases are useful to know, but the influence of maintenance on the failure and recovery parameters will be considered separately. Assessing these planned outages is therefore outside of the scope of this research, and the outages themselves will be omitted from all results henceforth.

## 2.3 BREAKDOWN OF AFFECTED ASSETS AND FAILURE CAUSES

The first step taken to assess the outage database is to break down the proportions of the outages. This is done to obtain a broad overview of the data, in terms of the proportions of each asset type failing, and the proportions of different failure causes. This process establishes the assets which should be the focus of analysis when conducting parameter estimation. It can also reveal patterns in the data which can explain phenomena seen in parameter estimation. Finally, this analysis can be used to present the nature of the data to the reader, or other stakeholders, by highlighting the most important assets and failure causes. The methodology used here has been adapted from [48].

The breakdown analysis will be done in three parts; a proportional analysis of Affected Assets, of Causes of Failure and of the Causes of Failure of specific assets. Analysis will observe how the breakdown of each of these three perspectives of the

outage data are proportioned for the overall grid, and then separately for rural and urban environments. The results will be presented as pie charts, showing how the ratios of the three perspectives change. The intention is to identify which assets are the most prominent in the data, and can be used in later analysis. A discussion of the need for differentiating rural and urban environments is given in Section 2.3.1. Because of the need for anonymity, specific data counts will be omitted from this analysis and only percentages given.

For each of these three perspectives, supplementary to the breakdown presented in pie charts, a temporal analysis of the proportions will be conducted. The aim of this is to identify how each breakdown trends over the duration of the database, and also will highlight how consistent the proportions are. This will be done by splitting the data into biennially proportioned data bins.

### 2.3.1 Urban and Rural Outages

It is important to stress the differences between urban and rural distribution grids within the database. The differences in these environments can have a significant impact on the results; in the same way it has a significant influence on the methods and processes used to maintain the two environments. The two major differences are as follows:

1. An urban distribution grid spans a much smaller area with many more interconnections while a rural distribution grid is spread over a much larger area with less interconnections.

2. Urban grids use a high proportion of underground cables, while rural grids use a high proportion of overhead lines.

These differences have an significant impact on the reliability of the two environments.

The reason that urban distribution varies greatly from rural distribution is that the urban environment has a significantly higher population density. An outage in an urban area typically affects many more customers, and thus it is justified for utilities to invest in underground cable infrastructure. These are more reliable than overhead lines. This point will be demonstrated in later sections where cable failure rates are estimated from the data. An advantage of high population density and the resulting infrastructure density is that feeders are closer to each other. This means they have more interconnections and therefore more reconfiguration options. This further reduces the recovery time of many customers within the grid.

Conversely, rural feeders tend to be much more sparse than urban feeders. They cover larger areas, meaning it is not feasible to use underground cables, except in some densely populated towns. This generally results in a higher number of failures per unit time, due to more exposed assets and fewer options for reconfiguration. However, due

to having fewer customers, the impact of these outages is generally smaller than what it would be in more populated regions.

The breakdown analysis work and parameter estimation work, will place emphasise on the difference between these environments when data is presented. This is intended to ensure more accurate and appropriate data can be obtained for use in later models. In general, all results will be first given for the original sample data, and then separated into the two environments. This will be done for all of the following data analysis sections, including the recovery and failure parameter estimation, in cases where it is applicable to do so.

### 2.3.2 Affected Asset Breakdown

The aim of this section is to assess which asset types fail most often in the outage database, and how this changes over time. The first result looks at the breakdown of overall portions of assets attributed to failures. This is done for the overall system, and also separated into rural and urban results for the purpose of conveying the differences between the two environments. Following this, analysis will be conducted from a temporal perspective. The goal of this is to investigate how the proportions of asset failures has changed over the span of the database, and also to determine if it trends over time.

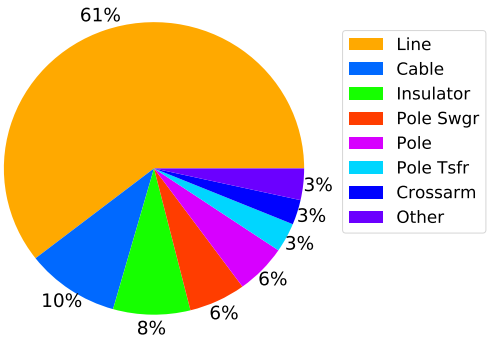


**Figure 2.1** Breakdown of failed assets for combined urban and rural environments

The breakdown of affected assets for both environments can be seen in Figure 2.1, and for rural and urban environments in Figure 2.2. It is immediately obvious that overhead line faults dominate in all three graphs. The results show that underground cables represent a much lower proportion of faults in the rural environment compared to the urban environment. This is due to two reasons. Firstly, underground cables tend to be much less likely to fail than overhead lines, as they are not exposed to the environment and wildlife. Secondly, there are less underground cables used in the rural distribution grids. Underground cables are mostly used in densely populated areas, while the rural grid primarily utilises overhead lines.

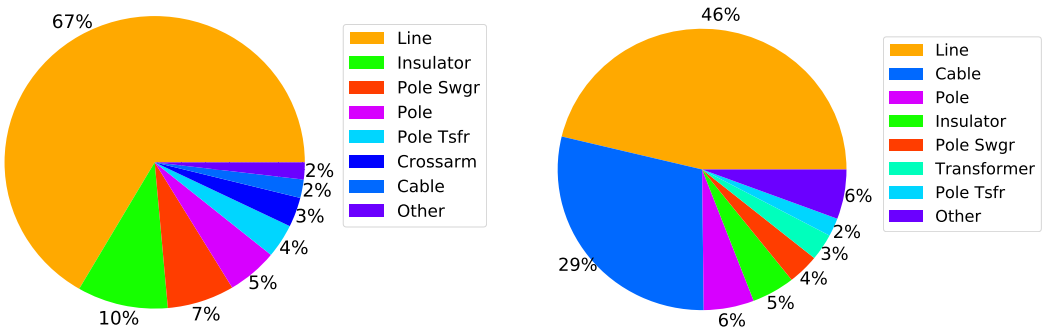


(a) Breakdown of rural asset failures (b) Breakdown of urban asset failures

**Figure 2.2** Breakdown of failed assets for urban and rural environments

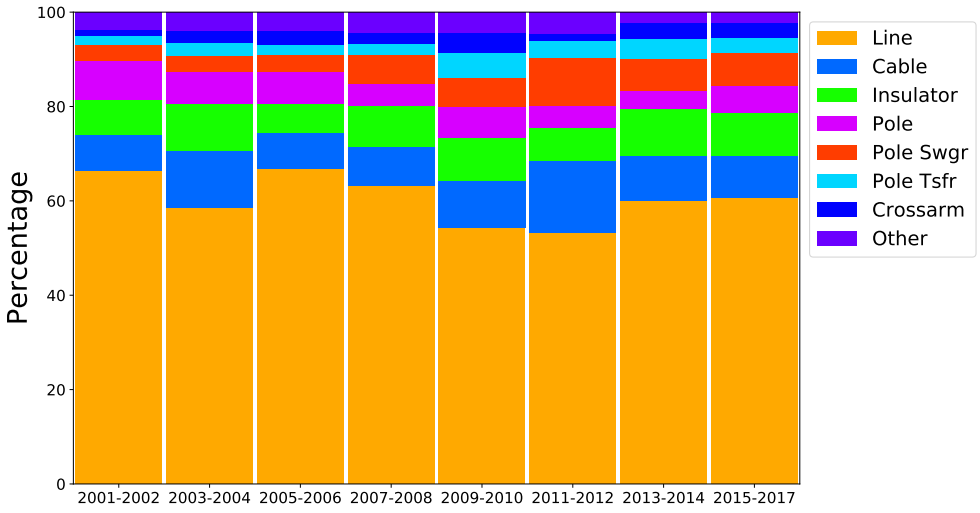


**Figure 2.3** Biennial breakdown of overall asset failures

Finally, we look at this breakdown from the temporal perspective. Figure 2.3 shows a biennial breakdown of assets. The results show that the proportion of failures attributed to each asset has remained constant for the duration of this database's collection. There is some variation, but no obvious trend.

### 2.3.3 Failure Cause Breakdown

This section observes how each cause of failure is distributed in the data. It will also investigate how they change over time, and if each are distributed differently in urban and rural environments. The goal to establish the most common failures in the data, and how likely each cause of failure is. This knowledge will allow specific causes of focus to be identified. It will reveal which are most common and therefore most important. These causes will be the subject of future discussion in later analysis.

This analysis will first consider the overall distribution of failure causes, and then

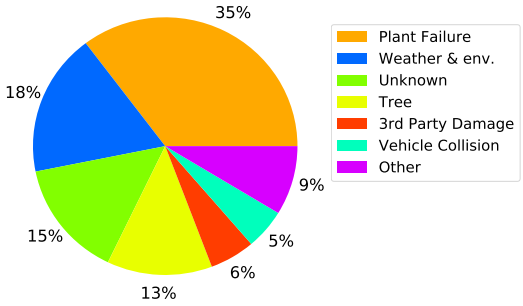


**Figure 2.4** Breakdown of failed assets for combined urban and rural environments

distributions in rural environments and urban environments. The overall breakdown for cause of failure is shown in Figure 2.4. Specific breakdowns for rural and urban environments are shown in Figure 2.5

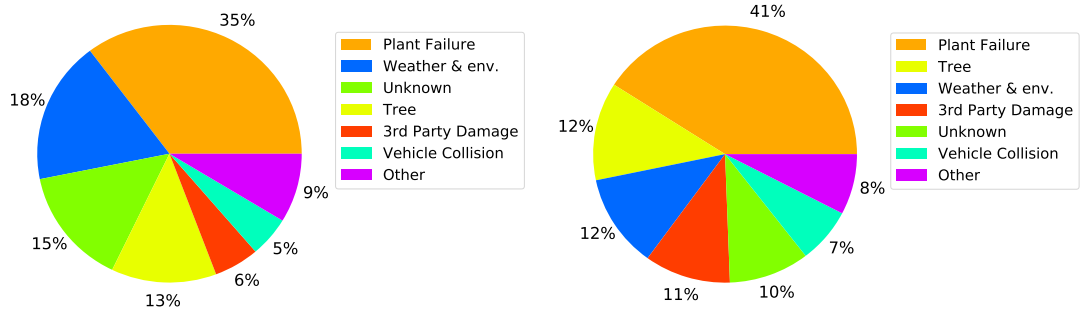


(a) Breakdown of rural cause of failures (b) Breakdown of urban cause of failures

**Figure 2.5** Breakdown of failed assets for urban and rural environments

The first point of note is that unlike the breakdown of affected assets, the results show much less difference between the breakdown in urban and rural environments. This implies that causes of failure are not dependent on the environment, although further analysis is needed to confirm this.

It is clear that a major cause of failure in this database is “Plant Failure”. These failures are those which involve the breakdown of assets due to age and general use. There are a number of reasons why this cause of failure is the most common. One could be that failures due to other causes are well managed, so assets failing due to expected deterioration is more likely. Another reason could be due to the assets not being maintained, so are requiring general repair more often. Assets may be deteriorating faster than expected due to a lack of ongoing care from the utility.

Other prominent causes of failures are Weather and Environment (W&E), “Unknown”, and “Trees”. Weather and environment can be attributed to specific events such as earthquakes or storms. This will become an important area of research in future resilience assessment, to be discussed later. Analysis of specific assets will provide additional insight below. “Unknown” cause of failure refers to outages where the cause

of failure was never confirmed. This situation occurs when the fault was not physically located. An assessment of the lines was undertaken, but the utility was unable to attribute a specific cause to the protection equipment operating. “Tree” as a cause of failure means situations where trees damage the lines or other assets, typically through falling. This mainly effects assets above ground.

As with the affected assets breakdown, there is merit in observing the breakdown of cause of failure over the lifespan of the database. This can be seen in Figure 2.6. The chart shows that there is some variation in W&E as a cause of failure over each two year period. A likely reason behind this fluctuation is storms and other High-Impact Low-Probability (HILP) events which cause W&E failures are sporadic and inconsistent in terms of impact, with differing amounts of damage. All the other causes of failure appear to remain relatively consistent, with “Plant Failure” continuing to dominate in all three charts. It was seen in Figure 2.5 that W&E-caused outages were responsible for a greater proportion of outages in rural environment, therefore having a greater impact. This is most likely due to the fact that overhead lines are more common in the rural distribution. These overhead lines are more exposed to the weather than underground cables, which are used prominently in urban environments. Thus the rural distribution, as shown in this chart, is more likely to be impacted by extreme weather damage than the urban environment.

The problem with W&E (HILP events) as a cause of failure is the variability of the data. This presents a problem because the failures are not predictable, and therefore need to be assessed differently to a cause of failure which is relatively consistent year on year e.g. “Plant Failure”. This presents motivation for resilience assessment, as resilience is a measure which is independent of the severity or the frequency of events. This point will be demonstrated further when MTTR estimation is conducted in Section 2.4.

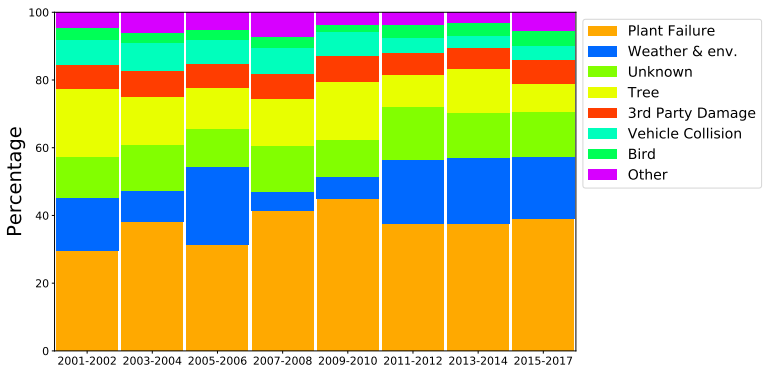


**Figure 2.6** Cause of failure broken down biennually

### 2.3.4 Failure Cause Breakdown of Overhead Lines and Underground Cables

This section considers the failure cause breakdown of two specific important assets - overhead lines and underground cables. The physical differences between overhead lines and underground cables are more relevant in this analysis. Unlike overhead lines, underground cables are less exposed to the weather. This physical quality will contribute to differences in the failure cause breakdowns.

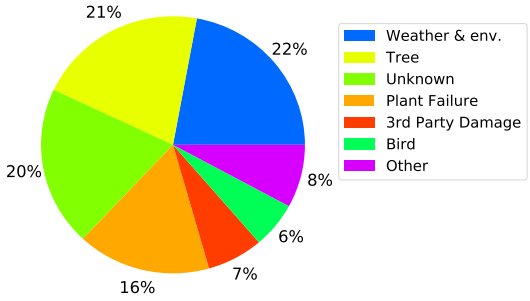


**Figure 2.7** Breakdown of cause of failure for overhead lines in combined urban and rural environments

Overhead lines will be the first specific asset to be discussed. Figure 2.7 represents the cause of failures in overhead lines in both urban and rural environments. Figure 2.8 contains separate rural and urban breakdowns. The charts show that there are four major causes of failure in overhead lines: W&E, “Tree”, “Plant Failure”, and “Unknown”. The proportions of these four categories are relatively similar, however W&E dominates in the overall chart and the rural chart. “Tree” as a cause of failure dominates in the urban environment. A common reason for this is to the urban population not adhering to rules regarding tree trimming, resulting in damage [30]. Further analysis of this is needed to draw more definitive conclusions. “Plant Failure” is less common in the urban environment compared to rural. This could be related to line inspection or line inspection policy, which may favour urban environments because utilities would discover degrading assets before they fail, more often in an urban environment due to higher population density [31].

Underground cables are the other specific asset which will be discussed, as shown in Figure 2.9. The rural and urban charts have been omitted because they are almost identical. Few things can cause an underground cable to fail, which is why they are utilised whenever feasible. W&E has a low proportion of the failure cause breakdown. The greatest proportion in Figure 2.9 is “Plant Failure”, which includes general deterioration and ageing and therefore is unsurprising. The other dominant cause of failure is “3rd Party Damage”. This occurs when, for exapmle, digging equipment damages the underground cables. There does not seem to be a large difference in proportions for urban environments compared with rural environments, although there is a slightly

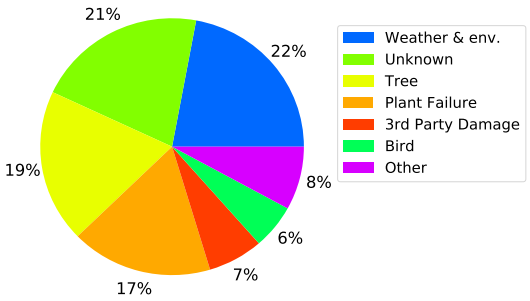


(a) Breakdown of rural cause of failures for overhead lines

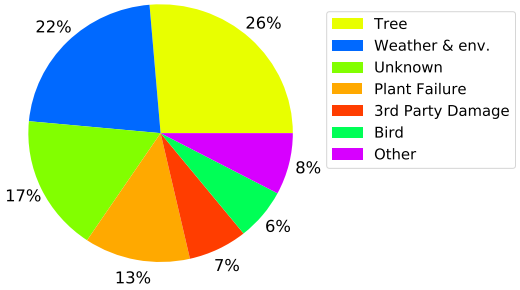


(b) Breakdown of urban cause of failures for overhead lines

**Figure 2.8** Breakdown of cause of failure for lines in urban and rural environments

greater proportion of "3rd Party Damage" in the rural chart.

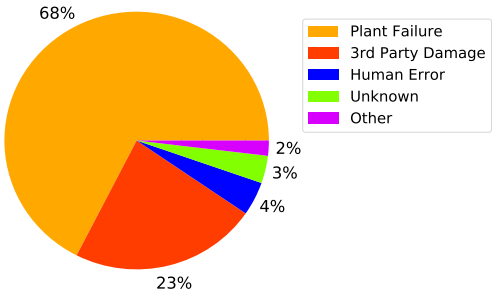


**Figure 2.9** Cable cause of failure for combined urban and rural environments

Although previous sections further analysed the data over time, there was not enough data available to confirm valid results in this situation so temporal charts were not included.

## 2.4 RECOVERY PARAMETERISATION

The focus of analysis will now move to parameter estimation. This section will use the outage data to fit a probability function which can estimate the MTTR of assets, for use in reliability and resilience modelling. The method used fits a range of different distributions to the data, and then evaluates and compares goodness of fit to identify the distribution that fits the data best. This distribution is used to estimate MTTR parameters. The three distributions fit are log-normal, exponential, and Weibull. These have been chosen from a group of well-established and commonly-used distributions [29], with no more than two parameters. These are the only distributions which have been successfully fit to a shape similar to the data. These distributions have been introduced in Background Section 1.3.1.3.

As was seen in the breakdown analysis, specifically in Figure 2.1, overhead lines are

the most prominently failing asset. This makes them the priority in a grid model, because they have the greatest influence on system reliability and availability. Additionally, because they are most common asset type in the data, it also has the highest number of samples, compared to other asset types. This means a better fit for their estimated recovery time distribution.

The amount of samples available within the data has directed the number of results in this section. It was difficult to fit failure data with a reasonable probability distribution when there is fewer than 1000 samples. This is because of the large variance attributed to the data, which will be revealed during the analysis results. The high variance has led to a limitation in the number of parameters which can be generated from the data. Despite this, the work will fit distributions to the main assets seen in the database. These are overhead lines, presented in Section 2.4.2, and underground cables, presented in Section 2.4.3

### 2.4.1 Methodology

Parameter estimation is the process of using statistic inference to assess a sample of data, and constructing a model to represent the data using Maximum Likelihood Estimation (MLE) [29]. This model can be used to represent the system which the data was sampled from. The steps involved are listed below:

1. Identify the focus of the analysis. Select the desired asset, the cause of failure, the environment (rural, urban, or overall), and any other relevant category to be considered.

2. Filter the outage database, to obtain data on specifically desired criterion.

3. Collect the timing values. Time To Recovery (TTR) values can be gathered using the technique described in Section 2.4.1.1 and Time To Failure (TTF) values can be gathered using the technique described in Section 2.5.1.

4. Fit a model data using MLE. This analysis used the Python package Scipy.

5. Assess the Goodness of Fit (GOF) using visual inspection, squared coefficient of variation and sum of squared residuals (SSR). The specifics are detailed in Section 2.4.1.2.

6. Extract requested parameters from the fit distribution.

The main two parameters needed from this analysis are MTTF and MTTR, which are the mean values of the fit distributions.

#### 2.4.1.1 Obtaining Time To Recover Values

The overall process of collecting TTR values is to gather the temporal differences, specifically the difference in time of failure and time of recovery. Within the outage database, each row represents an outage sample. Each sample contains the time when the outage began, and when the outage ended. Between these two times, the entire recovery process is performed. The length of this time is the TTR.

Once these values are obtained, they are fit with probability distributions. The best fitting distribution will be used to estimate the expected time that the system will take to recover. It should be noted that momentary or sustained outages can be differentiated through the use of filtering at this stage. The distinction and relevance of the two has been covered in Section 1.3.1.2.

#### 2.4.1.2 Goodness of Fit Testing Methods

Analysis in this chapter of work involves working with a large quantity of sampled data, and attempting to fit continuous distributions. The data itself is extremely variant (large standard deviation (SD)), however for most of the data there is a significant concentration at the mean, but also a number of outages with a much longer duration.

The difference between data and estimated distribution (i.e. the hypothesis) is measured by the p-value and the estimated distribution is constructed using an estimator. Consistent estimators have errors which shrink when sample-size increases. However, as sample size grows, the standard error becomes very small. The result is that even minuscule distances between the estimator and the null hypothesis become statistically significant [49]. Futhermore, simple GOF tests such as the $\chi$-squared test will fail because each of the chosen models have too few parameters to account for the complexity of real-life data, in such a large quantity. Using distributions with a higher number of parameters to fit the data is not feasible for this application, because stochastic modelling with these models is computationally expensive and complex [29].

Regardless of this, the purpose of this chapter of work is to fit a distribution which best represents that data. It is important to state that this is not the same as finding the distribution which the data follows. This purpose therefore means that the overall goal is identifying the best probability distribution available from the selection which can be used to represent the data reasonably enough to model it.

The two analytical methods will be used to compare the fit of each distribution, as well as visual inspection. The first being assessment of the squared coefficient of variation ($C^2$), and secondly by calculation the SSR, also known as the mean squared error.

The first method, $C^2$ is calculated as the squared ratio of the mean to the SD. For

the sample data, this is calculated as:

$$C^2 = \frac{\bar{X}^2}{\sigma^2}. \tag{2.1}$$

$C^2$ is a value commonly used to express the variability and is defined as the squared SD divided by the squared mean. It can be used as a measure of variability instead of the SD or variance because it has been normalised by the mean, and thus can be compared to among different distributions with different means [29, 50].

The second way of comparing the fit distributions will be observing the SSR. The SSR for distribution $f$ will be calculated as:

$$SSR_f = \sum_i \frac{N_i - np_{fi}\Delta x}{np_{fi}\Delta x} \tag{2.2}$$

for $i$ bins of width $\Delta x$. Where $n$ is the total number of samples, $N_i$ is the number of counts in bin $i$ and $p_{fi}$ is a probability value for bin $i$, based on the fit distribution. This method is summarised as calculating the sum of squared errors for a fit distribution and its data. This is a useful a method of comparing two distributions to calculate which fits the given dataset best. The SSR for each and then compared comparing them. Accompanied with visual inspection, this method can be used to obtain an estimate of parameters.

### 2.4.2 Overhead Line Recovery Parameter Estimation

The first asset to be considered is the overhead line. This has the highest number of samples in the outage database, indicating that overhead lines are the most likely to fail assets in the distribution grid. The large number of samples is beneficial because it allows for a higher quality fit distribution, as will be shown in the section.

Initially, the TTR of all line outage samples were collated and the three distributions were fit using MLE. This can be seen in Figure 2.10. The generated MTTR values and goodness of fit results can be seen in Table 2.2. Of the three possible distributions, the log-normal is the best-fitting solution. Visually, this fit appears to be mediocre, the reason being that W&E as a cause of failure degrades the results. The MTTR of 256 minutes (around 4.3 hours) is an unexpectedly large value. The reason and rectification of this is presented shortly. Additionally, the SD of the result is very high, reflecting the high variability of this data.

The exponential distribution is the worst fitting. This is because by its definition it always has a $C^2 = 1$, and hence cannot account for variability seen in the data. The best fitting distribution, and the on which matches the variability of the data is the log-normal distribution, however visual inspection confirms that it is not a good fit. Overall, this initial result is not sufficient. Additional adjustments will now be made to

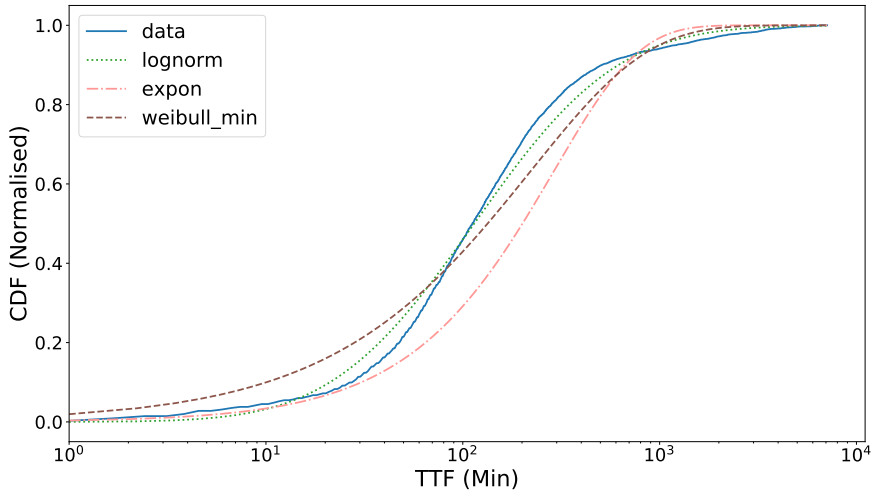


**Figure 2.10** Overhead line outage recovery data plotted as an empirical Cumulative Density Function (CDF), along with three fit probability distributions.

| | **MTTR (min)** | **SD** | $C^2$ | **SSR** |
|---|---|---|---|---|
| **Sample Data** | 290 | 648 | 0.2005 | - |
| **Log-Normal** | 256 | 490 | 0.2732 | 4.89E+13 |
| **Exponential** | 290 | 289 | 1.0000 | 4.99E+19 |
| **Weibull** | 305 | 522 | 0.3415 | 5.63E+13 |

**Table 2.2** Overhead line outage recovery data results for the three fit distributions.

the data to produce better results.

Outages caused by W&E, often during HILP events, are unlike other causes of failure for several reasons. These are as follows:

- Failures all occur in relatively short periods of time, thus are clustered together in time.
- The number of outages is directly related to the severity of the event.
- The clustering makes the number of W&E failures differ over time periods. In Figure 2.6, it was seen that some 2-year periods had more than 5 times as many W&E-caused outages than other periods.
- When W&E events occur, often utilities are unable to progress recovery or conduct repairs as it is unsafe to deploy operators. This adds additional delay to durations. It is also a key motivator for Distribution Automation (DA).

Collectively, these differences mean that W&E-related outages tend to not follow the same trends as other causes. [46] confirms this finding, where it states that W&E is the most prominent reasons for the variability in recovery time. Due to this, the resulting distribution shown in Figure 2.10 is not an ideal solution, and a better one can be produced if W&E-caused outages are omitted and assessed separately.

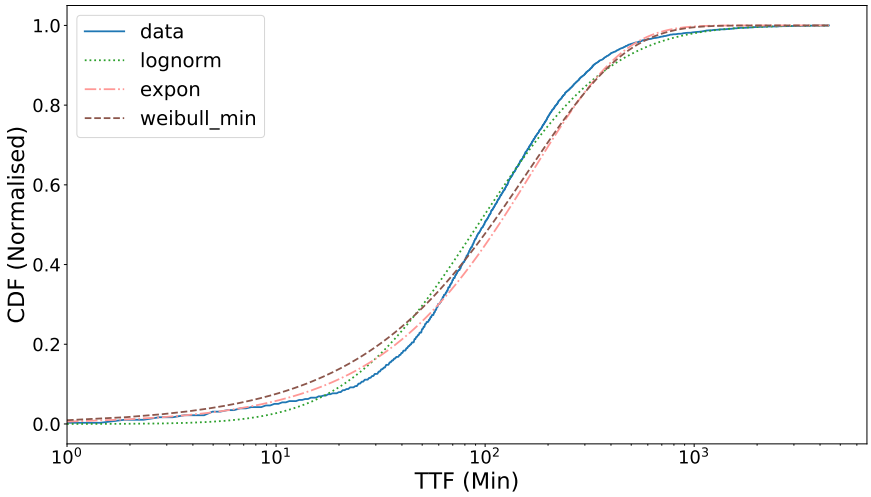


**Figure 2.11** Overhead line outage recovery data, excluding Weather and Environment related outages, plotted as an empirical CDF, along with three fit probability distributions.

| | **MTTR (min)** | **SD** | $C^2$ | **SSR** |
|---|---|---|---|---|
| **Sample Data** | 168 | 266 | 0.3967 | - |
| **Log-Normal** | 162 | 208 | 0.6066 | 7.53E+13 |
| **Exponential** | 168 | 167 | 1.0000 | 4.99E+19 |
| **Weibull** | 167 | 182 | 0.8351 | 2.77E+17 |

**Table 2.3** Overhead line outage recovery data, excluding weather and environment related outages, results for the three fit distributions.

The results for fitting the data with W&E-caused outages removed can be seen in Figure 2.11 and Table 2.3. The log-normal has the lowest SSR value, and visual inspection reveals it is the best fit. This result is superior to the previous, and overall a satisfactory one. The estimated MTTR of 162 minutes (2.70 hours) and SD of 208. Though this result is favourable, it is important to assess how the MTTR of lines change in rural and urban environments. Log-normal is clearly the best fit when compared to the other distributions, however it still doesn't capture the variability that the data contains. This is evident because that SD and therefore $C^2$ still remain high.

The rural distribution fit is shown in Figure 2.12, with results in Table 2.4. The MTTR generated by this distribution is 169, which is similar to that of the sample data. The $C^2$ is 0.5612, which slightly larger than the sample data.

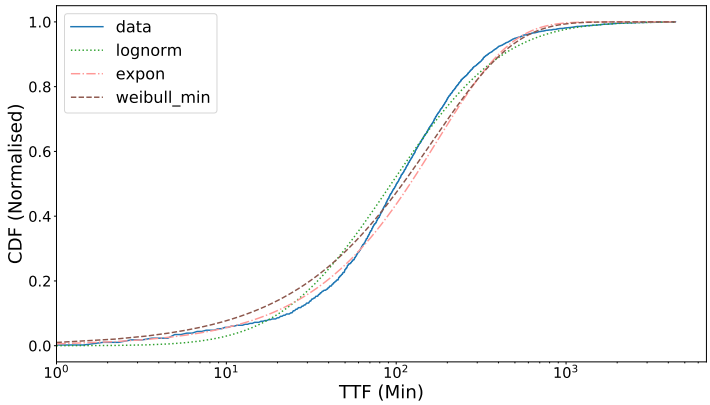


**Figure 2.12** Rural overhead line outage recovery data, excluding Weather and Environment related outages, plotted as an empirical CDF, along with three fit probability distribution.

| Best Model | Log-Normal |
|---|---|
| MTTR | 169 min |
| SD | 226 |
| $C^2$ | 0.5612 |
| SSR | 3.97E+13 |

**Table 2.4** Rural overhead line outage recovery data, excluding weather and environment related outages, results for the best fitting distributions.

The final result to assess here is the distribution of recovery for outages in the urban distribution grid. This can be seen in Figure 2.13 and the results are collected in Table 2.5. The MTTR and SD are 141 minutes and 157 respectively. Visual inspection reveals that this fit is better than the exponential and Weibull distributions.

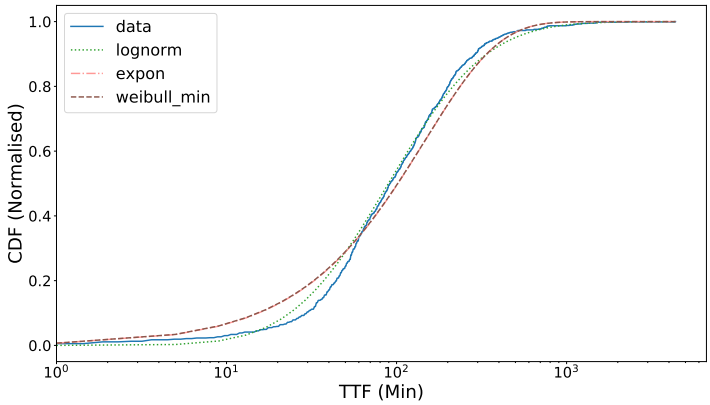


**Figure 2.13** Urban overhead line outage recovery data, excluding Weather and Environment related outages, plotted as an empirical CDF, along with three fit probability distribution.

| Best Model | Log-Normal |
|---|---|
| MTTR | 141 min |
| SD | 158 |
| $C^2$ | 0.8091 |
| SSR | 9.31E+13 |

**Table 2.5** Urban overhead line outage recovery data, excluding weather and environment related outages, results for the best fitting distributions.

It is clear that there is some difference between the MTTR results for rural and urban systems, not sufficiently explained by the lower-quality fit seen for the urban case. It is likely that this difference is due to the difference in geography seen in these two environments. As has been mentioned, urban environments can cover a smaller area. The result of this is that the area needed to search to locate an outage is generally smaller. Additionally, crews require less of a commute to reach an outage. It is reasonable that the 27 minutes difference is due to these factors. Also, the smaller geography could also explain the smaller SD in the urban result. There is less distance to cover in urban areas, thus the difference between the closest fault and the furtherest is smaller, hence a smaller variation in the result.

| | Model | MTTR (min) | SD |
|---|---|---|---|
| Both Env. | Log-Normal | 162 | 208 |
| Rural | Log-Normal | 169 | 226 |
| Urban | Log-Normal | 142 | 158 |

**Table 2.6** Overhead line outage recovery collected overall, rural and urban environment best fit results. All are excluding outages caused by the weather and environment.

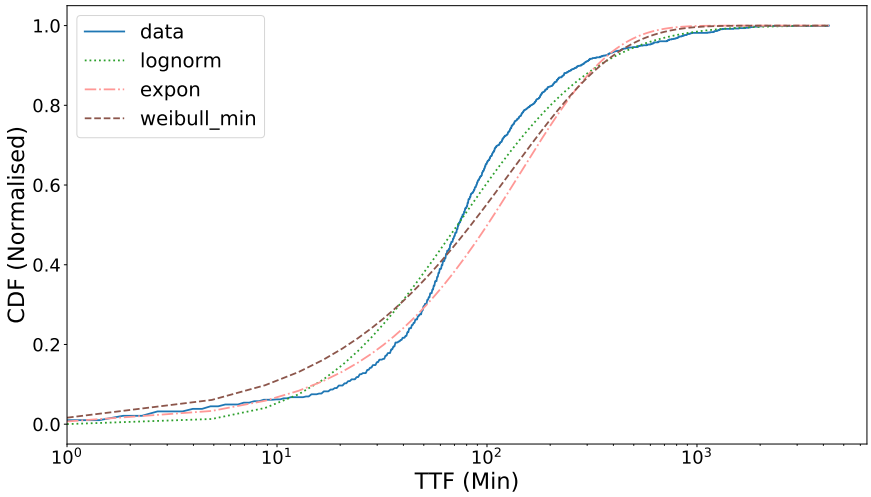


**Figure 2.14** Underground cable outage recovery data, excluding Weather and Environment related outages, plotted as an empirical CDF, along with three fit probability distributions.

Overall, the fits for these three results present useful repair times which can be used in later modelling. A summary of the results presented in this section can be seen in Table 2.6. All of the curves are best fit with log-normal curves.

### 2.4.3 Underground Cable Recovery Parameter Estimation

The next asset to be considered is underground cables. This asset has the second highest number of samples in the outage database. Despite this, there are only around 1000 samples, and so it is difficult to obtain accurate results. This section will analyse cable outages are not cause by W&E events. The reasoning for this is the same as that explained in Section 2.4.2, W&E-caused outages have too many additional external factors which influence them, compared to all other outage causes.

| | MTTR (min) | SD | $C^2$ | SSR |
|---|---|---|---|---|
| **Sample Data** | 144 | 262 | 0.3052 | - |
| **Log-Normal** | 133 | 186 | 0.5176 | 1.84E+13 |
| **Exponential** | 144 | 144 | 1.0000 | 2.34E+13 |
| **Weibull** | 137 | 160 | 0.7429 | 6.16E+13 |

**Table 2.7** Underground cable outage recovery data, excluding weather and environment related outages, results for the three fit distributions.

The fit distributions for the cable TTR data can be seen in Figure 2.14, with results in Table 2.7. The best fitting probability distribution is the log-normal distribution, based on comparison of both of the p-values and the $C^2$ value to other distributions. The MTTR estimated based on generated distribution is 133, with SD 186. As with overhead lines, the SD is very large, attributing to the many factors which influence the TTR. It's immediately clear that this is not as well fitted the results in the previous section. As was previously mentioned, the low number of samples has greatly affected the quality of the result. The goal therefore, is to find the best distribution available, in able to estimate a value for cable MTTR.

With regards to the results, the repair time of cables is clearly smaller than that of lines. At first glance, this may appear to be counter-intuitive, but after discussion with engineers at utility managing this system, it was clear that this is an expected result. The first reason is because in a many cases when a cable fails, it's immediately obvious and the customer is aware they have done the damage, for example when a cable is damage during excavation. As we saw in Figure 2.9, around 25% of cable failures are related to human interaction. In most cases, the culprit quickly contacts the utility, revealing the location. Secondly for other cases where the cable failed due to cause "Plant Failure", locating the section of cable where the cable occurred is easier than that of overhead lines. This is due to generally more sensors and detection being deployed for cable networks, as they tend to serve densely populated areas. Finally, cables are laid in a relatively dense mesh, so the search area is generally smaller when a section of grid is identified. This means technology such as heat sensors and pulse reflection equipment can be used with relative ease to locate the failed cable [30].

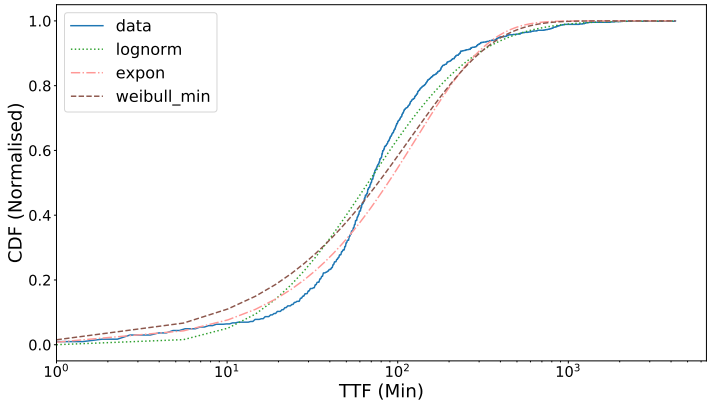


**Figure 2.15** Urban underground cable outage recovery data, excluding Weather and Environment related outages, plotted as an empirical CDF, along with three fit probability distributions.

| Best Model | Log-Normal |
|---|---|
| MTTR | 117 min |
| SD | 149 |
| $C^2$ | 0.6169 |
| SSR | 4.96E+13 |

**Table 2.8** Urban underground cable outage recovery data, excluding weather and environment related outages, results for the best fitting distributions.

The underground cable recovery times will now be evaluated for for cables within the urban environment of the distribution grid. Rural cannot be assessed in this way however, as there are very few samples available to fit. This is due to cables being much more practical in urban environments, as has previously been discussed.

The empirical data CDF and the fit distributions are presented in Figure 2.15, with fitting results show in Table 2.8. As with previous recovery parameters, the log-normal distribution is the best fit for this data. This distribution estimates an MTTR of 117 and SD of 149. This MTTR value is somewhat smaller than the sample data. This aligns with the results for overhead lines, where the urban MTTR was shorter than the rural, and overall. The expected reasoning for this is that urban outages occur in a smaller area, reducing the time to commute to the outage.

The overall results for cable recovery parameters are given in Table 2.9. For both the successful fit conditions, the log-normal curve is the best fitting probability distribution, as was the case with the overhead lines. In comparison with the results for overhead lines, the MTTR values are shorter in all cases, which is not an intuitive result. Despite this, discussion with the utility reveals that these results are feasible.

## 2.5 FAILURE PARAMETERISATION

The next stage of this chapter will present methods to estimate and evaluate the MTTF values of assets within a distribution grid using the outage data. This section will utilise TTF values for the purpose of generating MTTF values which can be used to model the failure rates. As with recovery parameterisation, analysis will focus on the two main components of interest, the overhead lines and the underground cables. Analysis of other components will be left for future work, as it will require a larger dataset, with a sufficient number of outages affecting other assets of interest. The output of this analysis will be the MTTR value estimated from the data, as well as additional parameters required to model using the fitted probability distribution.

Unlike the previous section, the data used will not have weather and environment related outages filtered out. This is because regular failures and weather and environment outages are not independent, because the TTF observes the timing differences between two separate outages. This is an acceptable result when considering that weather and environment events are likely to break assets which are weakening due to age or other conditions, and conversely, weather and environment events can damage assets so they are likely to fail sooner than they would otherwise.

The process for collecting these TTF values, outlined in Section 2.5.1, is different than the process for obtaining TTR values. The differences in the process have led to two important effects on the data available for this part of analysis. Firstly, there are

| | **Model** | **MTTR (min)** | **SD** |
|---|---|---|---|
| Both Env. | Log-Normal | 133 | 186 |
| Urban | Log-Normal | 117 | 149 |

**Table 2.9** Underground cable collected overall and urban environment best fit results. All are excluding outages caused by the weather and environment

fewer data samples. This means fewer available data to fit. Secondly, the samples are collected at a feeder-by-feeder basis.

### 2.5.1 Obtaining Time To Failure Values

The process of fitting distributions to estimate MTTF is similar to that of MTTR. The primary difference is the means of obtaining the data. This process is different to the TTR process detailed in Section 2.4.1.1 because it involves collecting the times between outages, while collecting TTR values requires only collecting the duration of each outage from the data.

TTF is the length of time between the start of an outage, and the start of the next outage [29]. This is collected from the database by calculating the difference in time between one outage sample and the next. Asset outages are heavily dependent on their environment. However, distribution grids span multiple different environments and therefore it is not valid to look at the timing difference between one outage and the next from the system perspective. This complicates the process, as TTF values must be gathered one feeder at a time. The procedure requires gathering all outages from each individual feeder, and then obtaining the difference in time between each chronologically ordered outage sample, for each feeder. These values are the TTF.

An issue that arises from the need to collect values feeder-by-feeder is that a smaller number of samples are available. Each feeder has $N$ outages and this it is only possible to obtain $N - 1$ TTF values. The reason for this is because there is a need to avoid using censored data. Censored data is data of which only a single bound of the lifetime is known [35]. Avoiding censored data can enhance the quality of the fit distribution, but means fewer data are available.

### 2.5.2 Weibull-Distributed Failure Rates

The Weibull distribution is a favourable result for failure modelling. It is a common result for capturing the failure pattern of a system [30]. The reasoning for this is it is able to accurately model the failure rate of an asset with it's shape parameter. The shape parameter can be defined to represent an increasing, decreasing or constant failure rate. Therefore, the Weibull distributioncan represent components at any stage of the asset lifecycle [29, 35].

The failure rate, (sometimes refereed to as the hazard function) of a Weibull distribution is related to it's Probability Density Function (PDF) (shown in Equation 1.15). This failure rate function is defined as,

$$h(t) = \lambda \alpha t^{\alpha - 1} \tag{2.3}$$

| **Asset** | **Env** | $\hat{\alpha}$ | $\hat{\lambda}$ |
|---|---|---|---|
| Line | Both | 0.6035 | 9.610E-03 |
| Line | Rural | 0.6139 | 9.388E-03 |
| Line | Urban | 0.5908 | 8.874E-03 |
| Cable | Both | 0.6013 | 3.850E-03 |
| Cable | Urban | 0.6191 | 3.261E-03 |

**Table 2.10** Weibull distribution parameter estimates for results from Section 2.5

The shape of this function is largely dependent on the shape parameter, $\alpha$. $\alpha$ affects $h(t)$ in the following ways:

- $\alpha < 1$: $h(t)$ decreasing at a decreasing rate
- $\alpha = 1$: $h(t)$ constant
- $1 < \alpha < 2$: $h(t)$ increasing at a decreasing rate
- $\alpha = 2$: $h(t)$ increasing

The parameters taken from the distributions in Section 2.5 are defined in Table 2.10. The shape parameter for all these distributions shows that the estimated failure rate for all of these distributions is decreasing, at a decreasing rate.

### 2.5.3 Overhead Line Failure Parameter Estimation

The first asset to be assessed will be the overhead line. It was shown in the asset breakdown analysis that these are the most commonly failing asset, and therefore the most prominent in the data. As was the case in the recovery analysis, this is beneficial for these purposes because there is the most data available for outages with these assets, allowing for a more accurate distribution.

The empirical PDF and the CDF of the fit distributions are presented in Figure 2.16. The results of these fits are shown in Table 2.11. It is clear immediately that the exponential distribution is the worst of the three, again not being able to capture the variability which is represented by its $C^2$ parameter. By visual inspection, both the log-normal and the Weibull have a reasonable fit. However, the log-normal greatly overestimates the variation in the data, and thus has a much lower $C^2$ than the Weibull distribution, and the data itself. Together, both of these factors imply that Weibull is the be fitting result. Furthermore, it was explained in Section 2.5.2 that the Weibull distribution is a more appropriate distribution for failure rates, so this will be favoured.

The Weibull distribution estimates the feeder MTTF of 3288 hours (0.37 years) and a SD is 5738. This value represents the MTTF of a feeder, caused by overhead lines. To further evaluate this result, it must be put into context, based on the methods used to obtain it. The TTF values were gathered on a feeder-by-feeder basis (see Section 2.5.1),

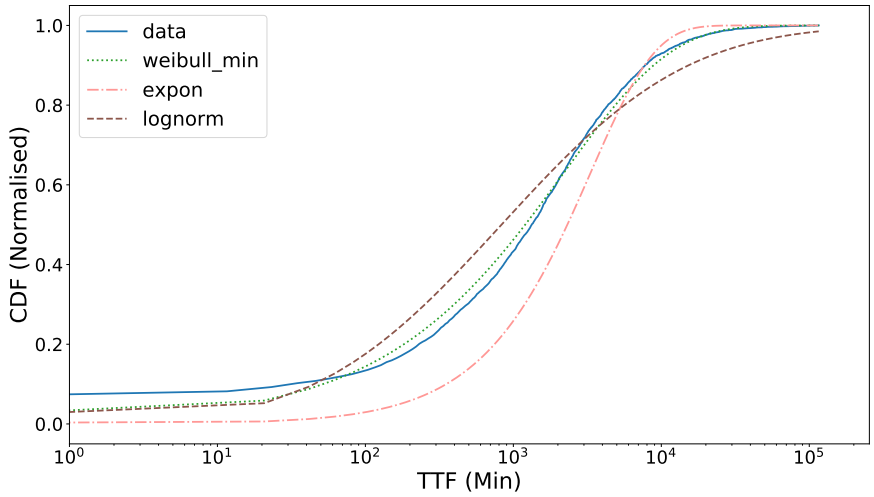


**Figure 2.16** Overhead line time to failure data plotted as an empirical CDF, together with three fit probability distributions.

and as such the resulting distribution represents the MTTF, of any feeder in the overall system, on average.

| | **MTTF (hr)** | **SD** | $C^2$ | **SSR** |
|---|---|---|---|---|
| **Sample Data** | 3298 | 6737 | 0.2395 | - |
| **Log-Normal** | 4962 | 23845 | 0.0433 | 6.46E+15 |
| **Exponential** | 3298 | 3298 | 1.0000 | 1.47E+26 |
| **Weibull** | 3288 | 5738 | 0.3282 | 5.41E+15 |

**Table 2.11** Overhead line time to failure data results for the three fit distributions.

The next item to discuss is rural overhead line TTF as seen in Figure 2.17 with results in Table 2.12. As with the previous dataset, the Weibull distribution is the best fit for this. The MTTF generated for this distribution is 2932 hours (0.34 years) per feeder with SD 5012. The MTTF in this situation is somewhat shorter than in the previous result. This implies that the MTTF of rural feeders in the system is shorter than the sample data and urban case.

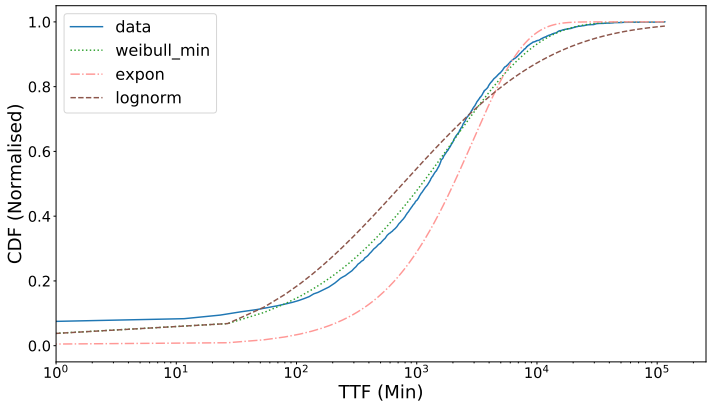


**Figure 2.17** Rural overhead line time to failure data plotted as an empirical CDF, along with three fit probability distribution.

| Best Model | Weibull |
|---|---|
| MTTF | 2932 hr |
| SD | 5012 |
| $C^2$ | 0.3423 |
| SSR | 6.09E+16 |

**Table 2.12** Rural overhead line time to failure data fitting results for the best fitting distributions.

The final overhead line TTF data fit is the urban environment. The empirical CDF and the three fit distributions are shown in Figure 2.18, with results given in Table 2.13. A Weibull distribution is again the most appropriate distribution for this data.

The estimated MTTF from the Weibull distribution is 4563 hours (0.52 years). This is greater than both the rural and overall datasets, as expected. This result shows that there are less overhead line failures in the urban distribution grid, however it does not necessarily mean that the urban grid is more reliable. Context, in the form of data about the quantity of overhead lines contained in each of these environments, is required in order to compare the reliability of each.

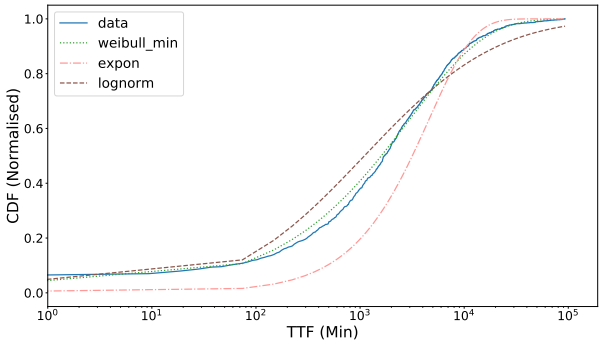


**Figure 2.18** Urban overhead line time to failure data plotted as an empirical CDF, along with three fit probability distribution.

| Best Model | Weibull |
|---|---|
| MTTF (hr) | 4563 |
| SD | 8180 |
| $C^2$ | 0.3112 |
| SSR | 8.53E+14 |

**Table 2.13** Urban overhead line time to failure data fitting results for the best fitting distributions.

### 2.5.4 Underground Cable Failure Parameter Estimation

This section will attempt to fit the underground cables with an MTTF value. There is fewer data for this perspective, and as such, the results cannot be confirmed as accurate as the previous. The empirical data CDF, and the three fit distributions, are shown in Figure 2.19, results can be seen in Table 2.14.

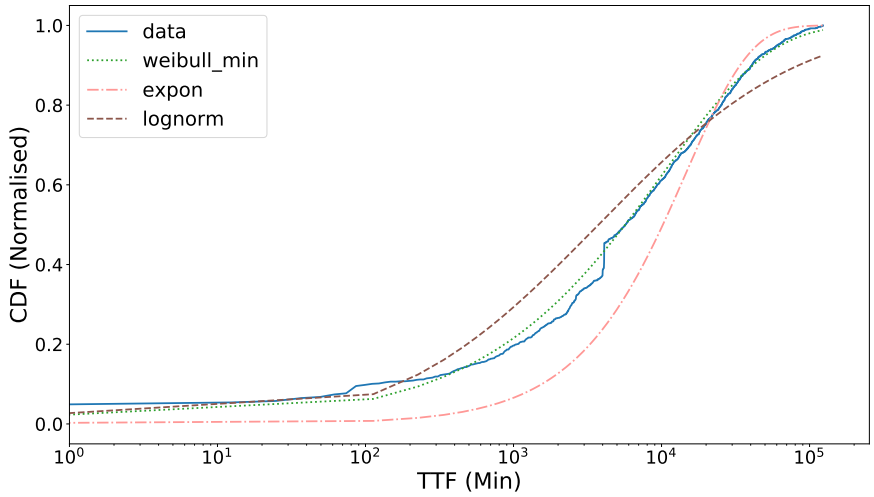


**Figure 2.19** Underground cable time to failure data plotted as an empirical CDF, together with three fit probability distributions.

| | MTTF (hr) | SD | $C^2$ | SSR |
|---|---|---|---|---|
| **Sample Data** | 14751 | 20820 | 0.5020 | - |
| **Log-Normal** | 28440 | 175553 | 0.0262 | 1.23E+14 |
| **Exponential** | 14751 | 14751 | 1.0000 | 1.13E+15 |
| **Weibull** | 25628 | 46285 | 0.3066 | 7.41E+13 |

**Table 2.14** Underground cable time to failure data results for the three fit distributions.

It is immediately clear from this result that visually, the data is not very favourable to fit. The Weibull is the best of the three, but the empirical CDF appears slightly jagged, which makes the fit less true to the data. The estimated MTTF value for this fit distribution is 25628 hours (2.93 years), with a SD of 46285 hours. Based on this, it is clear that the cable failure rate is significantly lower than that of overhead lines.

The final cable data to be evaluated will be that of the urban distribution grid. It was observed in Figure 2.2 that cables are significantly more dominant in this environment compared to the rural environment, and the discussion of this figure justified this claim. There was also insufficient data to conduct analysis on rural underground cable. The empirical CDF and fitted probability distributions can be seen in Figure 2.20 and the results in Table 2.15.

The the best fit distribution for this data is the Weibull distribution. This estimates a MTTF of 14566, and a SD of 24159. This result is notably similar to that of the sample data distribution. The overall results for fitting underground cables can be seen in Table 2.16.

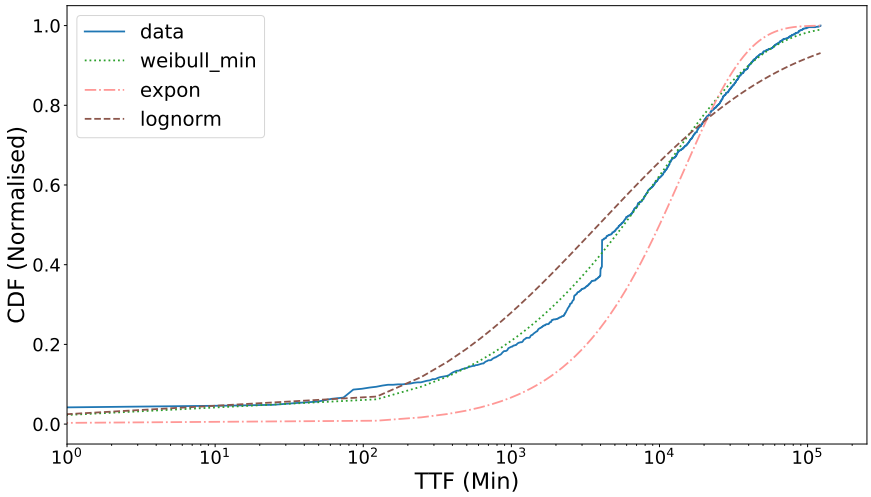


**Figure 2.20** Urban underground cable time to failure data plotted as an empirical CDF, together with three fit probability distributions.

| | MTTF (hr) | SD | $C^2$ | SSR |
|---|---|---|---|---|
| **Sample Data** | 14438 | 20207 | 0.5106 | - |
| **Log-Normal** | 28440 | 175553 | 0.0262 | 1.23E+14 |
| **Exponential** | 14751 | 14751 | 1.0000 | 1.13E+15 |
| **Weibull** | 14566 | 24159 | 0.3635 | 1.52E+14 |

**Table 2.15** Underground cable time to failure data results for the three fit distributions.

| | Model | MTTR (hr) | SD |
|---|---|---|---|
| Both Env. | Weibull | 14751 | 20820 |
| Urban | Weibull | 14566 | 20207 |

**Table 2.16** Underground cable time to failure collected overall, rural and urban environment best fit results.

## 2.6 RESILIENCE ASSESSMENT

### 2.6.1 Introduction

The previous work in this case study has been concentrated on the performance of the distribution grid on a day-to-day basis. This was done by first assessing proportions of affected assets, as well as failure cause. Following this, recovery and failure performance was assessed using statistical inference through parameter estimation. These methods are all based on the goal of reliability evaluation. This section aims to complete the analysis of the outage database by evaluating the performance from the perspective of resilience. It will look at the events which are outside of normal, predictable range, known as HILP events. This analysis aims to provide a high-level assessment of the resilience of the distribution grid, based on only the data provided in the outage database.

Resiliency is a measure of how a system can withstand and recover from unpredictable HILP events. To quantify resilience, it is shown in previous work, and discussed in Chapter 1, that introducing parametric or structure the changes to a system which are well outside of normal range produced changes to system parameters which can be quantified, thus quantifying resilience. However, this is method is analytical, and requires a model which is developed in later sections.

At this point in analysis, it is desirable to assess the resilience of the system based soley on the available outage data. This can be considered a preliminary analysis to what will be a more detail approach in later sections. A similar, but empirical version of the resilience quantification can be conducted with this data. HILP events are events which can be generally thought of as outside of normal range, and these events affect the standard parameters (such as MTTR) of the system. Thus the MTTR during HILP events can be a reasonable quantification of resilience, by observing how the overall component MTTR changes when these events occur. A smaller change in MTTR represents a more resilient system. This section will conduct this quantification by looking at the differences in recovery rates, specifically during W&E events - ones considered unpredictable and often substantial, thus qualifying as HILP.

It was presented in Section 2.4 that outages caused by W&E are different from other outage types, and inclusion caused in a a poor result. The work of [4] presented a similar analysis by inspecting the down time (DT) durations during Super Storm Sandy. This stage of analysis will specifically look at recovery outages with this cause, and contrast the difference to the recovery of other causes. Rural and Urban environments will be separated too, as this distinction is still relevant at this point in analysis. The specific asset which will be analysed is the overhead line. Underground cables will not be analysed because the outage data used contained only a small number W&E-caused failures for cables, as shown in Figure 2.9.

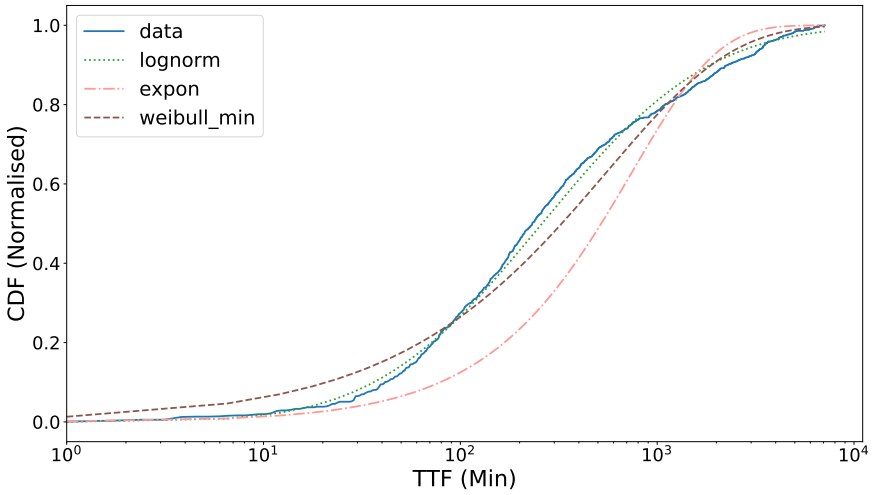


**Figure 2.21** Overhead line outage recovery data for Weather and Environment-caused outages, plotted as an empirical CDF, together with three fit probability distributions.

For the analysis itself, the data is collected and parameterised in the same way as the recovery data. The only difference is that all outages which have not been caused by HILP events have been filtered out. The fit distributions will now be presented and evaluated.

### 2.6.2 Overhead Line Overall Analysis

The plotted data's empirical CDF, as well as the three fit distributions can be seen in Figure 2.21. Results for the fitting can be seen in Table 2.17. As with the previous recovery results, the best-fitting distribution for this data is Log-normal distribution.

| | **MTTR (min)** | **SD** | $C^2$ | **SSR** |
|---|---|---|---|---|
| **Sample Data** | 750 | 1204 | 0.3877 | - |
| **Log-Normal** | 824 | 2450 | 0.1132 | 8.05E+11 |
| **Exponential** | 750 | 750 | 1.0000 | 1.08E+13 |
| **Weibull** | 660 | 990 | 0.4445 | 1.44E+12 |

**Table 2.17** Overhead line outage recovery data for W&E-caused outages results for the three fit distributions.

The fitted Log-normal distribution estimates an MTTR of 824 mins (13.7 hours), with an SD of 2450. This result shows that the MTTR is much larger for outages of this type. There are a number of possible reasons for this. Firstly, generally speaking, a large portion of these outages are either severe storms or lightning. In both of these cases it is not safe to deploy crew to begin reconfiguration and repairs until the worst of it has subsided. This is an area where DA can aid significantly. Secondly, there is generally a high number of outages in a short period of time during these events, thus the utility must prioritise some outages. This would greatly increase the MTTR during

these events.

Another significant feature of the resulting distribution is the large SD compared to the MTTR. It has been observed in most previous results that the SD is relatively large, attributed to the large amount of variables which influence the recovery time, including location, severity and how difficult the outage is to locate. The $C^2$ of this distribution is much smaller than previous results however, emphasising a larger-still variation. The reason for this is likely to only partially due to the reasons which the cause the amount of variation seen in previous results. The main reason for this variation is likely to be the variation of impact of W&E events. Many factors influence the impact of an HILP event on a system, such as frequency, location and duration. All of these factors can have a large influence on the resulting recovery time and therefore the amount of variation is likely to be large.

The final feature to note from this distribution is the quality of fit, despite the small number of samples. This quality of fit implies that though occurrence of HILP events is unpredictable, the recovery time seems to follow the an established model fairly well.

### 2.6.3 Overhead Line Rural and Urban Analysis

The analysis will now compare the outages of urban and rural environments for overhead lines. It is likely that the urban part of a distribution grid will have a smaller SD (and thus larger $C^2$) compared to the rural case. This is predicted based on the previous data, and due to the rural grid features of a large-spanning area and more exposure to storms and events. It is also predicted that the urban grid will have smaller MTTR, due to the population supplied making outages a priority, and also due to the urban grid's smaller and more meshed area.

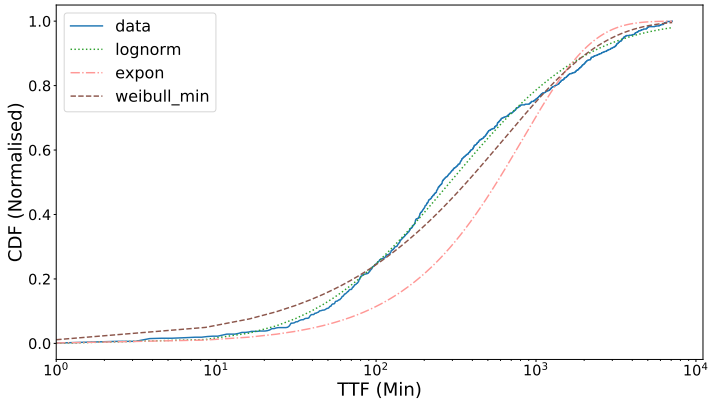


**Figure 2.22** Rural overhead line outage recovery data for Weather and Environment-caused outages, plotted as an empirical CDF, along with three fit probability distributions.

| Best Model | Log-normal |
|---|---|
| MTTR | 925 min |
| SD | 2795 |
| $C^2$ | 0.1119 |
| SSR | 5.02E+11 |

**Table 2.18** Rural overhead line outage recovery data for Weather and Environment-caused outages fitting results for the best fitting distributions.

The first of these two cases is the Rural environment. The plotted data's empirical CDF, as well as the three fit distributions can be seen in Figure 2.22. Results for the

fitting can be seen in Table 2.18. As with the previous recovery results, the best-fitting distribution for this data is Log-normal distribution.

The MTTR of the the rural overhead lines for outages due weather or other environmental causes is estimated by the fit distribution to be 925 minutes (15.42 hours). The SD of this is 2795. The first point to note is that the MTTR is very high - much higher than the sample data. Additionally, the $C^2$ is also very small, due to the large SD relative to the MTTR. This suggests that the outage data has a significant amount of variation, a point which has been seen in previous results. This supports the interpretation that there rural environment's larger area compared to the urban case makes the TTR more variate.

The fit of the distribution is relatively good compared to previous results, especially considering that there is a limited number of data available for this perspective. Overall, this result highlights the previous points, that rural distributions have a high variance, and that MTTR is higher than the urban case.

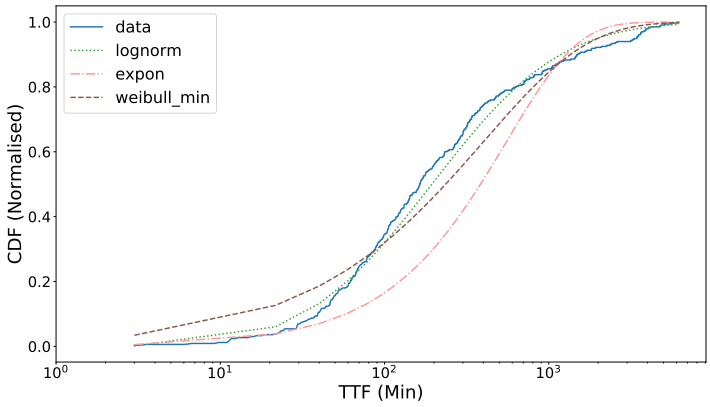


**Figure 2.23** Urban overhead line outage recovery data for Weather and Environment-caused outages, plotted as an empirical CDF, along with three fit probability distributions.

| Best Model | Log-normal |
|---|---|
| MTTR | 536 min |
| SD | 554 |
| $C^2$ | 0.3111 |
| SSR | 2.60E+11 |

**Table 2.19** Urban overhead line outage recovery data for Weather and Environment-caused outages fitting results for the best fitting distributions.

The second of the two cases is the Urban environment. The plotted data's empirical CDF, as well as the three fit distributions can be seen in Figure 2.22. Results for the fitting can be seen in Table 2.18. As with the previous recovery results, the best-fitting distribution for this data is Log-normal distribution.

The fitted log-normal distribution estimates an MTTR of this 536 minutes (8.93 hours), with a SD of 554. The urban environment produces a lower MTTR than the rural environment. The SD is also significantly smaller, as predicted earlier. This could be attributed to a geographically smaller area which contains the failed overhead lines. The fit of the distribution itself is reasonable, especially considering the limited number of data the was available. The main two points of note from these results agrees with the previous results. First, the urban distribution fit has a smaller variance than the rural distribution. Second, the MTTR is lower than in an rural distribution.

Comparing these distributions together, it's clear that there are significant differences in the recovery process. This is likely due to two key factors. Rural distribution grids are exposed and span large areas. Urban distribution grids are much more dense, and much more sheltered but surrounding buildings and other infrastructure. Additionally, it is likely that the urban grid has a higher priority, due to more customers being supplied by them, and also due to more priority services such as emergency and communications services being dependent on it. It is also confirmed that the urban grid TTR has smaller variation.

### 2.6.4 Discussion and Interpretation of Results

This section analysed overhead line outages caused by the weather and the environment. Comparing the results from Table 2.3 and Table 2.17, there is significant difference in MTTR of the W&E caused outages compared to the standard case. Numerically, the different in log-normal estimated MTTR is $824 - 162 = 662$ minutes.

This methodology a useful basis for comparison of long-term system resilience performance. Using this technique, it is possible to evaluate the changes in resilience which enhancements to the recovery process provide. This is done by comparing the overall difference in MTTR changes from W&E outages, with upgraded versions of the system. Overall it can provide basic analysis of resilience quantification.

This methodology has some limitations. One issue with using this measure is that a single calculation cannot independently be used to assess the resilience of the system. The values of this form must be compared to some other value, in order to evaluate which is more resilient. This limitation does not affect the measures ability to optimise resilience however, as the relational value is capable of being enhances. The cause of this limitation is that the results are not independent of the impact of the event. It has been previously discussed that resilience is a measure which is independent of severity of an HILP event. Despite this, the results being analysed are a result of an event of a certain impact and therefore cannot be used without either comparison, or some form of context given.

## 2.7 DISCUSSION

The following contributions have been made in this chapter:

- A breakdown of the quantitative distribution of different affected assets and causes of failure was presented.
- The process of fitting the distribution of outage data, to estimate MTTR and MTTR, was demonstrated

- An analysis of the resilience of the system represented by the outage data was conducted.

The results of the breakdown analysis in Section 2.3 highlighted several important points about the outage data. A large majority of outages within the outage database are attributed to lines and cables. Despite being a long-spanning database of distribution grid outages, there are insufficient outage samples which can be used for the other asset types. To build a complete model of this distribution grid, knowledge of these assets would be required, particularly if failure rate was the overall focus. However, this work is centred around recovery process and the aim is to enhance resilience by improving this recovery. Thus, these shortcomings do not impede the overall goal of this work.

Sections 2.4 and 2.5 undertook parameter estimation from the outage data to calculate the distribution and mean of TTR and TTF, respectively. The results of recovery parameterisation revealed that Log-Normal was the best fitting distribution for the recovery time in all cases. This is a common distribution for recovery. The results of the failure parameterisation demonstrated that the Weibull distribution was the best fitting result. This is a common two-parameter distribution for failure data, because it enables the ageing of an asset to be incorporated in its failure model. Section 2.5.2 provides further details about the Weibull distribution.

Models presented in later chapters of this thesis primarily utilise exponentially distributed failure and recovery parameters. The justification for this is to reduce the complexity required to present the developed methodology. Despite this, the presented models are capable of utilising the non-exponential statistical models developed in this chapter. Methods for doing so have been detailed in Section 1.3.

An issue which occurred through this analysis was limited information about specific assets. There are methods which can be applied if there is not enough data to model an asset. Lines and cables are the only type of asset which has parameters that deviate greatly from different distribution grids [45]. Other components tend to have similar failure rates. This is because the failure rates of other distribution grid assets tend to be more a of function of the components themselves. The most inconsistent asset parameters between different distributions are the components which have already been modelled; overhead lines and underground cables. It is therefore feasible to combine failure data of assets not of these types, such as transformers and insulators, and fit this combined data to estimate parameters. Standard components (transformers etc) generally have specifications provided by their manufacturer. These often document the expected lifetime of the asset, and it is reasonable to substitute these in cases of lacking data.

Overall, this chapter presented an analysis of outage data of a real-life distribution grid. The purpose of this analysis is to examine the outage data to extract information about the nature of the recovery and failure parameters. The context provided by this

examination will be referenced in the follow Chapters, which develop novel models utilising data which the methods presented in this chapter produce.

# Chapter 3

# RELIABILITY GRAPH MODEL OF DISTRIBUTION GRIDS

## 3.1 INTRODUCTION

In recent years, the majority of presented methodologies for the analysis of distribution grids have been based on state-space models[3]. The reason for this stems from the nature of distribution grids. They are complex structures which span vast areas, and have a large number of assets with complex interconnections. Further to this, the behaviour of distribution grids when a failure occurs involves complicated interactions between the assets, protection equipment and utility procedure. Continuous-Time Markov Chains (CTMCs) are the most common approach to evaluate this complex behaviour [30]. This is because they are capable of modelling the complex interactions between assets in a distribution grid, including the relationship between asset failure and protection operation.

An important limitation of CTMCs and other stochastic models is that they quickly suffer from a state explosion problem for even moderate sized systems. There are two core problems that stem from using existing stochastic models for large-scale distribution grid analysis. The first is that large models are typically computationally expensive. Secondly, established stochastic models are bulky, unintuitive and prone to error when constructed and analysed [29]. These limitations are a problems which can be overcome through the use of different techniques for different parts of the model, and this is a core part of this thesis. This chapter presents a methodology to produce an analytical model for distribution grids which overcomes these limitations.

In this chapter a non-state based technique for analysis of distribution grids is proposed. Hierarchical models utilising Reliability Graphs (RGs), a modelling formalism commonly used in other fields of reliability engineering such as distributed computing [29], are used for the reliability and availability analysis of distribution grids. These are a non-stochastic reliability formalism which provide an structured means of building an analytical load point (LP) model for reliability and availability. Instead of modelling the complex interactions of protection equipment, RGs are used to concisely and analytically

calculate the influence of specific assets on a system, based purely on the reliability of the assets and how they are interconnected.

RGs are a tool which can highlight the assets which most strongly affect overall reliability and resilience. The advantage of their approach is that the analysis is based purely on the reliability of components and the components they interconnect with. This means they are not burdened by the complex relationship between grid assets and the protection and reconfiguration equipment. At first look, RGs appear to be an inappropriate tool for the objectives of this thesis. Analysis which ignores the behaviour of protection equipment means that it cannot directly be used to plan its placement. However, rather than directly modelling the behaviour of protection systems, RGs can evaluate the impact of their application.

Analysis in this chapter examines how the distribution grid can be enhanced by the deployment of Distribution Automation (DA). The deployment of this technology can greatly reduce the time required to reconfigure the grid after an outage occurs. There are a number of examples where this technology reduced reconfiguration time to seconds or less. In one such case in the USA, 40,000 out of 80,000 customers had their power restored within 2 seconds after a wide-spread failure due to distribution automation [51]. A perfect knowledge of outage location, and the ability to reconfigure the grid in a short period of time will be referred to as Fully Automated Reconfiguration (FAR). With RGs, it is possible to evaluate the achievable benefits of such technology. This chapter provides a method of assessing and identifying assets and sections which are in need of reconfiguration equipment to enhance their availability and resilience. Further, it presents analysis of how well the system performs when DA technology is deployed.

The goals of this chapter are twofold. Firstly, it demonstrates the use of RGs and accompanying hierarchical models, and utilises them for the applications of sensitivity and resiliency analysis. This analysis shows the performance of a system, on a day-to-day basis, and also when HILP events occur. Secondly, these demonstrated methods to compare and evaluate the gains and shortfalls of FAR systems. This methodology can be used for detailed analysis of distribution grids, and also for assessing the achievable benefits of distribution automation.

The contributions of this chapter are as follows:

- Demonstrate the construction of a three-level hierarchical model which utilises Markov or semi-Markov chains, RGs and system reliability metrics to analyse the reliability and availability of distribution grids. (Section 3.3)
- Extend the developed model of the analysis for a system which has deployed technology to enable fully automated reconfiguration. (Section 3.4)
- Analyse and compare the sensitivity of load point and feeder availability for the base system and the system enhanced with FAR. (Section 3.5)

- Analyse and compare the resilience of load point and feeder availability for the base system and the system enhanced with FAR, using the analytical resiliency analysis method introduced in Section 1.2. (Section 3.6)

Additional to the works above, Section 3.2 presents a comparison of RGs with existing methods and Section 3.7 summarises the results, and discusses the benefits and shortfalls of this methodology.

## 3.2 COMPARISON WITH RELATED METHODS

RGs are categorised as a series-based analysis, meaning that the model takes the form of a connected graph. A method of series-based analysis similar to this was a prominent means of analysis when the field of distribution grid reliability analysis was relatively young [52]. This method, known as network reduction, utilises the series-parallel structure of distribution grid LPs to compute failure rate and availability.

The method of network reduction for distribution grid analysis is summarised as creating a sequence of equivalent components, obtained by gradually combining series and parallel connected components. It is based on the assumption that failure and recovery rates are exponentially distributed (thus Markovian and memoryless) and therefore can be combined together. This methodology is scalable and straightforward to implement, but it does have limitations which must be addressed. There are three long-standing limitations to this technique, summarised in reference [31]:

1. Assets must be in series or parallel.

2. Critical assets become 'absorbed' into their surrounding area, masking their effect on the network more as the network grows.

3. The technique is not able to describe different modes of failure, maintenance or weather, etc.

These limitations are all able to be overcome with the hierarchical model which is proposed in this chapter, and which utilises RGs.

RGs have a fundamental advantage over other series-based analysis methods, including reliability block diagrams or fault trees without repeated components [53]. This is because, as the first limitation states, traditional network reduction methods can only be used to model series-parallel connected systems. A system which is series-parallel is one which is composed of interconnected subsystems which are either connected in series, or in parallel [53]. RGs, however, model individual components as edges. This makes them able to be solved using a factoring algorithm detailed in reference [53] to solve systems which are not series-parallel.

The RG in this chapter will make up part of a hierarchical models which provides additional advantages to further address the limitations listed above. In hierarchical models, each individual asset within a system is contained separately in the model. As such, sensitivity analysis can be used to assess the influence of the parameters of each of these assets on the LP or system. Assets are modelled with CTMCs or semi-Markov Chains, which are state-based models, instead of series-based. This allows for various states, such as maintenance and bad weather, to be analysed. Further, if semi-Markov processes are utilised to model individual assets, the influence of time on the failure rate of assets can be incorporated. This means that there is no requirement for exponentially distributed parameters.

RGs have a limitation which is shared with other series-based models. They require the assumption that each of their components is independent all others. This is also a requirement of hierarchical models also. It means that each asset or subsystem within the model must be treated as independent of other assets within the system [29]. This limitation means that dependent assets, such as protection devices and switches, cannot be incorporated into models completely. The result is that the reconfiguration process of distribution grids cannot be completely modelled using this technique.

State-based models such as CTMCs don't have this limitation, so they are often considered a more appropriate tool for distribution grid reliability analysis. This is true in certain types of analysis, however RGs also hold several advantages over state-based models which make them an equally valid analysis tool, albeit for different purposes. RGs, and series-based models in general, do not suffer from the state-explosion issue which is a significant limitation of state-based methods. This has been discussed in Section 1.3.2 and restricts the scalability of state-based models, unless additional measure are taken. Due to this restriction, there are no state-based modelling techniques which scale as well as series-based methods such as RGs.

## 3.3 RELIABILITY GRAPH METHODOLOGY

This section demonstrated the use of RGs with hierarchical models for the analysis of a distribution grid feeder. The overall model structure is presented, and each of the levels of the model is described. An example analysis is given at the end of this section.

### 3.3.1 Overall Model Structure

RGs are models which require two main sets of data. The first is the failure and recovery rate of individual assets. The process of obtaining that data was described in Chapter 2. The second is the topology of the feeder or network which is modolled. Both of these datasets are available to all utilities.

The overall process is based on the concept of hierarchical modelling [29]. Hierarchical models can be summarised as a strategy which employs several different tiered models for different parts of a system. For this application, a three-tier hierarchical model is employed.

The three stages of this hierarchical model are as follows:

1. Individual Assets. These are modelled as two-state CTMCs. These aggregate all the various states of each asset into a state for "online" and a state for "offline".

2. Load Points (LPs). These are modelled by RGs, and are capable of calculating the reliability and availability of each LP based on the two-state CTMCs, and the topology by which they are connected.

3. Feeder. The final tier collects each LP model and aggregates them into the system indices System Average Interruption Duration Index (SAIDI) or System Average Interruption Frequency Index (SAIFI).

This three-tier model allows for the reliability of each individual asset to be analytically incorporated into the equation for the feeder SAIDI and SAIFI, by assessing each LP using RGs. RGs are able to model the connections between each of these assets. The result is a straightforward and structured means of evaluating the availability and resilience of each LP and feeder.

### 3.3.2 Asset Model

Individual distribution grid assets are commonly modelled using Markov processes [54]. Their utilisation enables the different modes of operation and failure of individual assets to be captured as states within them. The background of Markov processes, and specifically CTMCs, is covered in Section 1.3.2.

Markov processes are used to represent and aggregate the various modes of operation and failure for each asset in to a smaller collection of states. These models can then be solved to evaluate the probability that the model of an asset is in a given state. For the first tier of the hierarchical model, they represent the empirically calculated failure and recovery parameters as two states, *Ok* and *Failed*. If the parameters are exponentially distributed, two-state CTMCs can be utilised. These have a steady-state solution, meaning that they can be solved analytically. CTMCs have been introduced in Section 1.3.2.

Alternatively, if the empirically generated parameters for failure and recovery are not exponentially distributed (such as the Weibull-distributed failure parameters in Chapter 2), assets can be modelled with two-state semi-Markov models [29]. Semi-Markov models are used for non-exponentially distributed parameters, instead of CTMCs. CTMCs can not be used for non-exponentially distributed systems because CTMCs

utilise the memoryless property unique to exponential distributions. They have a failure rate, $\lambda$, which is does not change in time. Semi-Markov models do not have the memoryless property, so they must be solved numerically because they cannot be formed into a steady-state solution or be solved analytically. This is demonstrated in Section 1.3.3.

A two-state Markov model have two parameters; a failure rate, $\lambda$ and a recovery rate, $\mu$. These can be used to calculate the availability and reliability of the asset and they will be used as inputs to the second tier of the hierarchical model. They can be evaluated using the methods introduced in Section 1.3.2.

### 3.3.3 Load Point Model

The second tier of the hierarchical model is the LP. Representing distribution grid LPs with RGs within a hierarchical model is novel. This tier evaluates the interconnected components which supply each LP, and calculates their combined reliability and availability based on evaluation of the interconnected asset model outputs. The fundamentals of LPs have been introduced in Section 1.3.5.

Construction of an RG based on a distribution grid LP requires the collection of all assets that will force the LP offline if they fail. All assets which are not separated by instantly-operation protection and switching equipment must be collected for the construction of an RG. The reason for this is that assets which cannot be immediately separated from one which has failed will be brought offline when the failed asset goes offline. Therefore any LP connected to any of these offline assets must consider them in its model. These assets must be modelled as though they are in series, despite them not physically being in series.

For example, it is common for laterals which stem from a feeder to have a fuse at the junction. When any of the assets along this lateral fail, the fuse at the junction will operate, bringing any LP supplied from this lateral offline. Similarly, if any line along a feeder fails, and the circuit breaker at the base of this feeder operates, the whole feeder will be brought offline.

This overall methodology can be used to design a RG which represents each LP. Outputs from this section, the availability, down time (DT), and reliability, are used in the indices to evaluate the system. For additional reduction in computational complexity, factoring algorithms such as Binary Decision Diagrams (BDD) exist [29], which can be implemented using software packages such as SHARPE [37]. These were discussed in Section 1.3.5.

### 3.3.4 System Model

The system-level tier of the hierarchical model uses well-established reliability indices, commonly used to represent distribution grid reliability. Once each RG is calculated, their outputs can be aggregated using the system-wide indices. The background of SAIDI and SAIFI has been introduced in Section 1.3.1.2. These are used because there are several advantages to utilising standard system-wide measure for the system tier of the hierarchical model. Firstly, they already exist as well-known measures for utilities. This means that they are a proven method of expressing reliability and availability. Secondly, utilities in New Zealand and other countries are regulated by these metrics [55]. This means that they are a large driver of the investment and operational planning, as the goal of utilities is to maintain their values to acceptable levels. By deriving these measures from the model, it means that there is a direct analytical means of determining the influence that each individual asset has on the overall system reliability.

Traditionally, both the SAIDI and SAIFI indices are calculated by utilities empirically. Primarily this is done using outage databases, which was covered in Section 1.3.1.2. This model, however, produces an analytical calculation of these values. They will have the same meaning as their empirically-calculated counterparts, but they are predictive measures which are based on the analytical model. Conversely, the outage database generated SAIDI and SAIFI indices are reflective, and assess past performance. The relationship between the empirical and analytical indices allow for the verification of analytical models by comparing model outputs to empirical data. If estimates of parameters are not correct, this can be used as a method of adjusting the parameters to correctly calculate SAIDI and SAIFI for the system. This can be done to ensure the model is correct before other changes are implemented in order to predict other effects and influences. For example, the influence of remote communications and sensors on distribution grid reliability and resilience can be predicted.

Both the SAIDI and SAIFI values which make up the third tier of this model are calculated directly from outputs of the RGs that make up the second tier, as well as the customer numbers of each LP. The benefit of hierarchical modelling is that this tier can be changed to use other common indices, such as the load-based Annual Energy Not Served (AENS).

### 3.3.5 Example Analysis

This section presents a short analysis of a simple example system to demonstrate the methodology of RGs, and the hierarchical model which contains them. Analysis is conducted on Bus 2 of the Roy Billinton Test System (RBTS) [56]. This example will consider Feeder 1 (F1) and Feeder 2 (F2) of this system. The circuit diagram for these feeders is displayed in Figure 3.1.

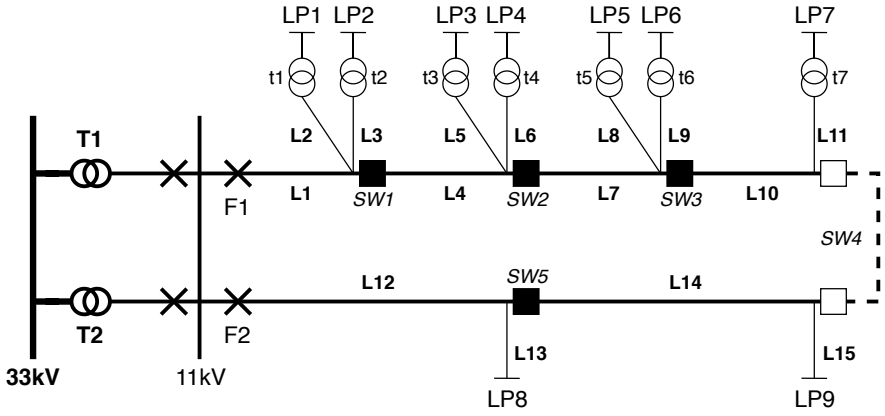


**Figure 3.1** Circuit diagram of the test system that is modelled for analysis.

| **Asset** | $\lambda$ $(yr^{-1})$ | **MTTR** $(hr)$ | **Availability** | **DT** $(hr\ yr^{-1})$ |
|---|---|---|---|---|
| Line 2, 6, 10, 14 | 0.039 | 5 | 0.99997774 | 0.195 |
| Line 1, 4, 7, 9, 12 | 0.048 | 5 | 0.99997260 | 0.240 |
| Line 3, 5, 8, 11, 13, 15 | 0.052 | 5 | 0.99997032 | 0.260 |
| Transformer t1-t7 | 0.015 | 200 | 0.99965766 | 3.000 |

**Table 3.1** Asset failure rates ($\lambda$) and Mean Time To Recovery (MTTR) from RBTS Bus 2 system [56], as well as their calculated availability and DT

There are several assumptions needed for analysis of this system. These are all stated in the paper describing this test system [56].

- Protection equipment such as circuit breakers (CBs), fuses, and sectionalising switches cannot fail.
- Protection equipment which operates in case of a failure (CBs, fuses) operates instantly, with no transient effects on the power flow.
- Failure rates are exponentially distributed.

Also note that at each junction of each lateral on both feeders, there is a non-load breaking switch on the downstream side of the connection (filled-in square in the circuit diagram). This switch becomes relevant during the FAR section of this chapter, and during later chapters when the reconfiguration after an outage is modelled.

The RG models used in this analysis are two-state, with failure rate and recovery times defined based on those given in the RBTS test system [56]. Table 3.1 presents the failure rates and recovery times for relevant RGs. Note that for this analysis, only the 11kV section of the network is considered, and therefore only the feeder RGs have been given in this table. Additionally, since these RGs have been specified by just two transition rates, their availability and DT can be calculated using Equation 1.25 and Equation 1.3, respectively. These are shown in the fourth and fifth column of Table 3.1.

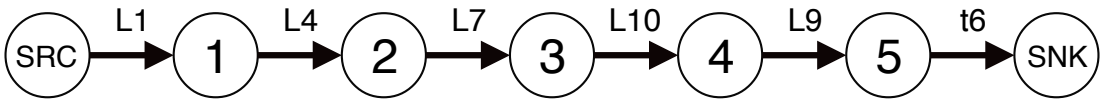


**Figure 3.2** RG for LP6 of the RBTS Bus 2 test system

Now that each asset failure rate and availability has been presented, they can be collected into a RG for each LP within the system. This is the second tier of the hierarchical model. Observing F1 of Figure 3.1 and noting the previously mentioned fuse at the base of each lateral, the following groupings are separated by instantly-operating protection equipment:

- L1,L4,L7,L10
- L2,t1
- L3,t2
- L5,t3
- L6,t4
- L8,t5
- L9,t6
- L11,t7

Each grouping can be selected for each LP, and construct an RG. LP6 is used to demonstrate this. For LP6, the relevant component set, based on selecting relevant groupings, is $I = \{L1,\ L4,\ L7,\ L10,\ L9,\ t6\}$. The RG for this presented system is shown in Figure 3.2.

As can be seen in Figure 3.2, the system is in series, and thus can be evaluated with little complexity. The reliability function of LP6 is based on Equation 1.39 calculated as,

$$R(t) = \prod_{i \in I} R_i(t) = e^{-\Sigma\lambda_i t} = e^{-0.246t}. \tag{3.1}$$

Where $\lambda_i$ is the failure rate of asset $i$.

And Mean Time To Failure (MTTF) is calculated as,

$$MTTF = \int_0^\infty R(t) = \frac{1}{\Sigma\lambda_i} = 4.065\ yr. \tag{3.2}$$

Availability of LP6 is calculated with Equation 1.40, using the results in Table 3.1. This is calculated as,

$$A = \prod_{i \in I} A_i = 0.999525858. \tag{3.3}$$

Therefore the DT of this LP is 4.153 hr/year.

The MTTF, availability and DT results for all of the LPs of F1 and F2 of the test system can be seen in Table 3.2.

The final calculation of this 3-tier model is the SAIDI and SAIFI results. These are calculated using Equation 1.5 and Equation 1.7, and the results in Table 3.2. The SAIFI

| Load Point | No. Cust | Availability | DT ($hr\ yr^{-1}$) | MTTF ($yr$) |
|---|---|---|---|---|
| 1 | 210 | 0.99953099 | 4.109 | 4.219 |
| 2 | 210 | 0.99952358 | 4.173 | 4.000 |
| 3 | 210 | 0.99952358 | 4.173 | 4.000 |
| 4 | 1 | 0.99953099 | 4.109 | 4.219 |
| 5 | 1 | 0.99952358 | 4.173 | 4.000 |
| 6 | 10 | 0.99952586 | 4.153 | 4.065 |
| 7 | 10 | 0.99952358 | 4.173 | 4.000 |
| 8 | 1 | 0.99952358 | 4.173 | 4.000 |
| 9 | 1 | 0.99952358 | 4.173 | 4.000 |

**Table 3.2** Results for Availability, DT and MTTF of each LP in RBTS Bus 2.

| Feeder | SAIDI | SAIFI |
|---|---|---|
| F1 | 4.152 | 0.246 |
| F2 | 0.695 | 0.139 |

**Table 3.3** SAIDI and SAIFI results for F1 and F2

and SAIDI values for these two feeders are given in Table 3.3. These results are the same as those given in the test system, for the case where there is no reconfiguration.

## 3.4 FULLY AUTOMATED RECONFIGURATION

This thesis focuses on the recovery process after an outage has occurred, and the enhancement of the reconfiguration stage of the recovery process with sensors and automation technology. Whilst being important, especially to customers which can be completely separated from an outage, this is only a part of the whole recovery process. This means there is an upper limit to the enhancement which DA can provide.

The goal of a smart grid, from the perspective of reliability, availability and resilience, is a system which is able to locate a fault and reconfigure in a very small amount of time, in the order of minutes or seconds. This is what can be considered the "best case" for DA placement, if an unlimited budget was available. When a system has achieved this, the resilience of a system will depend purely on the reliability of individual assets, and how they are connected, instead of how quickly the reconfiguration and protection equipment and processes operate.

This overall concept is referred to as FAR, and is an application to further demonstrate the use of RGs with hierarchical modelling. The specifics of modelling FAR systems with RGs are described in this section.

SAIDI and SAIFI are indices which only consider sustained outages. A sustained outage is one which lasts longer than 1-2 minutes, depending on the country where the managing utility operates. With the deployment of FAR, the duration of outages from the perspective of each LP is often below the threshold time for an outage classed as

'sustained'. If a fault is isolated in a time less than the threshold of a 'sustained' outage, this means that the outage is not considered for system reliability indices. Remotely controlled switches which can operate faster than the aforementioned threshold can be considered immediately operating.

The process of collecting assets for an RGs considers assets which can't be instantly separated from each other. This means that previously manual switches which are now immediately-operating should be considered. The result of this is that the alternate routes provided by redundant supply, such as tie-switches to other feeders, are now a relevant part of the analysis. A sustained outage on a FAR system only occurs when there is no longer a route or redundant route available to supply a LP. Because of this, FAR allows for system analysis to focus on grid assets, and their influence on the metrics and not the recovery process.

### 3.4.1 Example Analysis

The test system presented in previous examples is modified for the purpose of demonstrating this model. The overall hierarchical approach of Section 3.3 adopted, as has been the case with previous examples. However the system itself now operates with the assumption that normally-closed sectionalising switches and normally-open tie switches both operate immediately when a fault occurs, thus there is no interruption to LPs which can be supplied through alternate routes after reconfiguration.

The overall methodology for this analysis is the same as is demonstrated in Section 3.3.5. The only difference is the connected assets which are modelled within the RG. The following groups exist for the system with the new configuration:

- L1
- L4
- L7
- L10
- L12
- L14
- L2,t1
- L3,t2
- L5,t3
- L6,t4
- L8,t5
- L9,t6
- L11,t7

The feeder lines are now modelled separately. It is also now relevant to include the feeder lines from feeder F2. This is because these make up the alternate supply for LPs on F1. Based on these groupings, the RGs are constructed. For this demonstration, the RG for LP6 is produced. This can be seen in Figure 3.3.

Using this RG, the availability of LP6 can be calculated. Using Equation 1.25, the availability of each LP is given in Table 3.4

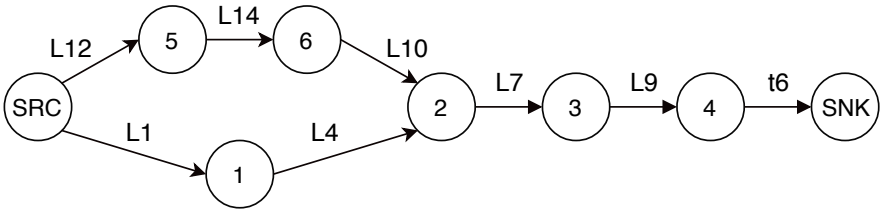


**Figure 3.3** RG for LP6 of the RBTS Bus 2 test system with FAR

| LP | Availability | DT ($hr\ yr^{-1}$) |
|---|---|---|
| 1 | 0.999608013 | 3.434 |
| 2 | 0.999600596 | 3.499 |
| 3 | 0.999600593 | 3.499 |
| 4 | 0.999608010 | 3.434 |
| 5 | 0.999600592 | 3.499 |
| 6 | 0.999602874 | 3.497 |
| 7 | 0.999605727 | 3.454 |

**Table 3.4** Results for Availability and DT each LP in RBTS Bus 2, with FAR deployed.

## 3.5 SENSITIVITY ANALYSIS

### 3.5.1 Introduction

The basic methodology for RG modelling has now been introduced. This section will now utilise the established model for the application of system evaluation. It will use the constructed RG model to evaluate the LP and system availability using sensitivity analysis. There are two important results which can be obtained from this methodology. The first is a means to validate the parameters which have been employed, The second is a means of highlighting the most influential, and most important sections and assets within a system.

Sensitivity analysis is a well-established methodology which utilises reliability models to evaluate systems [31]. The sensitivity of a function or a system to the parameters of an asset is defined as the partial derivative of the function with respect to the parameter [45]. It is approximated numerically by perturbing the parameters and observing the change to the function or system. This is presented as a chart in this analysis in order to convey the relationships between different models and their components.

If a function or system is sensitive to an asset, then changes in the reliability of the asset will result in larger changes to the overall reliability of the system. This knowledge can be used in two ways. Firstly it can be used to enhance the system by determining areas where the availability should be improved. Secondly, it can be used to tune models of the system. The parameters of assets which a system is most sensitive to can be adjusted to ensure a model is accurately representing a expected system performance [45].

The process of using RGs for sensitivity analysis is demonstrated using the example systems from Section 3.3 . First, the sensitivity of LP DT to asset parameters is assessed, and secondly a similar process is used for feeder SAIDI. The sensitivity of DT is presented instead of availability, because availability is bounded between [0,1], so the change is less intuitive. DT is calculated using Equation 1.3. As with previous examples, LP6 is analysed. The overall purpose of this analysis is to demonstrate the methodology, and also to present the enhancements achievable by FAR by contrasting the FAR system with the base system.

The results of this analysis are relatively straightforward, but this methodology can be applied directly to other models, and is used in later chapters. From this analysis, the lines which have the greatest influence on the LP DT and feeder SAIDI are identified. Similar analysis is conducted in a paper published by the author [44].

### 3.5.2 Load Point Availability Sensitivity

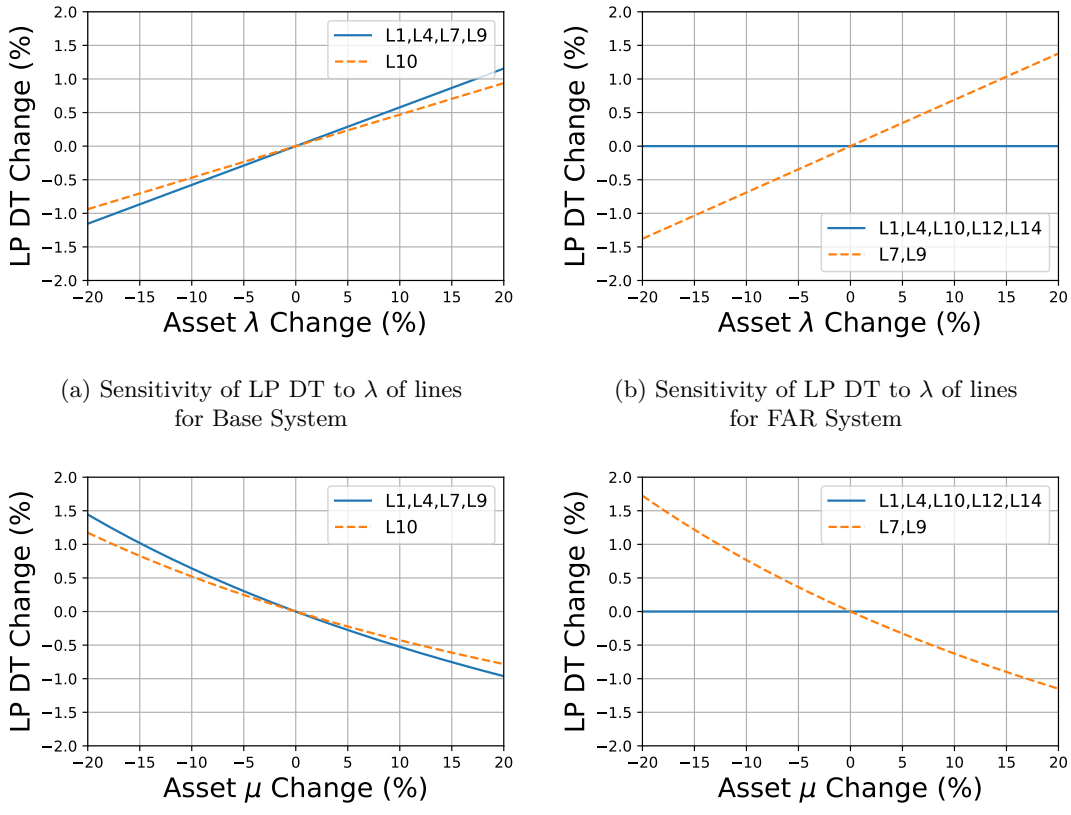


(a) Sensitivity of LP DT to $\lambda$ of lines for Base System

(b) Sensitivity of LP DT to $\lambda$ of lines for FAR System

(c) Sensitivity of LP DT to $\mu$ of lines for Base System

(d) Sensitivity of LP DT to $\mu$ of lines for FAR System

**Figure 3.4** Sensitivity analysis of LP6 availability to $\lambda$ and $\mu$, for Base and FAR system model.

The LP DT sensitivity analysis is done for LP6 of the test system. There are four

separate results which are all shown in Figure 3.4. Subfigures (a) and (b) show the results of sensitivity analysis of the availability of LP6 for the base system and FAR system, respectively, against the failure rate, $\lambda$, of lines L1,L4,L7,L9 and L10 for both systems, and additionally L12 and L14 for the FAR system. The subfigures (c) and (d) are similar, but for the recovery rate $\mu$.

First looking at the subfigures (a) and (b), showing sensitivity to $\lambda$, it can be seen that there are clear differences between the two systems. Subfigure (a) contains two curves, one for L1,L7,L7 and L7, the other for L10. Both of these have a clear influence on the DT. This is to be expected as the RG for this is purely a series-connected system. Thus, all contribute equally to the overall availability. The reason that one curve represents four lines is because according to the test system parameters, these all have the same length, and the same failure rate per unit length.

Comparing subfigure (a) to subfigure (b), there is a clear difference in the contribution of a majority of the lines in the system model. Specifically, it can be seen when viewing the chart alongside the RG in Figure 3.3, that lines L1,L4,L10,L12 and L14 have almost no influence on the overall DT. This is because it is extremely improbable for this section to fail, as it would require two separate series-connected routes to fail. The system is still extremely sensitivity lines L7 and L9, as these are not contained in the redundant section. Overall, It is demonstrated that there is a large reduction in sensitivity to $\lambda$ gained by introduction of alternate supply routes.

In subfigure (c) and (d), where sensitivity to $\mu$ is assessed, similar results are seen. All line $\mu$ values have an influence on the base system's LP availability. But in the FAR model, only the lines L7 and L9, which cannot be replaced by a redundant path have an influence on DT.

It should be noted that for the FAR system, $\mu$ has a much smaller effect on the system in the parts which have redundant paths. Assets which have the largest effect on availability are ones which, when failed, cannot have their effect mitigated by alternate routes to supply LPs. This is because the ratio of $\mu$ to $\lambda$ is very high, and therefore the system has significant availability and DT. Both supply paths need to have failed for the LP to go offline. This is unlikely in a day-to-day perspective. This point is important when considering resilience, and is discussed further in Section 3.6

### 3.5.3 Feeder SAIDI Sensitivity

The feeder SAIDI sensitivity analysis is undertaken for F1 of the test system. There are four separate results which are all shown in Figure 3.5. Subfigures (a) and (b) are sensitivity analysis of SAIDI for the base system and FAR system respectively, against $\lambda$ of the various lines which are contained within the RG model. The subfigures (c) and (d) are similar, but for $\mu$.

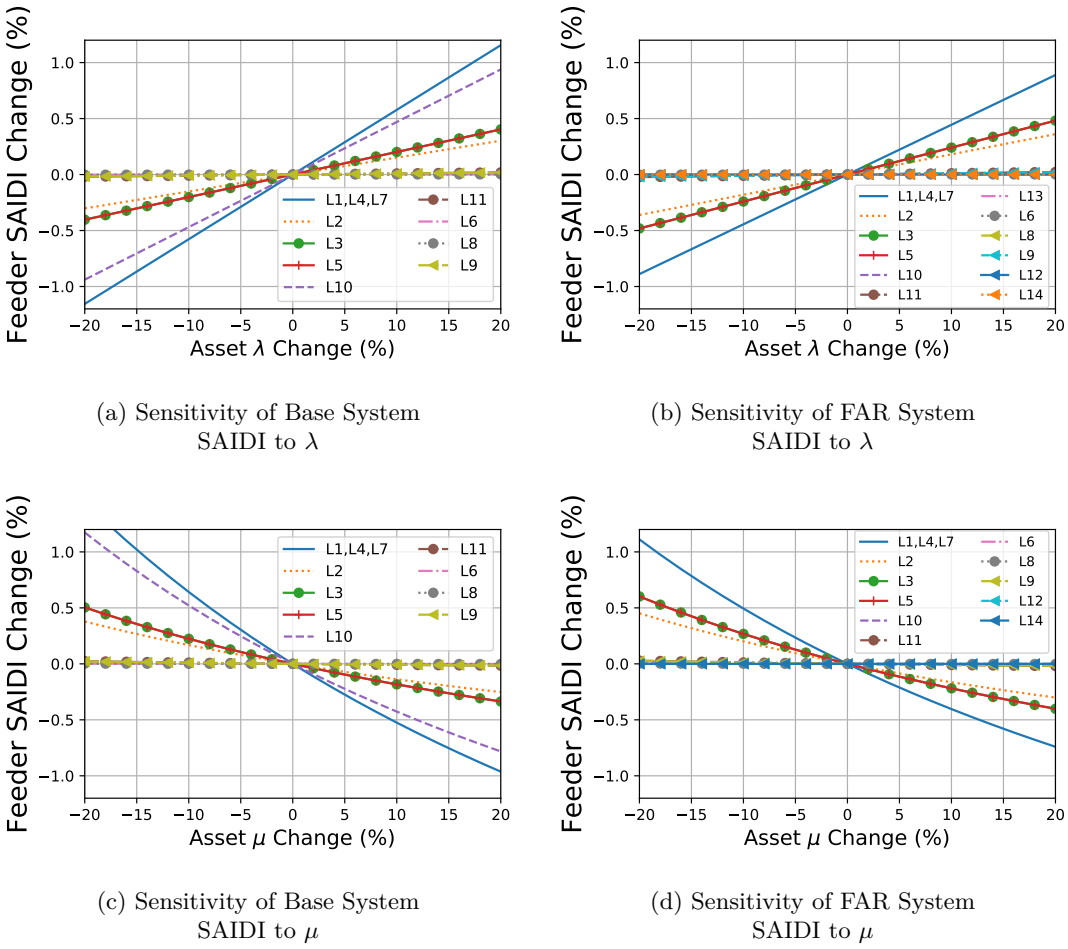


(a) Sensitivity of Base System SAIDI to $\lambda$

(b) Sensitivity of FAR System SAIDI to $\lambda$

(c) Sensitivity of Base System SAIDI to $\mu$

(d) Sensitivity of FAR System SAIDI to $\mu$

**Figure 3.5** Sensitivity analysis of Feeder 1 SAIDI to $\lambda$ and $\mu$, for Base and FAR system model.

In Figure 3.5 (a), it can be seen that $\lambda$ of the feeder lines L1, L4, L7 and L10 has the largest influence on overall system availability. This is an intuitive result, since these lines supply all LPs contained on the feeder. Other lines of significant influence on the SAIDI are the ones which supply the LPs containing a large number of customers. As was seen in Table 3.2, LP1-LP3 supply a large portion of customers, and thus the lateral lines supplying these have a large influence on the system.

Comparing these results to Figure 3.5 (b), there is a clear drop in the sensitivity of the system to the $\lambda$ of three of the feeder lines. The alternate route via L10, enabled by FAR, has removed the system dependence on a number of feeder lines. The only one which still has a large influence on feeder SAIDI is L1. This is due to the number of customers supplied at the LPs at the base of the feeder, and because these LPs cannot be supplied by any feeder line other than L1. Overall, this sensitivity analysis helps to highlight key assets and sections of interest from the customer-weighted perspective.

### 3.5.4 Discussion of Results

The analysis shows a reduction in the sensitivity of SAIDI to the failure rate of a number of assets in the FAR system. The ability to reconfigure rapidly in order to utilise redundant supply paths means that the influence of recovery and failure rates of the assets in these paths on the overall system was reduced significantly. This is because there must be a failure of an asset in each of the multiple paths to cause an outage to the LP supplied. Additionally, it is demonstrated that FAR deployed to a system has little influence on the systems sensitivity to assets which cannot be bypassed using redundant routes. It is clear that this is a limit of the deployment of this technology, as it can only enhance a system based on the assets which are already deployed.

The methodology demonstrated in this section is straightforward for a small system, but less so for larger system. An important advantage of RGs is that they are scalable to much larger systems, because their size grows linearly with each additional asset added. Distribution grids tend to grow feeder-by-feeder and mostly are operated in a radial structure. This means that sensitivity analysis, utilising RGs, is feasible to be used for larger systems. It can provide valuable and intuitive insight into the most significant assets of a system influencing LP availability and feeder SAIDI and SAIFI.

## 3.6 RESILIENCY ANALYSIS

### 3.6.1 Introduction

This section will demonstrate this established method of resiliency analysis from Section 2.5.2 using an RG model to compare the LP and the overall feeder hierarchical models from Section 3.3 and Section 3.4.

The resiliency analysis has been performed by introducing changes to the MTTF of several lines within the Base and FAR system. These lines have had their $\lambda$ increased to $\times 100$ their original values, and the overall availability is calculated. DT has a very close relationship with availability, but availability is bounded by between [0,1]. Because of this bounding, DT will be used to convey the availability in the results of this section because this is a more intuitive result. Figure 3.6 shows the results of this analysis for the base system, and Figure 3.7 the results for the FAR system.

### 3.6.2 Load Point Resilience

Figure 3.6 shows the results for analysis of the base system. Parametric changes have been introduced to three lines. L1 and L10 are feeder lines, and L9 is a lateral line which connects an LP to a feeder. It can be seen that the each of the LP's availability changes significantly for the reduction in both feeder line MTTF values. The lateral line, L9, only affects the availability of a single LP, LP6.

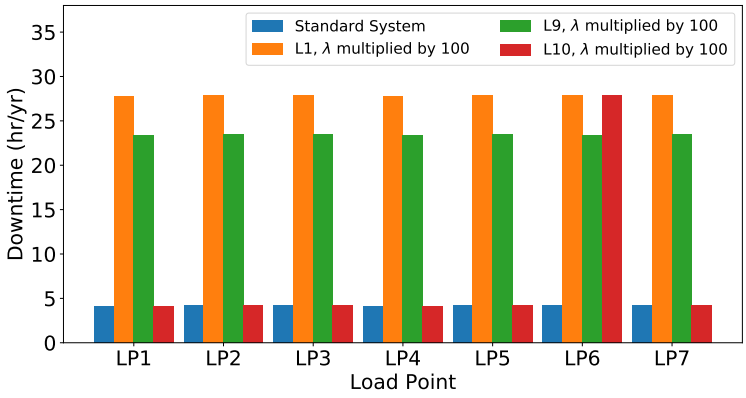


**Figure 3.6** Base system LP DT for parametric changes to L1,L10 and L9 $\lambda$.

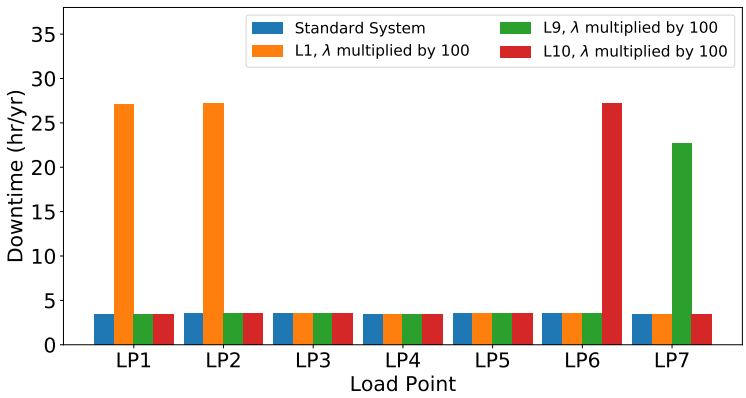


**Figure 3.7** FAR system LP DT for introduced changes to L1,L10 and L9 $\lambda$.

Figure 3.7 shows the results for analysis of the FAR system. As with the base system, parametric changes have been introduced to three lines. The increase in feeder line $\lambda$ has an influence on only directly connected LPs. As with the base system, the lateral line only affects LP6.

From these two results, several conclusions can be drawn about the resilience of the two systems. In the base system, all LPs are affected significantly when the $\lambda$ of any feeder line increases. Comparing this result to the FAR system, it can be seen that the ability to quickly reconfigure means that LPs in most cases are no longer forced offline and the reduction in MTTF of individual feeder lines has no effect. It is clear that the FAR system has increased LP resilience to feeder line $\lambda$. The exception is when the unreliable feeder line is directly connected to the LP with no sectionalising switch. In this case, FAR cannot enhance resilience. It is also shown that FAR provides no increase to the resilience of LPs to reduced MTTF of lateral lines, as reconfiguration cannot aid LPs in this case.

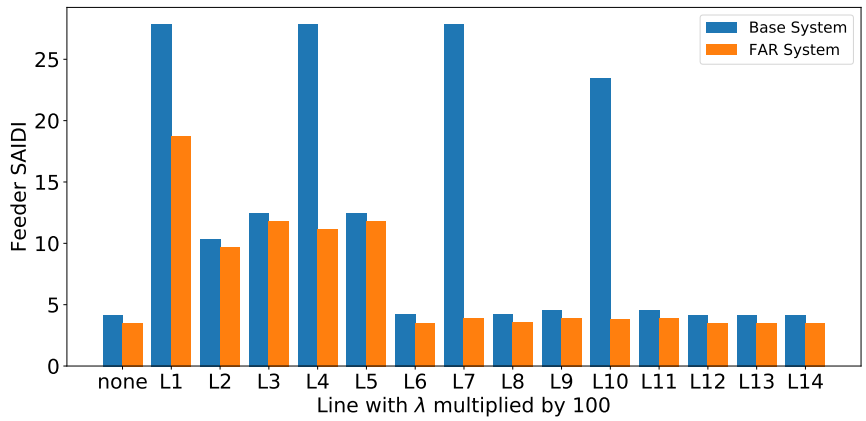


**Figure 3.8** Feeder F1 SAIDI for the Base and FAR system, with introduced parametric changes to $\lambda$ of each asset.

### 3.6.3 Feeder Resilience

The second part of this resiliency analysis demonstration is the feeder SAIDI resilience to line $\lambda$. This analysis assesses the impact of increasing each linesâĂŹ $\lambda$ to $\times 100$ their original value. This has been done for both the base system and the FAR system. The results can be seen in Figure 3.8.

The base system has the largest increase in SAIDI for any lines change in line failure rate. This is comparable to what was seen in the pervious LP analysis, where feeder lines which can't be disconnected from load points after an outage. This is attributed to the L1-L4-L7-L10 grouping seen when the RG was constructed in Section 3.3.5. It can also be seen that the laterals serving high customer LP also cause large increase.

The FAR system, by comparison, is only influenced by feeder lines which cannot be disconnected from the high-population feeders. L1 is the feeder line which can't be disconnected from LP1 and LP2, two LPs which serve a relatively large number of customers. This means that when L1 $\lambda$ is reduced, the impact on the system SAIDI is similar to the base system, despite being able to disconnect L1 from all but two of the LPs.

The key result from this example is that at a system perspective, there is a lack of resilience to changes in $\lambda$ of feeder lines and laterals which serve the high population LPs. This is revealed by the large increase in SAIDI for changes in L1, and similarly but to a lesser extent L4. This is despite the deployment of automation to reconfigure when these lines fail. It is also shown that lateral linesl have a great deal of influence on the feeder resilience if the LP serves a large number of customers. There is a clear limitation of this system, from a resilience point of view, in which there are a significant number of customers concentrated in a small section of grid.

### 3.6.4 Discussion of Results

Overall, this resiliency analysis provides a means of analysing distribution grids in order to identify how resilient a system is to individual parameters of lines and sections of grid. Asset failure during High-Impact Low-Probability (HILP) events does not necessarily depend on the normal failure rate of an asset, so design should not assume that the least reliable component is the most likely to cause the most problems. When planning for these events, it is important to know areas of the system where a failure will have the greatest impact on the grid. The analysis method presented in this section provides a means of conducting this analysis.

## 3.7 DISCUSSION

There are four contributions presented in this chapter:

- Demonstrate the construction and analysis of RGs to describe distribution grids in order to assess reliability and availability.
- Introduce a model which evaluates a give system with FAR. This is considered the 'best case' achievable by only placing sensors and deploying communications, serves as a means of evaluating shortfalls in the example system that are not related to the protection and reconfiguration equipment, but to the layout of the assets themselves.
- Compare and analyse the two models by conducting a sensitivity analysis, observing the impact of individual line failure and recovery rates on LPs and the feeder
- Apply the developed RG model to demonstrate the proposed resiliency analysis method and compare the two models.

This section summarises and discusses the demonstrated methodologies, and present the conclusions drawn from its applications.

All forms of analysis show that the FAR system performs better in terms of reliability and availability, compared to the non-automated base system. The FAR system is able to utilise redundant routes to ensure there is brief or non-existent interruption to customers who can be separated from a failed asset. There is an upper limit of improvement achievable with FAR however, in terms of availability. RGs and their applications in this chapter are able to show the maximum achievable gain, and also to show the assets which are the most important when upgrades and improvements are being considered.

The first application of RGs to using sensitivity analysis to highlight how each asset affect the day-to-day performance of distribution grids. It has been shown that

LP availability depends mostly on the reliability of non-isolatable assets, and that the introduction of redundant routes, by the use of FAR, increases the availability of the feeder section significantly.

Resiliency analysis, was used to evaluate the performance of a system when strained by HILP events which cause values of $\lambda$ well above system design ranges. This methodology highlights the assets which have the greatest influence on load point and feeder resilience. Failure during unpredictable events is not just dependent on the reliability of specific assets, and therefore a resilient system design should not make the assumption that the least reliable asset is the most likely to fail. Analysis of this type allows system designers to ensure that even if the most reliable asset fails, the system can withstand and mitigate the impact.

The overall purpose of this thesis is to construct a method of evaluating distribution grid availability and resilience, and enhance distribution grids by identifying locations to place DA. The main purpose served by DA technology is to hasten the recovery process by reducing the time taken to locate outages and reconfigure the grid. Whilst being able to assess the resilience and reliability of distribution grids, there are fundamental requirements of RGs that restrict their ability to evaluate the recovery process. Specifically, RGs require the assumption that all components are independent. This means that RGs cannot fully model the operation of switches and protection equipment, when an outage occurs. This limitation is addressed in Chapter 4, where a different model is developed.

RGs are capable investigating individual asset influence on the on an LP or feeder. They are intuitive and straightforward to develop, and can be used to identify critical assets which influence both availability and resilience. This makes them an effective tool to use alongside the later contributions which evaluate the system using state-based methods.

# Chapter 4

# STOCHASTIC REWARD NET MODEL OF DISTRIBUTION GRIDS

## 4.1 INTRODUCTION

This thesis develops a methodology to evaluate the resilience of distribution grids obtained by placement of Distribution Automation (DA) equipment. To assess the contribution of this technology, it is necessary to model the interactions between the two main parts of a distribution grid: the protection and reconfiguration equipment, and the assets for which the protection and reconfiguration equipment operates. This technology operates based on the state of distribution grid assets and so there is dependence between the protection equipment, and the assets the equipment monitors. For example, when there is a failure on an overhead line, a Fault Indicator (FI) could report this, and procedure be followed to isolate it. Modelling protection events and procedures is a complex problem, due to its dependence on the state of assets. This chapter will introduce Stochastic Reward Nets (SRNs) to model this behaviour and overcome a number of limitations which affect existing methods.

Evaluating the dependent procedures following events in distribution grids is traditionally done using Markov processes. Most commonly Continuous-Time Markov Chains (CTMCs) are used.[1] However, due to the number of assets which are modelled, generalisations are often made in order to reduce complexity. Hierarchical modelling is a common approach used to address this [33], and was key concept for the model of Chapter 3. An important assumption made in existing models for the purpose of reducing the state-space, and also reducing complexity, is that only a single failure can occur at any time. This assumption is made in order to reduce the number of states of the model, but with it comes an important limitation, particularly for this application.

Resilience is the assessment of systems during high impact, low probability (HILP) events. During such situations, multiple simultaneous failures become probable. Therefore, analysis of system resiliency cannot be conducted effectively with the assumption that only single failures can occur. This is because the probability of multiple failures

[1] CTMCs have also been covered in Section 1.3.2

during HILP events is not based on the reliability of the assets which can fail, but on the severity of the event. A different type of state-based model is proposed in this chapter, using SRNs, to overcome the restrictions of this assumption.

This chapter will develop an SRN model for distribution grid load points (LPs), which can be used to evaluate availability, System Average Interruption Duration Index (SAIDI) and resilience. The first step of this will be to present the base SRN model which has been developed. This model will then be the subject of a sensitivity analysis conducted to highlight important features of the model, and provide insight into the method itself. Following this will be the development of an extended model, where the reconfiguration process will be modelled by incorporating the distributed switches. The final portion of this chapter presents a method to evaluate the contribution to availability and resilience provided by different switch operating times in the model. The purpose of this is to enable the investigation of the advantage gained by deploying Automation Enabling Communications (AEC) to deployed switches

The following specific contributions are made within this chapter:

- An SRN model is used to evaluate availability, down time and SAIDI of distribution grid feeders and LPs (Section 4.3).
- Sensitivity analysis to gain insight into the model, and the system which it represents (Section 4.4).
- An extension is made to incorporate the operation of individual switches, allowing for the evaluation of their affect on a distribution grid (Section 4.5).
- Finally, the extended model is utilised for sensitivity and resiliency analysis to identify suitable locations to deploy remote communications in order to enhance resilience and availability (Section 4.6).

Additional to these contributions, Section 4.2 compares SRN modelling to existing state-based methods of assessing distribution grid. And Section 4.7 discusses the results of the analysis.

## 4.2 COMPARISON WITH RELATED METHODS

Existing modern reliability analysis methods for distribution grids are based on historic continuous Markov process models [30, 36] (i.e. CTMCs). The models reduce complexity and model additional features of by using hierarchical Markov models [33]. These methods build large CTMCs which can be used to analyse distribution grid reliability. The technique is widely used, and is a core part of analysis of modern distribution grids.

The technique known as construction of *switchable section equivalents* [30], otherwise known as *sections of branches* [57] is often used for feeder analysis to reduce the overall

complexity, and also the large number of states. The algorithm to construct these algorithm can be summarised as aggregating assets in a system into groups, with the boundaries being switches or protection equipment (such as fuses, sectionalising switches, etc.). The reasoning for this is that any outage within one of these groups will have the same influence on the system, regardless of where it occurs within the group [30]. This method has been adopted for the construction of SRNs, and is further explained in Section 4.3.

An advantage of SRNs compared to CTMCs is that the transitions are defined before the underlying reachability graph CTMC is generated, and so the change in failure rate for a section of line is propagated when the CTMC is defined - only a single variable is changed. An explanation of the generation of CTMCs using SRNs is given in Section 1.3.4. Additionally, SRNs can assign guard functions to transitions, so that when their underlying reachability graph is generated, unwanted state changes are excluded. This allows for a straightforward definition of the dependence of assets to each other. An example of this is the sequence of operation reconfiguration which occurs after a failure has occurred. This is demonstrated in Section 4.5.

Compared to existing state-based methods, SRNs enable definition of systems to be compactly modelled and altered for evaluation. They do not enforce independence between assets, so multiple failures can be modelled. Finally, they provide an intuitive model, with the parameters of asset state changes requiring only a single definition. This enables the straightforward introduction of changes to asset parameters for sensitivity and resiliency analysis.

## 4.3 STOCHASTIC REWARD NET METHODOLOGY

This section demonstrates the methodology to construct an SRN for a specific LP, in order to evaluate reliability and availability. The overall model structure is presented, and the individual parts are described. The section concludes with a detailed example analysis.

### 4.3.1 Overall Model Description

An SRN model will be used to represent a distribution grid feeder. After this is constructed, individual reward functions will be defined for each LP to assess availability and down time (DT). These are then aggregated using system-wide metrics such as SAIDI. A notable difference between this SRN model, and the three-tier model presented in Section 3.3 is that each LP is evaluated from a reward function of a single SRN model. Each feeder has a single SRN model. Hierarchical models require each subsystem to be independent; but having LPs with dependent assets is a requirement of this model in order to accurately model protection operation.

Each LP reward function contains all assets relevant to the LP. This allows for a analysis of LP availability while considering individual assets and their dependence on other assets. The developed model can be used to assess the influence of any asset parameter on the availability and resilience of the system. This model has been published in Reference [43].

### 4.3.2 Feeder Model

SRNs have been introduce and their concepts explained in Section 1.3.4. The power of SRNs come from their ability to utilise functions in their definition which can interact with the model. A reward function can be defined which applies a logical evaluation of the number of tokens in specified states. The other useful type of function, guard functions are also logic-based. They are applied to transitions in order to enable or prohibit them firing, again based on the number of tokens in specified states. It is demonstrated that these two types of function allow for the modelling of the complex interactions between assets and reconfiguration equipment which occur after a fault.

The procedure for constructing an SRN model begins by aggregating the feeders connected assets in order to reduce the overall complexity. This is the process which was introduced as constructing switchable section equivalents and was introduced in Section 4.2. Assets that are not separated by reconfiguration or protection equipment are aggregated into individual subsystems. Each of these groups represents a subsystem in the SRN model.

The SRN must model process of reconfiguration to connect LPs to redundant supply after a failure. Lines and feeders which are not usually connected to an LP, but are used after reconfiguration if a failure occurs, are incorporated into the model to do this. As can be seen in the example analysis in Section 4.3.4, these generally become a two-place subsystem; $P_{ok}$ when the section of line is online and $P_{fa}$ when the it is offline. Incorporating these subsystems into the SRN allows for it to model the possibility that a line has failed, but reconfiguration is not possible due to an alternative supply already having an outage. It has been discussed in previous chapters that occurrences of this are very unlikely during day-to-day operation, however these occurrences do become relevant when HILP events occur.

Laterals generally have a fuse at their junction with a feeder, but otherwise often have no other equipment which divides the assets along them. As such, these can usually be modelled as a single two-place subsystem. It contains the place $P_{ok}$, for when the lateral is online and $P_{fa}$, for when the it is offline. They contain a place for the token when the system online, and likewise for when the system is offline. Figure 4.1 (a) is an example of this.

Unlike laterals, feeder lines generally have several switches or reclosers which may be used to separate or isolate sections of line. Each of these sections has its own subsystem

in the SRN, and is a four-state system. The four states of a feeder are modelled as four places in the SRN subsystem. An example of a four-place subsystems is shown in Figure 4.1 (b). Note the distinction between transitions with repaired/repairing (rp) and recovered/recovering (re).

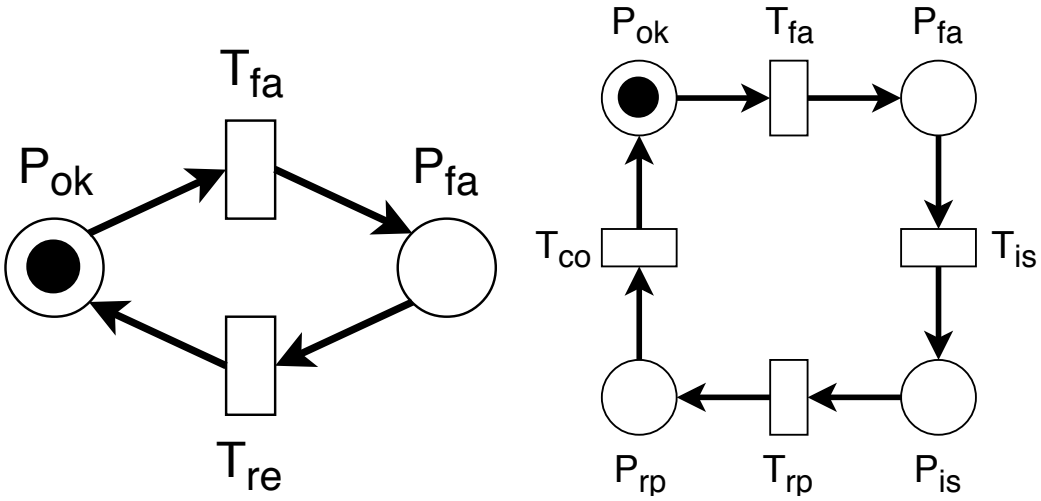


(a) Two-place subsystem for asset subsystems

(b) Four-place subsystem for asset subsystems with reconfiguration.

**Figure 4.1** Example two-place asset subsystem and a four-place asset subsystems for modelling with reconfiguration.

The four places for the SRN feeder line subsystem are $P_{ok}$, $P_{fa}$, $P_{is}$ and $P_{rp}$. The overall reasoning for these states is that feeder outages can be contained to a certain section of line. Four places enables the model to incorporate this factor by evaluating if a feeder has been isolated from it. The four places are defined as follows:

- $P_{ok}$ is the default place, where the subsystem's token remains for the largest portion of time. It represents the state where the asset is operating as intended.
- $P_{fa}$ where *fa* denotes 'failed', is the place representing the state where the line has failed. It is entered from $P_{ok}$ via the transition $T_{fa}$, where *fa* denotes 'failure', at the rate of $\lambda = 1/\text{MTTF}$ for an exponentially distributed transition.
- $P_{is}$, where *is* denotes 'isolated', represents the state of the line when the fault has been located, and all possible sectionalising switches have been operated to contain the outage, and if possible, resupply assets downstream of the outage. All of these events, and thus the transition into this state, $T_{is}$ where *is* denotes 'isolating', is modelled by the parameter $\sigma = 1/\text{MTTI}$, where MTTI is the mean time to isolate the outage.[2]

[2] $\sigma$ is referred to as the isolation rate. This is not the same as the switching rate $\tau$, which will be defined in Section 4.5.

- $P_{rp}$, where *rp* denotes 'repair', represents the state where the failure on the asset has been repaired, but the asset is still not connected to the rest of the feeder. It is entered from the $P_{is}$ place via $T_{rp}$ where *rp* again denotes 'repair', at a rate of $\mu' = 1/\text{MTTRe}$ for an exponentially distributed transition. Notation for repair is defined in the next paragraph.

- $P_{ok}$ is entered from $P_{rp}$ via $T_{co}$ where *co* denotes 'reconnection', at rate $c = 1/\text{MTTC}$, where MTTC is the mean time to connect the asset.[3]

At this point, the distinction between recovery and repair should be made clear. The mean time to *recover* is represented as $\text{MTTR} = 1/\mu$. This encompasses the reconfiguration, repair and reconnection states. To distinguish the difference, the mean time to *repair* is represented as $\text{MTTRe} = 1/\mu'$. This parameter is used on the transitions denoted with *rp* in the four-place model, and represents the repair part of the recovery. For clarity, the relationship between MTTR, MTTI, MTTRe and MTTC is,

$$\text{MTTR} = \text{MTTI} + \text{MTTRe} + \text{MTTC}. \tag{4.1}$$

For this base model, the isolation and reconnection transitions are represented by single parameter, constant-rate (thus, exponentially distributed) transitions. This allows for the complex reconfiguration and recovery process to be reduced to a single parameter, therefore reducing the overall model complexity. In Chapter 5, this parameter is expanded to a separate model, in order to holistically model this recovery process. At this point however, it is assigned a constant rate. Further discussion of this is contained in Section 4.7, where the context and use of this model is discussed.

When each of the relevant subsystems for the feeder have been added to the SRN model, the final stage is to define reward functions for each LP in order to evaluate their availability. This is done by inspecting the modelled system and determining the assets which are required to be online for the LP to be online, whether through a default supply path, or a redundant path through reconfiguration. This stage is best explained with an example, and this is given in Section 4.3.4.

### 4.3.3 System Model

The second part of this model for evaluating distribution grid feeders is the same as what was used for the previous RG hierarchical model. Section 3 provides a detailed definition and explanation of these metrics. To summarise this, the analytical SAIDI equation is used to aggregate each LPs reliability and availability values. SAIDI is defined in Equation 1.7.

[3] $c$ is referred to as the connection rate

### 4.3.4 Example Analysis

The two-feeder test system that was evaluated in Chapter 3, shown in Figure 3.1, is analysed in this section. The important insight obtainable from this section is how a model of this type can be constructed for a feeder. The calculated results obtained at this stage are not a point of interest, as they are equal to those given in the defined test system [56]. The reproduction of these values is evidence that the developed model is capable of correctly modelling the expected behaviour.

For the model to reproduce the load point availability results of the test system, the following assumptions are made:

- Protection and reconfiguration equipment cannot fail.
- Fault protection devices (CBs, fuses) operate instantly.
- All failure are detected at the time that they occur.
- All state transition rates are exponentially distributed, and thus are Markovian and unchanging in time.
- The isolation rate, $\sigma$ is not affected by the number of faults that have failed at any time.

These assumptions are typical and reasonable when considering a day-to-day system. However later analysis removes some of these assumptions, and these are discussed at that point in the chapter.

The first step of constructing an SRN is to evaluate and group the relevant assets, based on their adjacent assets, as well as adjacent protection and reconfiguration equipment. As stated, assets which are not separated by reconfiguration or protection equipment should be aggregated. The subsystems which correspond to these grouping will be now defined, and referred to in SRN which will be constructed using them, seen in Figure 4.1. The groupings are as follows, each of which has it's related subsystem denoted in the Figure 4.1:

- (a) Feeder lines L1
- (b) Feeder lines L4
- (c) Feeder lines L
- (d) A lateral line, comprised of L9. and 11/0.415kV Transformer (t5). This will later be referred to as Lat6.
- Substation and 33kV system.
- (e) F2 beyond the ring main (L12, L14).

- (f) Feeder lines L10

The two-place subsystems for laterals 1-5 and lateral 7 have been omitted because they are not used in LP6's reward function which is defined later.

Each of the feeder lines L1, L4, L7 and L10 are represented by the four-place subsystem which was described in Section 4.3.2 and shown in Figure 4.1. The complete SRN for the feeder is presented in Figure 4.2. Laterals not affecting LP6 have been omitted for clarity. This has a total of six subsystems, one for each of the four feeder lines, a two-place subsystem for each lateral and a two-place subsystem for the lines of F2. Due to F2 providing a possible alternate path for each of the LPs, there are two possible configurations of this system for which LP6 can be considered online. These configurations are defined logically in an availability function which will be defined later in this section.

For this analysis, the substation and 33kV section of the system is considered perfectly reliable. They are not included in the developed model or mentioned any further. Again, only the lateral assets relevant to LP6 have been listed. This is because the fuses at the feeder junction of other laterals are to be considered perfect, as was the case with the RG in Chapter 3. If there is a failure on any of the other laterals, the fuse ensures that the other LPs are unaffected.

There are further simplifications which can be made in order to decrease the complexity of the model by reducing the number of required subsystems. First, the lines of feeder F2 are combined into a single, two-place subsystem, with it's sectionalising switch ignored. This is subsystem (e) in Figure 4.2. The reason for this is that regardless of if the lines along the feeders are offline, or isolated, F2 is not available as an alternate supply source. Because of this, the normally-open ring main connecting the ends of feeder F1 and F2 does not open for an outage on F1, since there is no online redundant path available.

Another simplification which has been made is to combine the parameters of the assets on the lateral line which connects LP6 to the feeder, referred to as Lat6, and shown as subsystem (d) in Figure 4.2. There is no equipment dividing the transformer and lateral line, so a failure of either results in the loss of supply to the LP. Both F2 and Lat6 aggregated into two-place subsystems. Note that their transition for $P_{fa}$ to $P_{ok}$ is representative of the whole recovery process, and thus is denoted $T_{re}$.

Now that the feeder SRN has been constructed, each LP can be analysed. Two configurations must now be defined for the reward function, the default configuration, and the configuration which can be used when an alternate path is available. This alternate path is used after reconfiguration after a fault. Both of these configurations require the lateral to be online, because LP6 cannot be connected to the feeder in any configuration in which its lateral has fa iled. These configurations are now described in detail, but the overall approach being used can be applied to other LPs.

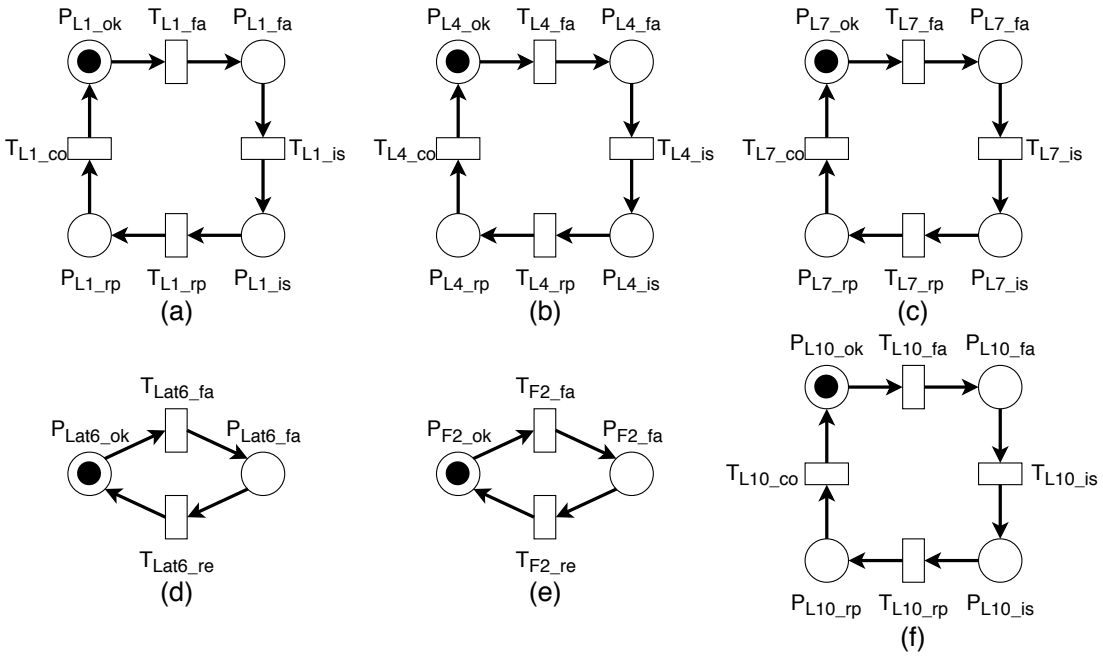


**Figure 4.2** SRN for LP6 of RBTS Bus2 Test system. Lat6 represents the combination of the lateral line L9 and transformer t6.

The normal path of supply for LP6 requires the three feeder lines which connect it to the source (L1, L4 and L7) to be online, and connected (i.e. their subsystem token must sit in $P_{ok}$). The final line of the feeder (L10) must either be online, or failed and isolated (i.e. the token must not sit in $P_{fa}$). This is due to the CB which sits at the base of F1. LP6 is not supplied through L10, but if L10 were to fail, the CB would operate and bring the whole feeder offline, and therefore LP6 too.

The alternate path of supply is used in situations where feeder lines L1 or L4 have failed. In these cases LP6 can be connected to the redundant feeder F2 through the normally-open ring main.[4] This path supplies LP6 if L1 and L4 are either online, or isolated from LP6. Note that as with the normal path, L7 must be ok and connected, since this is the feeder line that Lateral 6 connects to and therefore cannot be separated from LP6.

The final part of the SRN which must be defined for analysis is the availability reward function. This function is based on the two described paths, and also enforces that the lateral and L7 are online. For completeness, all of the availability reward functions are found, including that of LP6, in Table 4.2. The input parameters for the SRN model are defined in Table 4.1. The resulting availability values, as well as the system metrics, are equal to the ones given in the test system in reference [56].

[4]Note, as was mentioned earlier, operation of the ring main operation is incorporated into the isolation rate, $\sigma$

| Name | Attached Transition | Description | Assigned Value |
|---|---|---|---|
| $\lambda_{L1}$ | $T_{L1\_fa}$ | L1 Failure Rate | 0.048 $yr^{-1}$ |
| $\lambda_{L4}$ | $T_{L4\_fa}$ | L4 Failure Rate | 0.048 $yr^{-1}$ |
| $\lambda_{L7}$ | $T_{L7\_fa}$ | L7 Failure Rate | 0.048 $yr^{-1}$ |
| $\lambda_{L10}$ | $T_{L10\_fa}$ | L10 Failure Rate | 0.039 $yr^{-1}$ |
| $\sigma_{L1}$ | $T_{L1\_is}$ | L1 Isolation Rate | 8760 $yr^{-1}$ |
| $\sigma_{L4}$ | $T_{L4\_is}$ | L4 Isolation Rate | 8760 $yr^{-1}$ |
| $\sigma_{L7}$ | $T_{L7\_is}$ | L7 Isolation Rate | 8760 $yr^{-1}$ |
| $\sigma_{L10}$ | $T_{L10\_is}$ | L10 Isolation Rate | 8760 $yr^{-1}$ |
| $\mu'_{L1}$ | $T_{L1\_rp}$ | L1 Repair Rate | 2920 $yr^{-1}$ |
| $\mu'_{L4}$ | $T_{L4\_rp}$ | L4 Repair Rate | 2920 $yr^{-1}$ |
| $\mu'_{L7}$ | $T_{L7\_rp}$ | L7 Repair Rate | 2920 $yr^{-1}$ |
| $\mu'_{L10}$ | $T_{L10\_rp}$ | L10 Repair Rate | 2920 $yr^{-1}$ |
| $\sigma_{L1}$ | $T_{L1\_co}$ | L1 Reconnection Rate | 8760 $yr^{-1}$ |
| $\sigma_{L4}$ | $T_{L4\_co}$ | L4 Reconnection Rate | 8760 $yr^{-1}$ |
| $\sigma_{L7}$ | $T_{L7\_co}$ | L7 Reconnection Rate | 8760 $yr^{-1}$ |
| $\sigma_{L10}$ | $T_{L10\_co}$ | L10 Reconnection Rate | 8760 $yr^{-1}$ |
| $\lambda_{Lat6}$ | $T_{Lat6\_fa}$ | Lat6 Failure Rate | 0.063 $yr^{-1}$ |
| $\lambda_{F2}$ | $T_{F2\_fa}$ | F2 Failure Rate | 0.087 $yr^{-1}$ |
| $\mu_{Lat6}$ | $T_{Lat6\_re}$ | Lat6 Recovery Ratey | 170 $yr^{-1}$ |
| $\mu_{F2}$ | $T_{F2\_re}$ | F2 Recovery Ratey | 1752 $yr^{-1}$ |

**Table 4.1** Parameter defintions and values for LP6 SRN model

## 4.4 SENSITIVITY ANALYSIS

### 4.4.1 Introduction

This section conducts sensitivity analysis on the test system, using the model developed in Section 4.3. There are two goals for this analysis. The first is to demonstrate how sensitivity analysis is conducted with SRNs. The second is to present the insights which can be obtained and to contrast them with the results of the similar analysis performed in Chapter 3. Overall, this section presents a means of assessing important assets when considering the availability of distribution grid LPs, and including the influence of the recovery process to this result.

The approach for this analysis is looking at three of the different parameters which affect feeder lines related to each LP. First, the influence of the parameters failure rate ($\lambda$) and recovery rate ($\mu$) values is investigated. Analysis is applied to LP6, so the results can be compared with those of Chapter 3. This comparison can be used to verify each method, and also to assess the differences between them. The third parameter which will be evaluated is the isolation rate ($\sigma$) parameter. This will reveal how this parameter influences the LP availability, and what benefits could be achieved by reducing it. Note that the isolation rate encompasses all the location, and reconfiguration steps required to isolate a feeder line. As with the sensitivity analysis in Section 3.5, the recovery time

| **Reward Function** | **Load Point** | **Definition** | |
|---|---|---|---|
| $ss\_avail\_LP1()$ | LP1 | 1: if($\#P_{L1\_ok} == 1$ && $\#P_{Lat1\_ok} == 1$ && ($\#P_{L4\_failed} == 0$ && $\#P_{L7\_failed} == 0$ && $\#P_{L10\_failed} == 0$) | 0: otherwise |
| $ss\_avail\_LP2()$ | LP2 | 1: if($\#P_{L1\_ok} == 1$ && $\#P_{Lat2\_ok} == 1$ && ($\#P_{L4\_failed} == 0$ && $\#P_{L7\_failed} == 0$ && $\#P_{L10\_failed} == 0$) | 0: otherwise |
| $ss\_avail\_LP3()$ | LP3 | 1: if($\#P_{L4\_ok} == 1$ && $\#P_{Lat3\_ok} == 1$ && ($\#P_{L1\_ok} == 1$ && $\#P_{L7\_failed} == 0$ && $\#P_{L10\_failed} == 0$) \|\| ($\#P_{L1\_failed} == 0$ && $\#P_{L7\_ok} == 1$ && $\#P_{L10\_ok} == 1$ && $\#P_{F2\_ok} == 1$)) | 0: otherwise |
| $ss\_avail\_LP4()$ | LP4 | 1: if($\#P_{L4\_ok} == 1$ && $\#P_{Lat4\_ok} == 1$ && ($\#P_{L1\_ok} == 1$ && $\#P_{L7\_failed} == 0$ && $\#P_{L10\_failed} == 0$) \|\| ($\#P_{L1\_failed} == 0$ && $\#P_{L7\_ok} == 1$ && $\#P_{L10\_ok} == 1$ && $\#P_{F2\_ok} == 1$)) | 0: otherwise |
| $ss\_avail\_LP5()$ | LP5 | 1: if($\#P_{L7\_ok} == 1$ && $\#P_{Lat5\_ok} == 1$ && ($\#P_{L1\_ok} == 1$ && $\#P_{L4\_ok} == 1$ && $\#P_{L10\_failed} == 0$) \|\| ($\#P_{L1\_failed} == 0$ && $\#P_{L4\_failed} == 0$ && $\#P_{L10\_ok} == 1$ && $\#P_{F2\_ok} == 1$)) | 0: otherwise |
| $ss\_avail\_LP6()$ | LP6 | 1: if($\#P_{L7\_ok} == 1$ && $\#P_{Lat6\_ok} == 1$ && ($\#P_{L1\_ok} == 1$ && $\#P_{L4\_ok} == 1$ && $\#P_{L10\_failed} == 0$) \|\| ($\#P_{L1\_failed} == 0$ && $\#P_{L4\_failed} == 0$ && $\#P_{L10\_ok} == 1$ && $\#P_{F2\_ok} == 1$)) | 0: otherwise |
| $ss\_avail\_LP7()$ | LP7 | 1: if($\#P_{L10\_ok} == 1$ && $\#P_{Lat7\_ok} == 1$ && ($\#P_{L1\_ok} == 1$ && $\#P_{L4\_ok} == 1$ && $\#P_{L7\_ok} == 1$) \|\| ($\#P_{L1\_failed} == 0$ && $\#P_{L4\_failed} == 0$ && $\#P_{L7\_failed} == 0$ && $\#P_{F2\_ok} == 1$)) | 0: otherwise |

**Table 4.2** Availability functions for LP1-LP7 of RBTS Bus 2 test system.

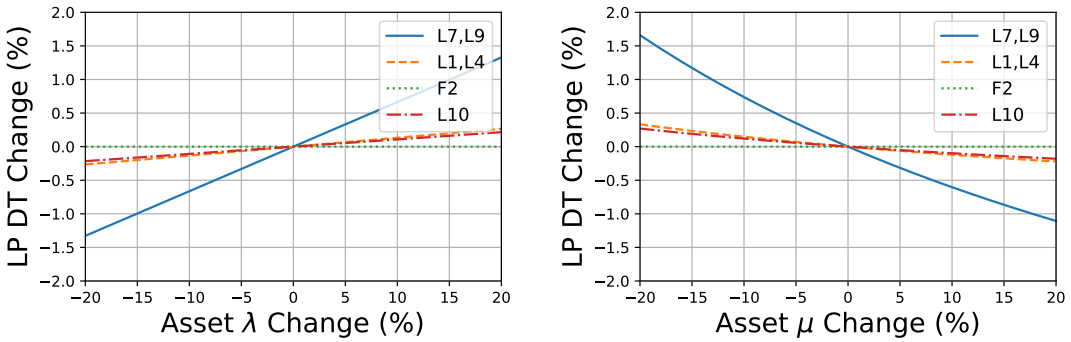


(a) Sensitivity of LP DT to $\lambda$ of each line.

(b) Sensitivity of LP DT to $\mu$ of each line.

**Figure 4.3** Sensitivity analysis of LP6 DT to $\mu$ and $\lambda$ using the SRN LP model.

is a combination of the isolation, repair and reconnection transitions. As such, all three of these have been perturbed by the given amount. Note that only L9 of the assets which make up Lat6 has been changed, and this is reflected in the results.

LP down time (DT) will be evaluated in this analysis, instead of availability. This is because availability is bounded between [0,1], and so a change in value does not intuitively convey the actual effect on the system. DT is expressed in units of $hr/yr$.

The sensitivity analysis methodology used in this chapter is the same as in Section 3.5. To summarise, specific parameters of a given model are perturbed by small amounts and the change in system DT calculated. Evaluating the magnitude of the system changes to individual parameter changes conveys how this parameter affects the system.

The main contribution of this section is demonstrating how SRNs can be applied to existing methodology. Often state-based models perturb failure and recovery rates for specific asset types within a system[45], evaluating how these parameters affect a system model. The method in this section conducts analysis differently to this. By assessing at specific asset parameters, rather than system-wide parameters (e.g. assessing L4 failure rate, instead of all line failure rate), individual assets are highlighted and important insight gained. The results in this section also build upon those of Chapter 3 by incorporating a more complex recovery process, in order to assess how this affects the overall system.

### 4.4.2 Load Point Availability Sensitivity

The first parameters to be analysed in this section are $\lambda$ and $\mu$. Sensitivity analysis of these parameters for the developed model is given in Figure 4.3 (a) and (b), respectively. For $\lambda$, L7 and L9 both have the largest slope, and that the feeder lines are fairly flat. The feeder F2 is extremely flat. For $\mu$, the results are similar, though the relationship is inverted because faster recovery leads to reduced downtime.

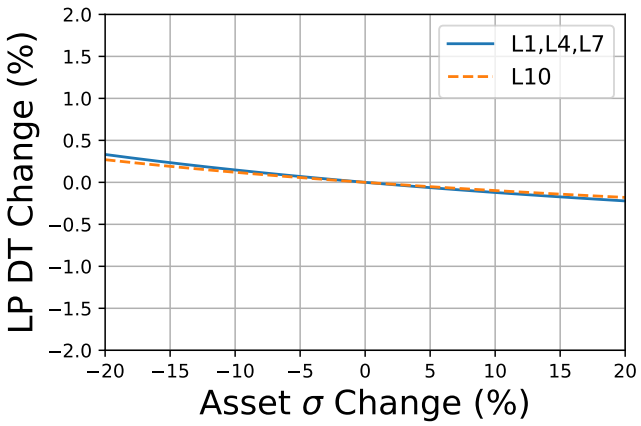


**Figure 4.4** Sensitivity analysis of LP6 DT to $\sigma$ of each line.

These results show that the system is most sensitive to changes in the lines L7 and L9, which are the lines that have no reconfigurable alternatives. The sensitivity to feeder line parameters is due to only the reconfiguration part of the recovery process affecting LP6, because reconfiguration can restore LP6 when any feeder line except L7 fails. The F2 has almost no influence because F2 only has effect on the LP if it fails when it is being used as a redundant source, or is to be used for one.

Comparing the results of the sensitivity analysis of this SRN model to that of the RG model in Section 3.5, the two agree in several parts. First, the effect of both $\lambda$ and $\mu$ of the lines L7 and L9 is the same for both models. This is due to the point raised in Section 3.5, that the reconfiguration time of a feeder line has no influence on the DT of an LP which cannot be isolated from it after an outage. These results also demonstrate that the base system and FAR system in Chapter 3 are the extremes of the contributions obtainable with and without post-outage reconfiguration.

The other parameter of interest for this analysis is the isolation rate parameter, $\sigma$. Only four-place feeder lines have been modelled with this parameter, and so these are the only ones which have been analysed in this section. The Figure 4.4 contains the analysis for the four feeder lines. The influence is almost linear for all of the lines in the result, and the sensitivity is low.

The results in Figure 4.4 convey that the $\sigma$ value has similar influence among all four of the feeder lines. The minor difference in L10 is due to that component having a smaller length and thus varying it has a slightly smaller effect on the DT than the other three. Aside from this, the result shows that the reconfiguration time amongst all feeder lines is equally important to any LP on that feeder.

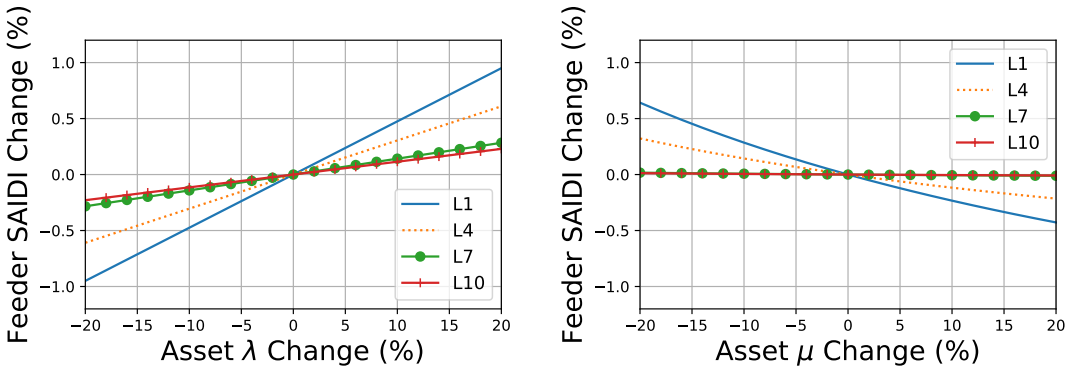


(a) Sensitivity of F1 SAIDI to $\lambda$ of each line.

(b) Sensitivity of F1 SAIDI to $\mu$ of each line.

**Figure 4.5** Sensitivity analysis of feeder SAIDI to $\lambda$ and $\mu$ using an SRN model for each LP.

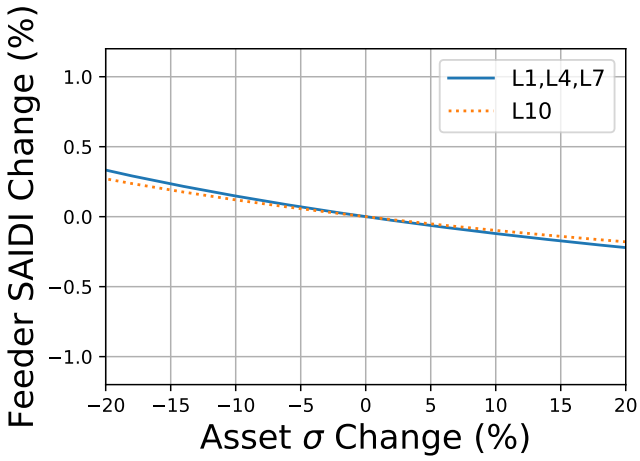


**Figure 4.6** Sensitivity analysis of F1 SAIDI to $\sigma$ of each line.

### 4.4.3 Feeder SAIDI Sensitivity

The SAIDI of F1 for varying $\lambda$ and $\mu$ is given in Figure 4.5. Only the four feeder lines have been included in this analysis, because these are the only four which can be reconfigured. The most influential feeder line is L1, and that L4, L7, and then L10 are next, in descending order.

The results in Figure 4.5 give similar implications to those of the FAR system modelled in Section 3.5. By incorporating a customer-weighted perspective of SAIDI, it is shown that the feeders which are closer to the high-population LPs, and which cannot be isolated from them, are the most influential on system availability measures. Comparing this result to those given in Section 3.5, the assessment of the two results from the RG analysis are edge cases, and the SRN model here lies between the two.

The final analysis of this section is that of the recovery rate ($\sigma$) of each individual

feeder line on F1 SAIDI. This is presented in Figure 4.6. Note that the scale of the axis in this figure spans a larger range. The result shows that the four lines are very similar, despite their locations in the system and the only difference being that of L10, which has a different length to the other three lines. The results show that the influence of $\sigma$ on the feeder SAIDI is not affected by the distribution of customers at individual LPs on the feeder. It should be noted that the sensitivity of F1 SAIDI to $\sigma$ is the same as LP DT.

### 4.4.4 Discussion of Results

Overall, there were two goals of this section. First, to demonstrate the methodology of sensitivity analysis using SRNs, and secondly, to present and compare the insights of the analysis, to those of the RG analysis in Section 3.5. With the LP analysis it was seen that the model is most sensitive to assets which cannot be isolated. This was also a result highlighted in the Reliability Graph (RG) sensitivity analysis. Comparing the results of the two models, RG and SRN, it was seen that the key assets to each LP and feeder model were the same, though their sensitivities change.

The results of the $\sigma$ parameter sensitivity analysis for LP and feeder showed that the influence of each feeder lines' $\sigma$ parameter does not depend on the location of that line along the feeder. This is because all load points are offline for the duration of the isolation phase of any failed feeder line, regardless of their location on the feeder. Because the $\sigma$ parameter is all-encompassing of the isolation process, it does not consider the difficulty of an outage to detect or locate, it's location, or the number of switches which must be operated in order to isolate the outage. An important result of this is that the SRN model is unable to analyse the actual contribution of switching time, or fault location time, in its current form. The next section will present an extension of this model which will allow for the analysis of how individual switches contribute to each LP and their residing feeder.

## 4.5 SWITCH RECONFIGURATION MODEL

### 4.5.1 Introduction

The model which have been developed thus far models LPs using a four-place feeder subsystem. This system accurately models distribution grid behaviour by aggregating the outage location, reconfiguration and recovery steps into a single transition and parameter, $\sigma$. The problem is that it represents the operation of multiple switches, and if interest was in the influence of a single switch, the model in it's existing form cannot convey such information. This section will extend the previous model, so that the distributed switches which are used during reconfiguration to resupply LPs using alternate routes can be analysed.

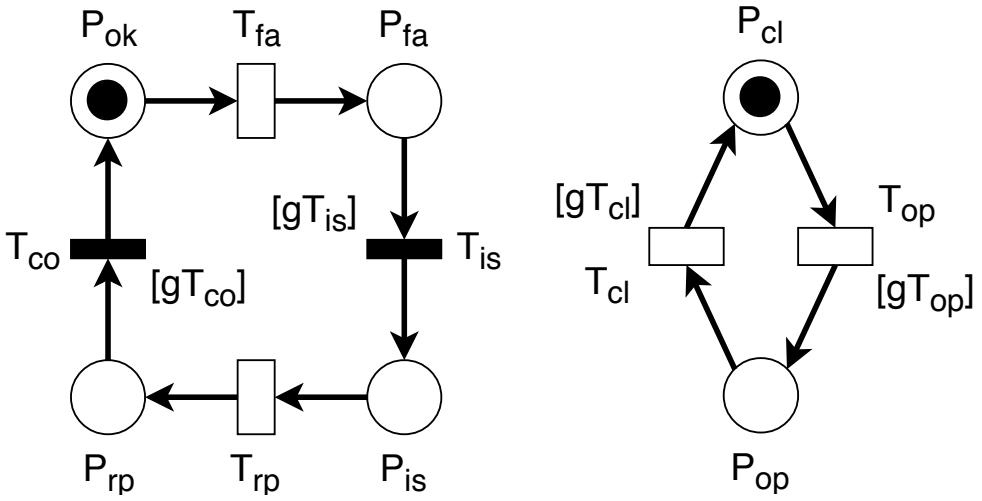


(a) Example modified feeder subsystem (b) Example modified switch subsystem

**Figure 4.7** Representation of four-place feeder subsystems for extended SRN model, with switch operation modelled with two-state subsystem.

By extending this model, specific analysis of the reconfiguration process can be analysed. The operating times of each switch can be altered and the overall effect on the system can be observed. With this, it is possible to determine the switches which are most important to the system, in terms of both availability, and also resilience. The remaining work in this chapter will be centred around investigating the influence of switches on distribution grid availability, and resilience. This section will explain the changes made to the SRN for the new model, and will then investigate the placement of remote communications to enhance availability.

### 4.5.2 Feeder Model

This section will present the methodology to construct the extended model. In the base SRN model, $T_{is}$, the transition between $P_{fa}$ and $P_{is}$, encapsulates the operation of however many switches are required to isolate a particular feeder. There are three core additions which will be added to extend the model. All of these relate to feeder line subsystems, as these are the subsystems which require the system to reconfigure when an outage occurs on them. The altered representation of feeder lines in the extended model is presented in Figure 4.7.

The most obvious change is the addition of a new subsystem for modelling a switch. Although one switch is shown, it is possible to model a number of these, depending on how many affect the given feeder line grouping. Also, an individual switch subsystem can interact with more than one feeder line. Because the operation of each individual switch is represented by one of these two-place subsystems, the parameters of their

| Guard Function | Transition | Definition | |
|---|---|---|---|
| $gT_{is}()$ | $T_{is}$ | 1: if($\#P_{op} == 1$) | 0: otherwise |
| $gT_{co}()$ | $T_{co}$ | 1: if($\#P_{cl} == 1$) | 0: otherwise |
| $gT_{cl}()$ | $T_{cl}$ | 1: if($\#P_{fa} == 1$) | 0: otherwise |
| $gT_{op}()$ | $T_{op}$ | 1: if($\#P_{rp} == 1$) | 0: otherwise |

**Table 4.3** Guard Functions for SRN feeder line example, Figure 4.7.

transitions can be adjusted, in order to evaluate their influence on the system. This will be discussed further in Section 4.5.3.

The second change made to the model, seen in Figure 4.7, is the addition of guard functions to control the dependence of the feeder line subsystem on the switch subsystem, and vice versa. These are assigned to specific transitions and prevent them firing unless specified conditions are met. They are presented in the diagram in square brackets. Their specific purpose is to prevent the switch from operating unless the feeder line is in a desired state. For example, the feeder line token can moved to $P_{fa}$ at any stage, governed by $T_{fa}$. When the token moves to $P_{fa}$, $T_{is}$ will not fire and move the token further unless the conditions of $gT_{is}()$ are met. The condition of $gT_{is}()$, seen in Table 4.3 amongst the definition of the other guard functions, requires that the switch token has moved to $P_{op}$. Opening and closing rates for the switches are represent by the parameters $\tau$ and $\tau_2$, respectively. Note that these are not the same as the $\sigma$ parameter, which models the whole location and reconfiguration process.

The final change made to the model is the introduction of immediate transitions, $T_{is}$ and $T_{co}$. These are defined as transitions which immediately fire and move a token through them, provided the guard function assigned to them has its conditions met. The symbol for these is a filled in rectangle. In this developed model, every immediate transition has a guard function.

These outlined changes are all that is required in order to incorporate switching time to the model. An example is now produced to demonstrate how the model differs from the base model.

### 4.5.3 Example Analysis

The example developed in Section 4.3.4 will now be extended using the methodology introduced in the previous section. Four switches are considered for the analysis of LP6. The fifth, labeled SW5 in the diagram, has been omitted as its state does not affect LP6, except in circumstances which are already considered in the F2 subsystem.

The first step is to establish the relationship between the switch subsystems and the feeder line subsystems. The three normally-closed sectionalising switches will be open when a feeder line adjacent to them has failed. From the perspective of the SRN

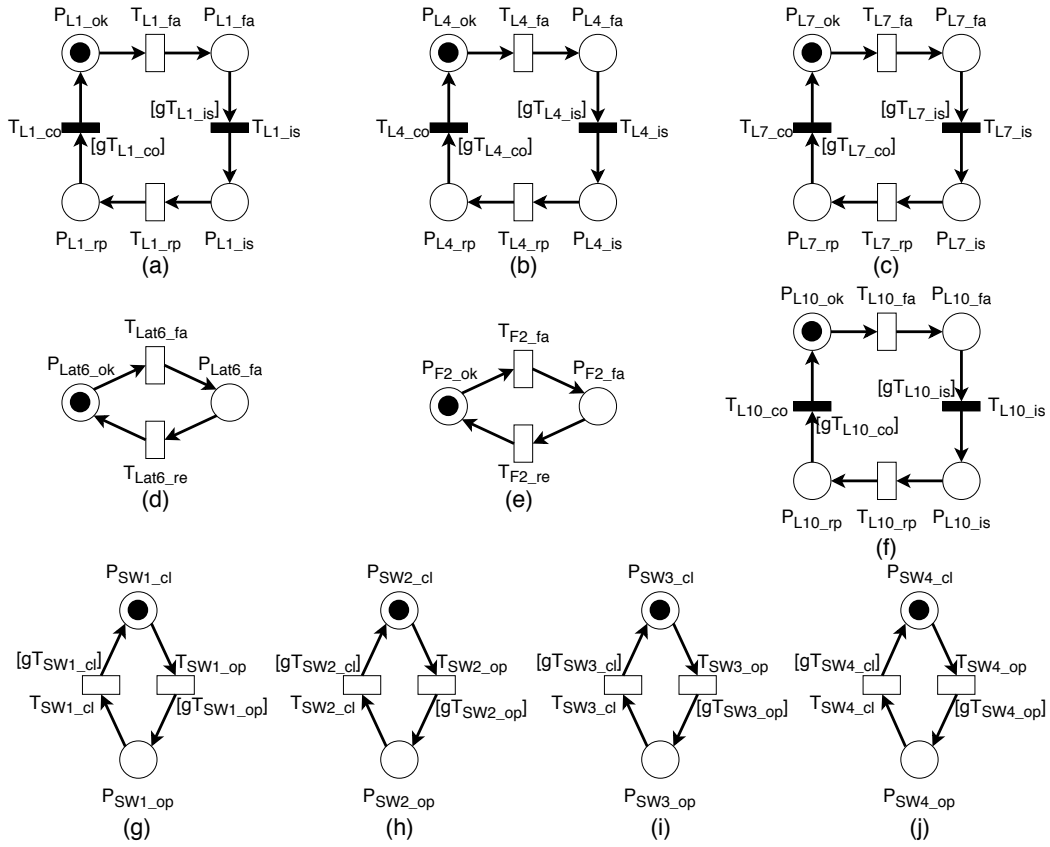


**Figure 4.8** Extended SRN for LP6 of RBTS Bus2 Test system.

and using SW1 as an example, if L1 or L4 have failed, then SW1's $T_{SW1\_op}$, transition should be enabled, allowing the token to move from $P_{SW1\_cl}$ to $P_{SW1\_op}$. *SW1_op* and *SW1_cl* denotes the opening of and closing of switch SW1, respectively.

For the feeder line subsystem, using L4 as an example, once the token is in $P_{L4\_fa}$, the guard for $T_{L4\_is}$, denoted as $gT_{L4\_is}()$, prevents firing until the necessary switches have operated, completing the isolation of L4. The guard functions for the designed model can be found in Table 4.4. For this example, this means that SW1 must have it's token in $P_{SW1\_op}$ and SW2 must have it's token in $P_{SW2\_op}$. Once this condition is met, the conditions of the guard function for $T_{L4\_is}$ will be met, and the L4's token will immediately move to $P_{L4\_is}$. There is no delay for $T_{L4\_is}$ because it is an immediate transition. The process is similar for all of the feeder lines, with the exception of L1, which only requires a single switch to be open for guard conditions to be met.

The normally-open ring main switch, SW4, behaves in a different way that the three sectionalising switches. This switch must close when certain switches have opened to isolate an outage. In order to resupply the LPs downstream of the outage via F2. SW4 must closed when any of the SW1, SW2 or SW3 subsystems have their token in $P_{SWx\_op}$, provided there are no failed assets between the two switches. It must open when any of other the feeder lines, including L10 and F2, fail, or when the isolated feeder line has been repaired.

The parameters for the model are presented in Table 4.5. The extended model is shown in Figure 4.8. Finally, the availability reward functions are defined in Table 4.6.

### 4.5.4 Discussion of Extended Model

This section will discuss the points of difference of this model, and the resulting limitations and benefits. The main difference of this model, compared to the base model, is that it is capable of assessing the system based on the switching time of individual switches. This is done by replacing the isolation transition on four-place substations by an immediate transition and assigning a guard function. This guard function is used to check whether the switches which are used to isolate the section of feeder have done so.

An important outcome of this difference is that the transition from $P_{fa}$ to $P_{is}$ is no longer a set time, but depends on the configuration of switches. Some feeder lines must wait for only a single switch, in order to be isolated (e.g. L1 only requires SW1 to be open), while other require multiple. A limitation stems from this feature. These transitions are exponentially distributed and therefore *memoryless*. The memoryless property means that the *expected time* for an SRN's transition to fire is independent of the time the token has spent waiting for it. This means that the expected time for two transitions to fire is equal to the sum of their mean time to fire values (e.g. mean time to open/close). The result of this property is that two switches are expected to take exactly twice as long as a single switch to operate, even though in the case of

| Guard Function | Label | Definition | |
|---|---|---|---|
| $gT_{L1\_is}()$ | $T_{L1\_is}$ | 1: if($\#P_{SW1\_op} == 1$) | 0: otherwise |
| $gT_{L4\_is}()$ | $T_{L4\_is}$ | 1: if($\#P_{SW1\_op} == 1$ && $\#P_{SW2\_op} == 1$) | 0: otherwise |
| $gT_{L7\_is}()$ | $T_{L7\_is}$ | 1: if($\#P_{SW2\_op} == 1$ && $\#P_{SW3\_op} == 1$) | 0: otherwise |
| $gT_{L10\_is}()$ | $T_{L10\_is}$ | 1: if($\#P_{SW3\_op} == 1$ && $\#P_{SW4\_op} == 1$) | 0: otherwise |
| $gT_{L1\_co}()$ | $T_{L1\_co}$ | 1: if($\#P_{SW1\_cl} == 1$) | 0: otherwise |
| $gT_{L4\_co}()$ | $T_{L4\_co}$ | 1: if($\#P_{SW1\_cl} == 1$ && $\#P_{SW2\_cl} == 1$) | 0: otherwise |
| $gT_{L7\_co}()$ | $T_{L7\_co}$ | 1: if($\#P_{SW2\_cl} == 1$ && $\#P_{SW3\_cl} == 1$) | 0: otherwise |
| $gT_{L10\_co}()$ | $T_{L10\_co}$ | 1: if($\#P_{SW3\_cl} == 1$) | 0: otherwise |
| $gT_{SW1\_op}()$ | $T_{SW1\_op}$ | 1: if($\#P_{L1\_fa} == 1$ \|\| $\#P_{L4\_fa} == 1$) | 0: otherwise |
| $gT_{SW2\_op}()$ | $T_{SW2\_op}$ | 1: if($\#P_{L4\_fa} == 1$ \|\| $\#P_{L7\_fa} == 1$) | 0: otherwise |
| $gT_{SW3\_op}()$ | $T_{SW3\_op}$ | 1: if($\#P_{L7\_fa} == 1$ \|\| $\#P_{L10\_fa} == 1$) | 0: otherwise |
| $gT_{SW4\_op}()$ | $T_{SW4\_op}$ | 1: if($\#P_{L10\_ok} == 0$ \|\| $\#P_{F2\_ok} == 0$ \|\| ($\#P_{SW1\_cl} == 1$ && $\#P_{SW2\_cl} == 1$ && $\#P_{SW3\_cl} == 1$) | 0: otherwise |
| $gT_{SW1\_cl}()$ | $T_{SW1\_cl}$ | 1: if(($\#P_{L1\_ok} == 1$ \|\| $\#P_{L1\_rp} == 1$) && ($\#P_{L4\_ok} == 1$ \|\| $\#P_{L4\_rp} == 1$)) | 0: otherwise |
| $gT_{SW2\_cl}()$ | $T_{SW2\_cl}$ | 1: if(($\#P_{L4\_ok} == 1$ \|\| $\#P_{L4\_rp} == 1$) && ($\#P_{L7\_ok} == 1$ \|\| $\#P_{L7\_rp} == 1$)) | 0: otherwise |
| $gT_{SW3\_cl}()$ | $T_{SW3\_cl}$ | 1: if(($\#P_{L7\_ok} == 1$ \|\| $\#P_{L7\_rp} == 1$) && ($\#P_{L10\_ok} == 1$ \|\| $\#P_{L10\_rp} == 1$)) | 0: otherwise |
| $gT_{SW4\_cl}()$ | $T_{SW4\_cl}$ | 1: if($\#P_{L10\_ok} == 1$ && $\#P_{F2\_ok} == 1$ && ($\#P_{SW1\_op} == 1$ && $\#P_{SW2\_op} == 1$ && $\#P_{SW3\_op} == 1$) | 0: otherwise |

**Table 4.4** Guard Functions for LP6 SRN Model in Figure 4.8.

| Name | Attached Transition | Description | Assigned Value |
|---|---|---|---|
| $\lambda_{L1}$ | $T_{L1\_fa}$ | L1 Failure Rate | 0.048 $yr^{-1}$ |
| $\lambda_{L4}$ | $T_{L4\_fa}$ | L4 Failure Rate | 0.048 $yr^{-1}$ |
| $\lambda_{L7}$ | $T_{L7\_fa}$ | L7 Failure Rate | 0.048 $yr^{-1}$ |
| $\lambda_{L10}$ | $T_{L10\_fa}$ | L10 Failure Rate | 0.039 $yr^{-1}$ |
| $\mu'_{L1}$ | $T_{L1\_rp}$ | L1 Repair Rate | 2920 $yr^{-1}$ |
| $\mu'_{L4}$ | $T_{L4\_rp}$ | L4 Repair Rate | 2920 $yr^{-1}$ |
| $\mu'_{L7}$ | $T_{L7\_rp}$ | L7 Repair Rate | 2920 $yr^{-1}$ |
| $\mu'_{L10}$ | $T_{L10\_rp}$ | L10 Repair Rate | 2920 $yr^{-1}$ |
| $\lambda_{Lat6}$ | $T_{Lat6\_fa}$ | Lat6 Failure Rate | 0.063 $yr^{-1}$ |
| $\lambda_{F2}$ | $T_{F2\_fa}$ | F2 Failure Rate | 0.087 $yr^{-1}$ |
| $\mu_{Lat6}$ | $T_{Lat6\_re}$ | Lat6 Recovery Rate | 170 $yr^{-1}$ |
| $\mu_{F2}$ | $T_{F2\_re}$ | F2 Recovery Rate | 1752 $yr^{-1}$ |
| $\tau_{SW1}$ | $T_{SW1\_op}$ | SW1 Opening Rate | 8760 $yr^{-1}$ |
| $\tau_{SW2}$ | $T_{SW2\_op}$ | SW2 Opening Rate | 8760 $yr^{-1}$ |
| $\tau_{SW3}$ | $T_{SW3\_op}$ | SW3 Opening Rate | 8760 $yr^{-1}$ |
| $\tau_{SW4}$ | $T_{SW4\_op}$ | SW4 Opening Rate | 8760 $yr^{-1}$ |
| $\tau 2_{SW1}$ | $T_{SW1\_cl}$ | SW1 Closing Rate | 8760 $yr^{-1}$ |
| $\tau 2_{SW2}$ | $T_{SW2\_cl}$ | SW2 Closing Rate | 8760 $yr^{-1}$ |
| $\tau 2_{SW3}$ | $T_{SW3\_cl}$ | SW3 Closing Rate | 8760 $yr^{-1}$ |
| $\tau 2_{SW4}$ | $T_{SW4\_cl}$ | SW4 Closing Rate | 8760 $yr^{-1}$ |

**Table 4.5** Parameter definitions and values for LP6 SRN model

| **Reward Function** | **Load Point** | **Definition** | |
|---|---|---|---|
| *ss_avail_LP*1() | LP1 | 1: if(#$P_{L1\_ok}$ == 1 && #$P_{Lat1\_ok}$ == 1 && (#$P_{L4\_failed}$ == 0 && #$P_{L7\_failed}$ == 0 && #$P_{L10\_failed}$ == 0)) | 0: otherwise |
| *ss_avail_LP*2() | LP2 | 1: if(#$P_{L1\_ok}$ == 1 && #$P_{Lat2\_ok}$ == 1 && (#$P_{L4\_failed}$ == 0 && #$P_{L7\_failed}$ == 0 && #$P_{L10\_failed}$ == 0)) | 0: otherwise |
| *ss_avail_LP*3() | LP3 | 1: if(#$P_{L4\_ok}$ == 1 && #$P_{Lat3\_ok}$ == 1 && ((#$P_{L1\_ok}$ == 1 && #$P_{L7\_ok}$ == 1 && #$P_{L10\_ok}$ == 1) \|\| (#$P_{SW1\_op}$ == 1 && #$P_{L7\_ok}$ == 1 && #$P_{L10\_ok}$ == 1 && #$P_{F2\_ok}$ == 1 && #$P_{SW4\_cl}$ == 1) \|\| (#$P_{L1\_ok}$ == 1 && #$P_{SW2\_op}$ == 1) \|\| (#$P_{L1\_ok}$ == 1 && #$P_{L7\_ok}$ == 1 #$P_{SW3\_op}$ == 1))) | 0: otherwise |
| *ss_avail_LP*4() | LP4 | 1: if(#$P_{L4\_ok}$ == 1 && #$P_{Lat4\_ok}$ == 1 && ((#$P_{L1\_ok}$ == 1 && #$P_{L7\_ok}$ == 1 && #$P_{L10\_ok}$ == 1) \|\| (#$P_{SW1\_op}$ == 1 && #$P_{L7\_ok}$ == 1 && #$P_{L10\_ok}$ == 1 && #$P_{F2\_ok}$ == 1 && #$P_{SW4\_cl}$ == 1) \|\| (#$P_{L1\_ok}$ == 1 && #$P_{SW2\_op}$ == 1) \|\| (#$P_{L1\_ok}$ == 1 && #$P_{L7\_ok}$ == 1 #$P_{SW3\_op}$ == 1))) | 0: otherwise |
| *ss_avail_LP*5() | LP5 | 1: if(#$P_{L7\_ok}$ == 1 && #$P_{Lat5\_ok}$ == 1 && ((#$P_{L1\_ok}$ == 1 && #$P_{L4\_ok}$ == 1 && #$P_{L10\_ok}$ == 1) \|\| (#$P_{L1\_ok}$ == 1 && #$P_{L4\_ok}$ == 1 && #$P_{SW3\_op}$ == 1) \|\| (#$P_{SW2\_op}$ == 1 && #$P_{SW4\_cl}$ == 1 && #$P_{L10\_ok}$ == 1 && #$P_{F2\_ok}$ == 1) \|\| (#$P_{SW1\_op}$ == 1 && #$P_{L4\_ok}$ == 1 && #$P_{SW4\_cl}$ == 1 && #$P_{L10\_ok}$ == 1 && #$P_{F2\_ok}$ == 1))) | 0: otherwise |
| *ss_avail_LP*6() | LP6 | 1: if(#$P_{L7\_ok}$ == 1 && #$P_{Lat6\_ok}$ == 1 && ((#$P_{L1\_ok}$ == 1 && #$P_{L4\_ok}$ == 1 && #$P_{L10\_ok}$ == 1) \|\| (#$P_{L1\_ok}$ == 1 && #$P_{L4\_ok}$ == 1 && #$P_{SW3\_op}$ == 1) \|\| (#$P_{SW2\_op}$ == 1 && #$P_{SW4\_cl}$ == 1 && #$P_{L10\_ok}$ == 1 && #$P_{F2\_ok}$ == 1) \|\| (#$P_{SW1\_op}$ == 1 && #$P_{L4\_ok}$ == 1 && #$P_{SW4\_cl}$ == 1 && #$P_{L10\_ok}$ == 1 && #$P_{F2\_ok}$ == 1))) | 0: otherwise |
| *ss_avail_LP*7() | LP7 | 1: if(#$P_{L10\_ok}$ == 1 && #$P_{Lat7\_ok}$ == 1 && ((#$P_{L1\_ok}$ == 1 && #$P_{L4\_ok}$ == 1 && #$P_{L7\_ok}$ == 1) \|\| (#$P_{SW1\_op}$ == 1 && #$P_{L4\_ok}$ == 1 && #$P_{L7\_ok}$ == 1 && #$P_{F2\_ok}$ == 1 && #$P_{SW4\_cl}$ == 1) \|\| (#$P_{SW2\_op}$ == 1 && #$P_{L7\_ok}$ == 1 && #$P_{F2\_ok}$ == 1 && #$P_{SW4\_cl}$ == 1) \|\| (#$P_{SW3\_op}$ == 1 && #$P_{F2\_ok}$ == 1 && PNUMSW4_cl1))) | 0: otherwise |

**Table 4.6** Availability functions for LP1-LP7 of RBTS Bus 2 test system SRN model with switch extension.

two switches, both are enabled. They do not operate in parallel. The result of this limitation on the example system is that in the model, the isolation transition of L1 is twice as fast as those of the other feeder lines because L1 only waits for SW1 while the other feeder lines wait for multiple.

The result of this limitation is a slight deviation of availability values for this model, compared to those of the base model. However, the purpose of this model differs from that of the base model, and therefore this limitation is not restrictive. This model is concerned with the influence of the timing values on the availability of the system, and how altering them affects the overall system. Despite not being able to simulate the operation of multiple switches simultaneously, the model is still able to observe how changing parameters of these switches can improve the overall model, in order to assess which are the most influential on LP and feeder DT and availability. Particularly, in the case of assessing the deployment of communications to enable remote operation of a switches, where the timing values are significantly smaller for the remotely controlled case.

The important point about this model is that it assumes that there is no time taken to detect and locate an outage before reconfiguration. This assumption restricts the applications of the model to only the reconfiguration stage, and therefore cannot be used for placing sensors. The reason this stage of recovery has been excluded from the model is that the focus of this is enhancing the reconfiguration time. The detection, location and remaining parts of recovery which are not considered in this model are given attention in the recovery process model which is developed in Chapter 5.

## 4.6 SWITCH COMMUNICATIONS PLACEMENT AND RESILIENCY ANALYSIS

### 4.6.1 Introduction

The result of Section 4.5 is an SRN model which is capable of modelling an LP with deployed switches modelled as individual subsystems. This extension enables the analysis of the specific contribution that each individual switch makes to the overall system availability, and resilience. The final goal of this chapter, and the focus of this section, is to utilise this modelling method to evaluate and enhance LP availability, feeder SAIDI, and overall resilience of a given distribution grid.

Enhancement of distribution grid switches is conducted by deploying automation enabling communications (AEC). Deployment of this technology allows for a utility to remotely operate distributed switches, and greatly reduce the time required to reconfiguration the distribution grid after a outage has occurred. If a specific number of switches are able to be upgraded, this method will identify the best choices which

provided the largest improvement to either availability and DT, or resilience, depending on the needs of the user.

Two separate approaches will be taken for this analysis. The first approach will be to identify switches on which to deploy AEC, with the purpose of maximising the improvement to availability and DT. The second approach will be to identify switches with which the deployment of AEC will maximise the benefit gained from the perspective of resilience. The enhancement of AEC is simulated by introducing a reduction in the expected time of a switch to open and close. The current models set this time to one hour, where the operation of a switch is manual. For AEC enhanced switches, the expected time will be one minute. Finally, once the two approaches have been taken, the section will compare the two results.

This section is structured as follows. Firstly, sensitivity analysis of the test system will be conducted, looking specifically at the influence of each individual switch. This will be conducted for both LP DT, and for feeder SAIDI. Following this, AEC will be deployed on different configuration of switches, identifying the configuration which produces the greatest improvement to LP availability, and then the same for system SAIDI. After improvements to availability have been determined, the focus will switch to resilience analysis. The configuration of AEC enhanced switches which provides the greatest contribution to resiliency, again at an LP and then feeder level, will be identified. Finally, the section will conclude by comparing the results of the two perspectives, and evaluating the overall method and results.

### 4.6.2 Sensitivity Analysis of Switches

This section will present a sensitivity analysis of the developed SRN switch reconfiguration model. The overall goal of this is to assess how each of the switches in the given distribution grid influences the overall availability of the LP. The approach taken will be the same as was taken in Section 4.4, except that only the parameter $\tau$ of each of the switches will be increased in the analysis. Additionally, the point of interest in this analysis is what benefit switches provide when they are enhanced, so the analysis will focus on the behaviour of the system when the switch operation time is reduced. After sensitivity analysis has been conducted on the LP6 availability, it will be performed for the feeder F1 SAIDI.

#### 4.6.2.1 LP6 Down Time Sensitivity Analysis

The sensitivity analysis of LP6 to its relevant switches can be seen in Figure 4.9. The four switches each have a different amount of influence on the overall LP DT. SW1 and SW3 have the highest amount of influence, but all of them have a noticeable impact on the system. For smaller increases in $\tau$, SW3 provides the greatest reduction to feeder DT. However, the later analysis is concerned with the impact of enhancing $\tau$ for

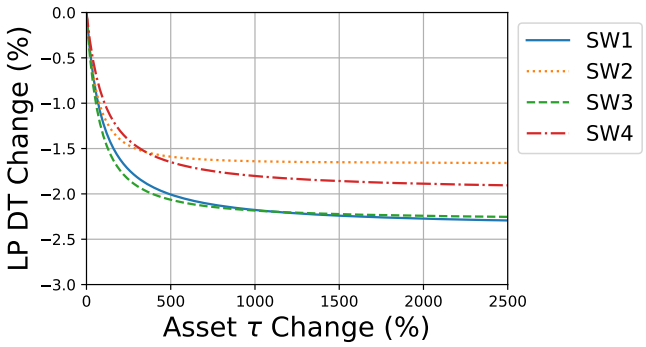


**Figure 4.9** Sensitivity analysis of LP6 DT to $\tau$ of each switch for the extended SRN LP model

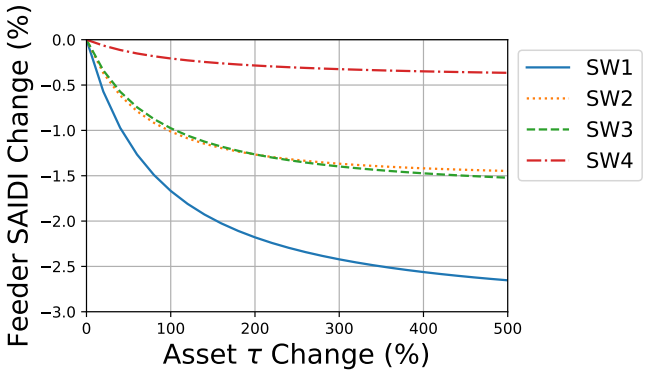


**Figure 4.10** Sensitivity analysis of feeder F1 SAIDI to $\tau$ of each switch for the extended SRN LP model

switches by a significant portion, so this analysis focuses on the affect of these switches by a significant amount.

#### 4.6.2.2 Feeder SAIDI Sensitivity Analysis

Analysis of the feeder SAIDI's sensitivity to each switch is shown in Figure 4.10. Again, only the influence of increasing the switching rate has been presented. It is clear that the most influential switch is SW1, and that SW4 has a relatively small influence of the overall system. As has been seen in previous analysis, an important factor in the sensitivity analysis of SAIDI is the location of customers along the feeder. A significant portion of customer are served by laterals connected to L1, and hence the switch which isolates this line, enabling repairs to start, understandably has the greatest influence on this overall measure.

An important point of note, which is relevant to these results, is how $\tau$ affects each LP. In Figure 4.10, it is seen that SAIDI is much more sensitive to SW1, compared to other switches. The main reason for this is that repair on a feeder does not begin until the isolation process is complete. Therefore, for the LPs on L1, the influence of $\tau$ is the same as that of $\mu$. This means that the contribution which is being provided by

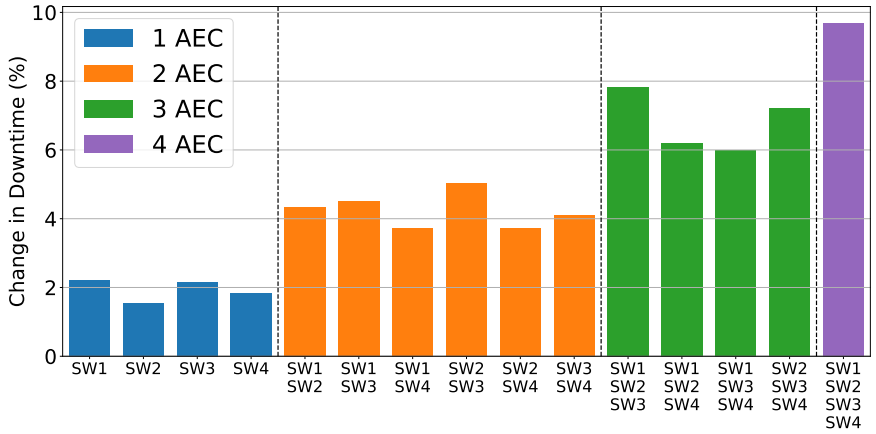


**Figure 4.11** Change in LP6 DT obtained by upgrading various switches with AEC.

SW1 to the system is not due to the isolation of the failed L1, so that the downstream LPs can be restore via F2. It is due to the isolation process delaying the repair of the line which supplies, and cannot be isolated from, two of the most populous LPs. In the case of the failure, the best policy may be to immediately begin repairs and bypass the isolation process, for the sake of overall customer-weighted impact. This might seem counterintuitive, but it is important to consider the impact of policy on this type of analysis.

### 4.6.3 Switch AEC Placement

Analysis of actual achievable reduction in DT which can be provided by enhancing switches with AEC will now commence. As with Section 4.6.2.1, LP6 will be analysed, followed by F1.

#### 4.6.3.1 LP6 Availability Analysis

Figure 4.11 presents the results of analysis of LP6. There are four different categories in this chart, representing different number of switches being upgraded with AEC. This upgrade has been simulated by changing the switches open and close time from one hour to one minute in the model. The figure shows that each additional switch introduced a reduction in expected DT, and the actual contribution is different among combinations.

The results in Figure 4.11 show that if a single switch is to be upgraded with AEC, the biggest expected reduction to LP6's DT can be achieved by deploying the upgrade to SW1, closely followed by SW3. If two upgrades are to be deployed, the best choice to upgrade are SW2 and SW3. Finally, if three are to be upgraded, SW1, SW2 and SW3 will achieve the greatest reduction in DT.

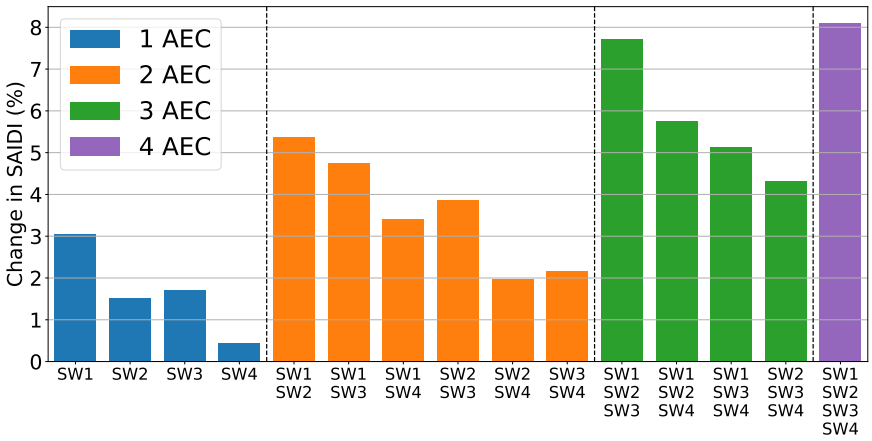


**Figure 4.12** Change in F1 SAIDI obtained by upgrading various switches with AEC.

#### 4.6.3.2 Feeder SAIDI Analysis

Figure 4.12 presents the results of analysis of F1. As with the LP analysis, there are four different categories in this chart and the upgrade has been simulated by changing the switches open and close times to one minute. These results can be used to identify the best combination of switches to choose for each category.

The results in Figure 4.12 show that if a single switch is to be upgraded with AEC, the biggest expected reduction to SAIDI can be achieved by deploying the upgrade to SW1. If two upgrades are to be deployed, the best choice to upgrade are SW1 and SW2. Finally, if three are to be upgraded, SW1, SW2 and SW3 will achieve the greatest reduction in SAIDI. These results will now be compared with the analysis of resilience.

### 4.6.4 Switch AEC Placement for Resilience

In this section, the focus is be on the possible improvement to resilience obtainable from deploying AEC to two switches. This will use the resiliency analysis demonstrated in Section 3.6. There is a total of four switches, and therefore six possible combinations. For this application, the approach will compare systems in a similar way; introducing changes and assessing how the system responds. This comparison will be made for each of the six possible combinations of AEC to two-switches, along with the case where no switches are upgraded, for comparison. The analysis will first look at placement of AEC for specifically LP6, and then for the feeder F1.

The results presented in this section show the DT of each combination of switch pairs along the x-axis, along with the case where no switches has been enhanced with AEC for comparison. Each of these combinations contains five results, the first of which is the case where no parametric change has been introduced. Alongside this result, there are four different parametric changes introduced to the system, one to each of the four feeder lines which make up the bulk of F1. It will be shown the different combinations

of switches deployed with AEC will have differing amounts of resilience to different feeder lines. This will be shown by introducing a significant parametric change to the failure rate of each of the feeder lines. For this analysis, the parametric change is a $\times 100$ increase to the failure rate parameter of the feeder line.

#### 4.6.4.1 LP6 Resiliency Analysis

Analysis of the LP resilience is presented in Figure 4.13. Seven sets of results are presented. It is clear that out of all the individual feeder lines, line L7 has the largest increase, as is expected. Aside from this, each of the remaining feeder lines vary a great deal; in terms of increase in DT due to the parametric change. As was explained in Section 3.6, a system is made more resilient to failures in a specific subsystem, if the change in the systems reliability or availability (in this case DT) is less than what it would be without the upgrade. In this analysis, the more resilient result is represented as a reduction in the resulting DT when a increased failure is introduced, for a given switch combination, when compared to the base system. The terminology used here is that the system is *more* resilience to failures in a given asset, due to the deployed upgrade.

The results show that enhancing SW2,SW3 provides the greatest increase to the resilience of LP6 to L7, which is the line that LP6 is least resilient to. However, the combination does little to increase the resilience of LP6 to L1, or L4; as can be seen by the small improvement when comparing to the system with no switches deployed. The combination of SW1 and SW4 provides the smallest benefit to the resilience of LP6 to failures in L7, but provides a favourable improvement to resilience to L4 and more so to L1. Enhancing SW1 and SW2 increases the the resilience of LP6 to L1 and L4 to the same amount as L10; as well as a increase to the resilience to L7.

Continuing the analysis, the combination of SW2 and SW4 could be considered the least beneficial of all the cases. This provides just a small increase to the resilience of LP6 too a lines. Enhancing SW3 and SW4 provides a similarly ineffective reduction to the resilience of LP6 to most lines, except for L10, which LP6 has been made significantly resilient against. Finally, the contribution from enhancing SW1 and SW3 provides a similarly ineffective benefit to LP6, as that of the SW3,SW4 combination. However, it does make LP6 very resilient to failures in L10.

The decision of which combination of switches should be enhanced with AEC to enhance resilience should be made with consideration of the priorities of the distribution grid utility, as well as environmental considerations. In lieu of this knowledge, it could be said that that combination of SW2 and SW3 provides the greatest gain to overall resilience, as the greatest overall enhancement when combining the four lines is gained from this result; including a significant gain to resilience to L7. However, L7 makes up just a part of the feeder, and it is presented that the improvement to resilience to the

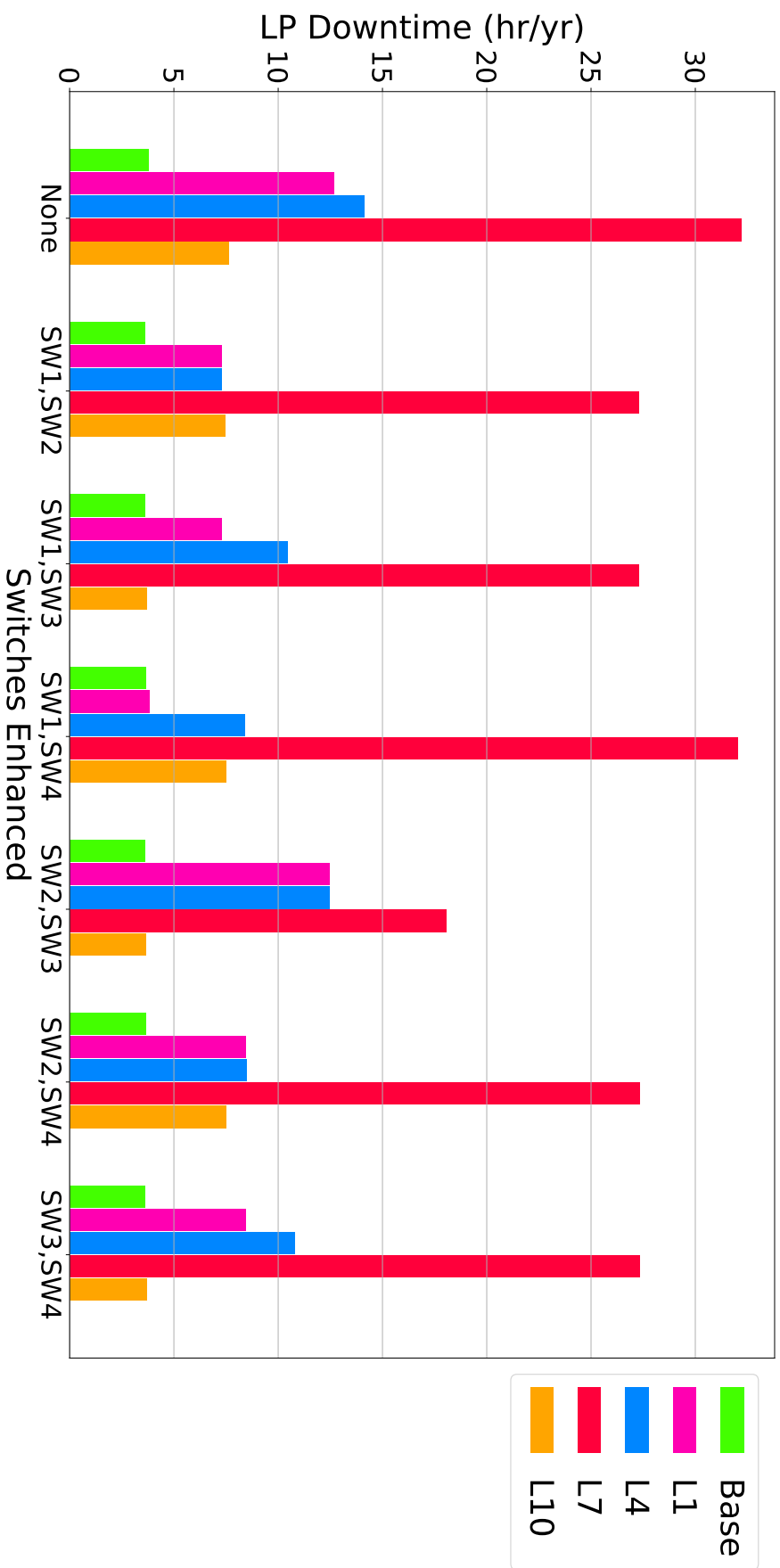


**Figure 4.13** Bar chart of the affect of introducing parametric changes to different feeder lines, for different combinations of switches enhanced with AEC, on LP6.

failures in the L1 and L4 was very small.

If all lines are equally prone to outages, the combination of SW1,SW4 could be considered the best option. This is because this arrangement provides a significant increase to the resilience of LP6 to L1 and L4. As LP6 is already relatively resilient to failures in L10, deploying AEC in this way makes LP6 resilient to all of the lines but L7. The likelihood of assets being affected by events should also be considered. If, for example, L10 runs beside a number of trees which cause frequent outages during severe storms, it could be considered prudent for LP6 to be made most resilient to this line, making SW3,SW4 a viable option.

To summarise these results, it is shown that enhancing each of the different combinations of two-switch pairs with AEC provides a range of different enhancements. The best general case could be considered SW2,SW3; but if more knowledge of the system is obtained, then other options must be considered.

#### 4.6.4.2 Feeder Resiliency Analysis

The resiliency analysis results for feeder F1 are presented in Figure 4.14. As with the LP analysis in Section 4.6.4.1, there are seven sets of results presented, one for each of the six possible switch combinations, and one for the case without any AEC enhancement deployed. Each feeder line has had a significant parametric change introduced to its failure rate. The resulting feeder SAIDI will be analysed to identify the resiliency of the feeder to each of the feeder lines.

The first combination of switches, SW1 and SW2, appears to provide a significant resilience increase of the system to failure of lines L1 and L4, and a slightly smaller increase to L7. It does not provide an increase to resilience to L10 however. The next, SW1 and SW3 provides a similarly significant increase to the resilience to L1 and L7, a lesser increase in resilience to L4, and a favourable increase to resilience to L10. SW1 and SW4 combination provides a reasonable increase in resilience to failures of L1, but less significant for the remaining feeder lines. In all of these cases, enhancement SW1 provides a significant increase to the resilience of the feeder to failures on L1. This can be attributed to reasoning presented in Section 4.6.2.2, where reductions in SW1 directly correspond to reductions in DT from L1.

Next, enhancing SW2 and SW3 is shown to provide a significant increase in the resiliency of the feeder to failures in L7 and L10; but only a small amount to L4 and almost none to L1. The combination of SW2 and SW4 appears to be unfavourable in when compared to the other combinations, in most cases. A small increase in resiliency to L1 is provided, as well as to L4 and L7. Finally, SW3 and SW4 provides a significant increase to resilience to failures in L10, as was the other cases containing SW3, but almost no other benefit to resilience to the other combinations of switches.

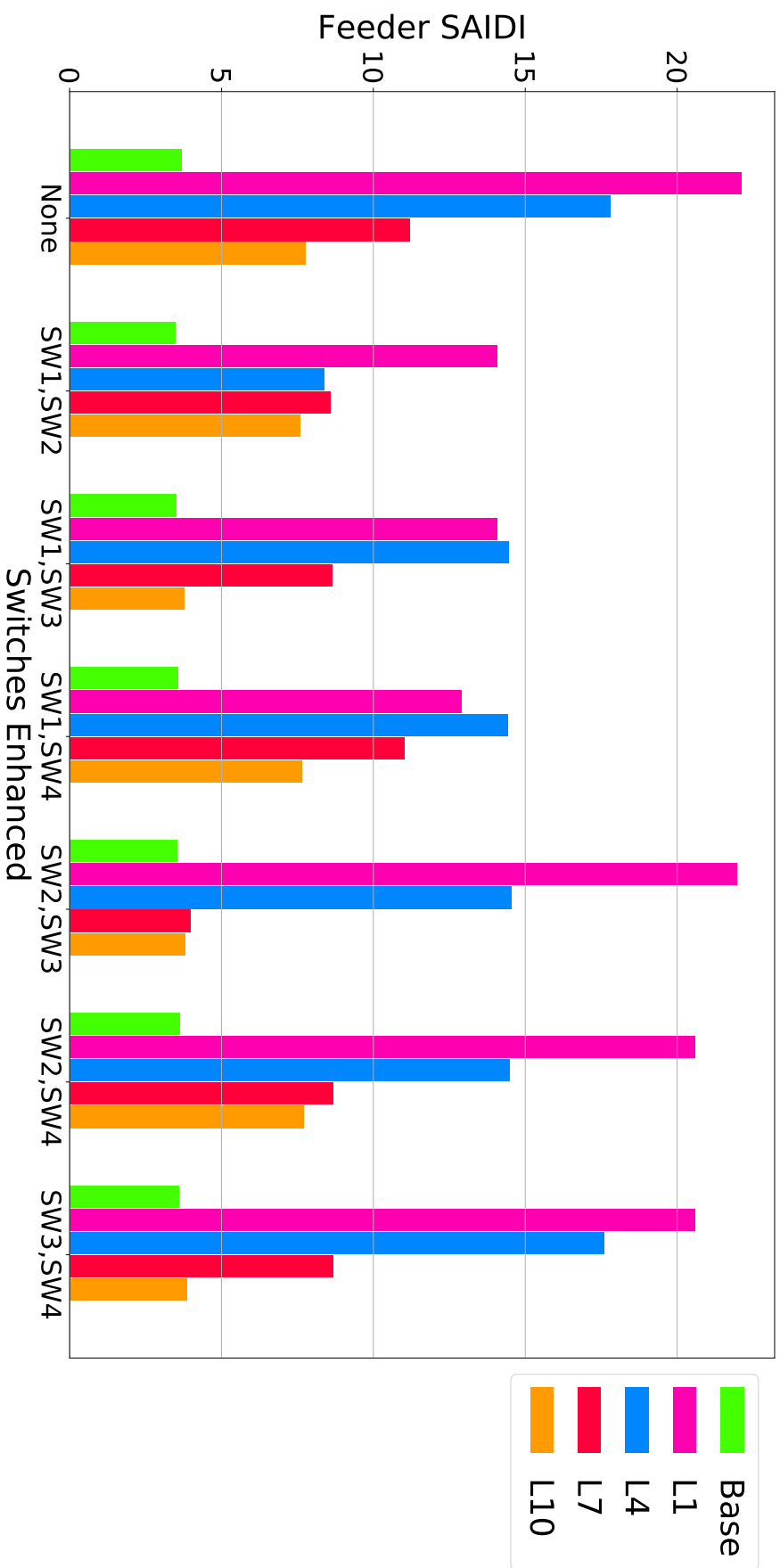


**Figure 4.14** Bar chart of the affect of introducing parametric changes to different feeder lines, for different combinations of switches enhanced with AEC, on F1

The decision of which switch combination provides the greatest contribution to resilience must again be made with consideration of the environment which the grid resides, and take into account any relevant external factors. If the system is taken without any additional information, then the best two switches to deploy AEC to enhance resilience would be SW1 and SW2. However, this solution provides the majority of enhancement through the increase of the feeders resilience to failures in lines's L1 and L4. If it is known that during severe storms, for example, L7 and L10 are more prone to failure than L1 and L4, then the may not be considered the best solution. In such a case, the combination of SW2 and SW3 may be considered a better choice.

### 4.6.5 Discussion of Results

The overall purpose of this section is to demonstrate how the SRN model developed in Section 4.5 is able to be used to analyse the influence of deploying switches on distribution grids. The goal was to utilise the model to evaluate the placement of AEC onto existing switches, to identify switches of which the enhancement would maximise the improvement of either availability, or resilience. It was demonstrated that either of these improvements could be assessed using the model.

The sensitivity analysis for both the LP and feeder showed that the the sensitivity of the systems to individual switches dependent on the magnitude of the perturbation. It is shown that for small perturbations of the switching parameters, LP6 was most sensitive to SW3, but for larger perturbations (10× and greater), SW4 became the most dominant. It was also shown that the two key ways that the deployment of AEC can enhance distribution grid feeders have different amounts of influence on overall availability. Deploying AEC firstly reduced the time take to reconfigure the gird after an asset fails. However, it was seen that the deployment of AEC had bigger influence on availability by reducing the duration recover process for a failed asset. This is evident in the sensitivity analysis of the feeder F1. SW1 has a significantly larger influence on the system that the other four feeder This is due to L1, which connects to a large portion of the population of the feeder, needed to wait for SW1 to isolate is before repairs can begin.

The placement of AEC on to distributed switches was demonstrated to provide a single solution which gives a maximum increase to availability. Placement for resilience however, shows there is potential to place different configurations, depending on the priorities and policies of the utility. This is due to different configurations providing increases in resilience to failures of different parts of the feeder. Knowledge about what effects the feeder, and how the assets behave in bad weather etc, could provide a different, more appropriate choice. This is related to the preparation and retrospective analysis phases which were discussed in Section 1.2.

In Section 3.6, it was seen that the system which has been analysed has a clear lack

of resilience to L1. This is due to the population being primarily fed at the base of the feeder. It was presented that even with the deployment of communications technology, the system will still be vulnerable to severe outages due to the lack of resilience the system has to failures in this line. This has been further reinforced with the results, and sensitivity analysis presented in this chapter.

To summarise this section, the extended SRN model has been applied to a specific analysis using sensitivity analysis and AEC placement methods in order to evaluate the most important switches on the feeder. The overall goal has been to demonstrate that this method is capable of assessing different configurations of AEC deployed to switches, in order to obtain the greatest enhancement to availability, and also to resilience.

## 4.7 DISCUSSION

To conclude this chapter, this section will discuss the overall contributions that have been made, and how this work fits in the overall context of this thesis. It will discuss advantages and limitations of this method, and then describe how this model is to be utilised in later chapters. The contributions are summarised as follows:

- An SRN model is developed to evaluate distribution grid feeders and LPs availability, DT and SAIDI .
- Sensitivity analysis using the developed SRN model was demonstrated.
- The SRN was extended to all the influence of each individual switch to be modelled.
- The extended SRN was used to evaluate the placement of AEC onto switches deployed onto a distribution grid. The AEC contribution to both DT and resilience can be analysed.

Two models have been presented in this chapter, both of which are a novel utilisation of SRNs. It was shown that by using these models, and the functions and other features which are contained within the framework, the complex interactions between distribution grid assets and protections systems can be modelled. By doing so, the performance of the system can be evaluated, and how each individual asset influences this performance can also be observed.

An important limitation which SRN models, one which is well-known for state-based models, is the state-explosion issue. This is a side-effect when attempting to account for dependence with a distribution grid feeder. Because the aim is to account for this dependence, the system state must account for all states of each asset. When an additional $N$-state asset is added to the system, the number of system states is multiplied by $N$, where $N \geq 2$. SRNs do not directly solve the issues of state explosion, but the methodology here reduced the state-space significantly, to a point where it is a

feasible size for any size feeder. The reduction is attributed to the number of switches and protection devices which exist on a feeder. The method of establishing switchable section equivalents to reduces the system to a number smaller subsystems based on the number of sections separated, and bordered by switches. It is proposed that the state-explosion limitation does not nullify the feasibility of this overall method.

The extended model, which was developed in Section 4.5, addresses the need for a model which can account for the influence of each individual switch on system reconfiguration time, and resulting yearly DT. The model does this by introducing individual two-place switches subsystems, with defined transitions rates, and introduces functions which transition a feeder line subsystem from a failed state to an isolated state, after the switch subsystems have operated. The problem with this approach, is the assumption that all of the reconfiguration time for a feeder line is attributed to the switch operation time. In practise, this is not the case. For a standard failure on a distribution grid, there are a number of steps taken to isolate a fault, including detection and location. As this thesis aims to place sensors on a distribution grid, it is important to mention that this model, with only switches, does not assist in the placement of sensors.

This point leads into the discussion of applications of these models in later chapters. The purpose of developing the extended switch model was that the isolation transition in the base model condenses what can be considered a complicated process into a single variable. The switch model approached this by extracting the switches from this transition. Chapter 5 will take a different approach. And additional layer of model will be added, which will replace the single transition value $\sigma$ used in the base model. The purpose of this, will be to holistically model the different parts of the recovery process, including that of detection and location. Both of these are factors important to sensor placement, and therefore must be part of the model. This is the purpose of the recovery model developed in Chapter 5, to extend the base SRN from this section by incorporating detail of the recovery process.

Overall, this chapter has presented a novel means of analysing the complex interactions of assets within a distribution greater, particularly during the recovery process. It presented a method which was used to identify the sensitivity of load points and feeders to individual assets. This was then extended to incorporate the operation of individual switches, and finally used to place communications on these switches in such a way that the overall benefit was maximised for both availability and for resilience.

# Chapter 5

# RECOVERY PROCESS MODELLING

## 5.1 INTRODUCTION

The time taken to recover from an outage on distribution grid can be influenced by many factors. Assets can fail for different reasons, in different locations, and at different times. For example, the location of a fault may be known very quickly after an outage occurs, due to a customer informing the utility that their vehicle has collided with a pole. Conversely, a line fault may be detected by substation circuit breaker operation, and the utility may have no further information. They may be required to reconfigure the feeder multiple times to locate it. This complexity causes a large variance in the recovery time, as was shown in Chapter 2.

Existing methods to model the recovery process apply assumptions which reduce complexity. The recovery process must be modelled with a high level of detail to assess the benefits of Distribution Automation (DA) on resilience. Considering the aim of this thesis, the assumptions which reduce model complexity are restrictive. DA only reduces the duration of specific phases of the recovery process, meaning to evaluate the effect of DA, the recovery process must be broken down so that the model can represent the phases of the process that DA affects.

A recovery process model, novel to distribution grid reliability analysis, is presented in this chapter. It is a phased recovery model, meaning that the durations of each part of the recovery are represented. The purpose this phased recovery model is to add depth to the modelling of the recovery process in order to represent the influence of the different phases. This model deconstructs the recovery process undertaken after an outage, based on the nature of the fault and the steps required to recover from it. It will be used to better analyse the influence of sensors and remote communications on a feeder, and then aid in their placement.

This phased recovery model will be used to evaluate the influence of the different recovery phases. This evaluation will be done using a sensitivity analysis, assessing the effect of altering the duration of each recovery phase on the overall system availability. After this sensitivity analysis, a Stochastic Reward Net (SRN) recovery model will

be utilised to evaluate the placement of sensors on a feeder. The sensor of interest in this analysis is a Fault Indicator (FI). Fault Indicators (FIs) enhance distribution grid recovery by reducing the time taken to locate faults. In their simplest form, they monitor the current of the line they are attached to and signal when they detect the current is at the level of a fault [11]. This operation reduces the fault location time by indicating which side of the FI the outage is on. If the FI has not signalled, the fault is upstream; if it has then the fault is downstream of the FI.

For this analysis, it will be assumed that any FI installed will be capable of signalling remotely, thus their reduction of the search area during an outage is immediate. Analysis of FI has been chosen because there is a well-used and methodology to assess how they affect fault location time. Other sensors could be placed using the developed model, if the effect of such a sensor on the fault location time can be estimated. A method of evaluating how FIs reduce the location time will be briefly explained in Section 5.6.2.

The contributions of this chapter are:

- Development and derivation of a phased recovery model which describes the recovery process, in order to evaluate how DA can contribute to different phases (Section 5.3).
- Evaluating the influence of the duration of different phases of the recovery process, by conducting a sensitivity analysis on the SRN recovery model (Section 5.4).
- Extending the SRN load point (LP) model presented in Chapter 4 by augmenting the recovery transition with the recovery model (Section 5.5).
- Utilising existing FI evaluation methods to extend the SRN recovery model to evaluate the placement of FI on distribution grid feeders (Section 5.6).

Additionally, Section 5.2 presents a comparison of the methodology presented in this chapter with existing methods. Section 5.7 discusses the results and how they fit into the context of this thesis.

## 5.2 COMPARISON WITH RELATED METHODS

Phased recovery modelling is a technique which has been applied regularly to distributed computing applications. References [58] and [59] contain methods which have developed phased recovery models to investigate the recovery methodology of escalating levels of recovery. Though similar, the models developed in the two papers are more focused on the likelihood of specific types of faults occurring, which require specific recovery actions. A distribution grid requires a model where the nature of recovery depends largely on the location of occurrence, and less on the cause of failure.

Reference [25] constructs a phased recovery model for a distribution grid, with the purpose of modelling part of the FDIR process, similar to this chapter. The solution developed in [25] is a model which considers the system response when a communications and automation technology fails, and whether alternate supply routes are available. This solution is not directly useable for the application in this chapter because it does not consider the effects of the location phase of the recovery process and instead it investigates the effects of having DA equipment which can fail. The model developed in this chapter does not allow DA equipment to fail. References [60] and [61] further extend this. [60] incorporates power flow models in the model, and [61] develops a non-Markovian state-space model. All of these existing distribution grid phased recovery models focus on the reconfiguration phase of the recovery process, and not on the other phases of the process. In particular; the process of locating faults, including by means of reconfiguration, has not been addressed.

The phased recovery model developed in this section will be applied to each individual asset. This is different from the existing models discussed, as these are constructed to analyse the recovery process from the perspective of the entire feeder. The fundamental advantage of assessing the recovery from an asset-by-asset basis is that the influence of recovery duration of an individual asset on the whole system be assessed, an important theme of this thesis. Because of this asset perspective, this recovery model can be used to evaluate how the reduction in the duration of specific phases of the recovery model can enhance overall system availability. Further, by extending the phased recovery model, it will be shown that the model can also be used to optimise the placement of FI on a distribution grid, to improve both availability and resilience.

## 5.3 DEVELOPMENT OF RECOVERY MODEL

### 5.3.1 Feeder Recovery

This section will introduce the central parts of the recovery process which will be considered with this model. The fault restoration process can involve all the following phases: detection, location, isolation, repair, and reconnection. These must be performed in this order, however, not every fault requires every phase in the process. For instance, in some situations, the detection/location phase is not required, as the location of the fault is known immediately.

There are a number of different failure contingencies that can occur on a distribution grid, and there are a number of different responses required. For example when sensors transmit information regarding the location of an outage, or when a customer informs a utility of an outage. Alternatively, a fault may occur on a line which is protected by a fuse. In this case, there is no isolation phase because the fuse has reduced the outage to the smallest possible section of feeder. These differences in failure contingencies

each have an influence on the recovery duration, as not performing unnecessary phases results in a reduction in the total time required for the recovery process.

FIs may influence some of the recovery phases, and therefore influence the duration of the recovery process. They are used to help locate faults by reducing the search area during the fault location phase. This includes reducing the number of reconfiguration switch operations needed when locating faults. This research is interested in the placement of these devices so it is essential that this behaviour is accurately modelled.

It has been seen that the recovery process duration is dependent on switch operation time. Chapter 4 quantifies how deploying remotely controllable Automation Enabling Communications (AEC) can reduce the time taken to recover from faults in several situations. Remote switching reduces reconfiguration time and enables restoration even if the location is not known exactly, but a knowledge of the approximate area is. Additionally, switching can play a key role in the location phase of the process. Automated switches enables pre-planned operations to be performed faster.

The purpose of this model is to allow for recovery process to proceed from all of the possible fault recovery phases, and determine which of these has the largest effect on the duration of the recovery process. By doing so, it will be able to assess how the deployment of DA technologies such as FIs and AEC can affect the overall availability of each LP and feeder of a distribution grid.

### 5.3.2 Feeder Recovery Phases

This section will outline the different phases of the phased recovery model, and how they fit into the process as a whole. The flowchart of the recovery process is given in Figure 5.1. It contains a phase-by-phase breakdown of the procedures which are required to recover from an outage on a distribution grid feeder line. There are two different probabilities in this model, representing the possible fault location requirements that different failure contingencies can have. Each of the labeled rectangles represents a time phase of recovery. These two probability values are:

- $p_{loc}$ - Probability that location of fault is discovered at the same time it is detected.
- $p_{ml}$ - Probability that the fault is located manually by a customer or operator, before the system is reconfigured.

Each of these probabilities influence the overall duration of the outage. This is due to the required phases that must be taken to recover from them.

Outages which recloser operation has cleared are not considered, as the outages resulting from these are brief. Common cases where reclosers clear fault is when a branch falls onto an overhead line. If a short circuit occurs and is detected, the recloser will open the circuit briefly, to extinguish the arc, thus in many case removing the outage.

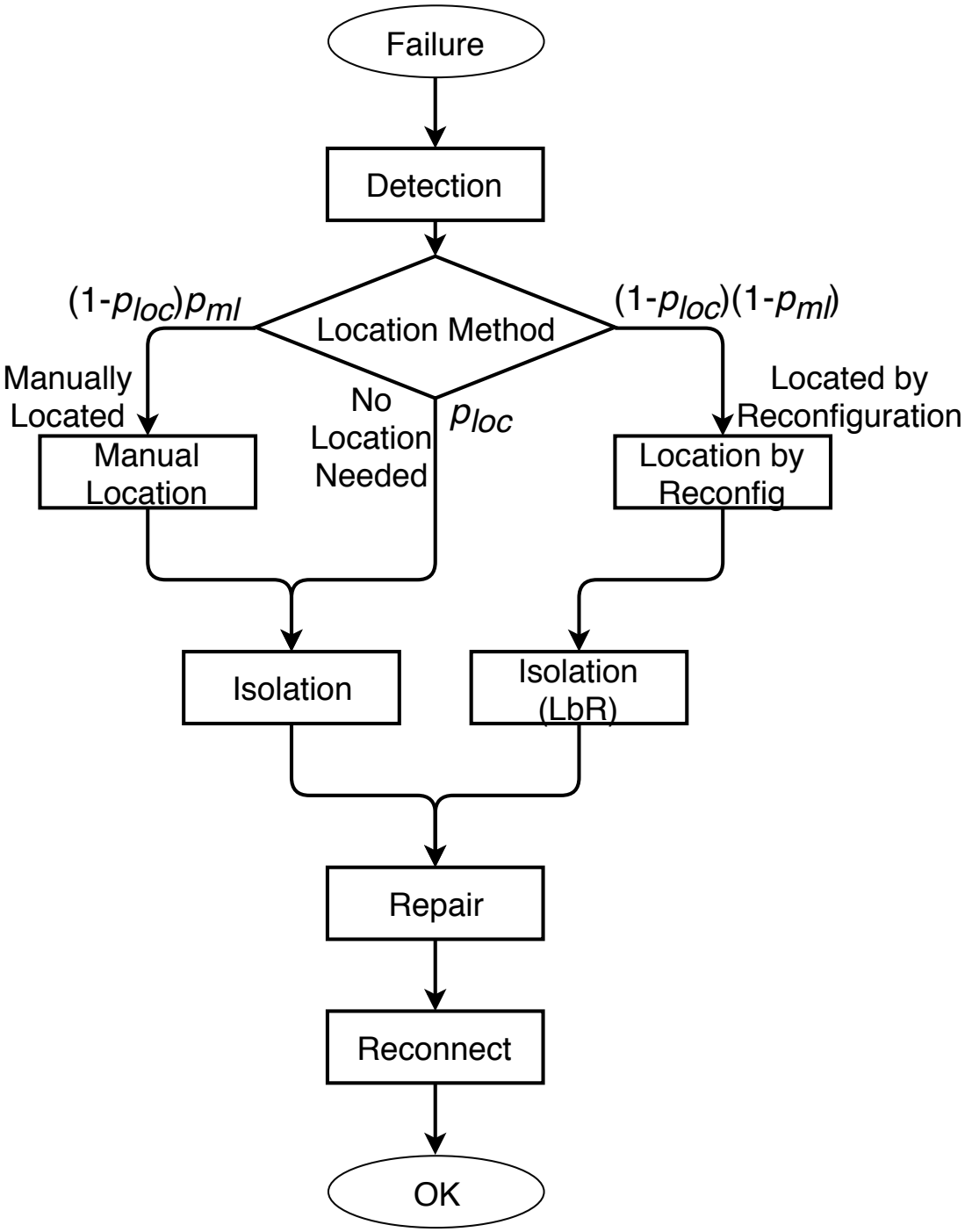


**Figure 5.1** Flowchart of recovery process after an outage.

In a scenario such as this, no recovery measures are required to be taken by the utility. Thus, this recovery model, and the SRN model of Chapter 4 do not consider recloser operation, unless the recloser clearing steps fail, and the recloser opens indefinitely.

A phase-by-phase breakdown of the flowchart will now be given. The first phase is detection. This represents the time taken for the utility to become aware of an outage after it has occurred. This can be as short as minutes or seconds but there are several external factors which can extend this duration. Most distribution grid protection, including fuses, reclosers and circuit breakers observe the current travelling through them.[1] If this current is over a pre-defined threshold, it is considered a *fault current* and the device will operate, opening the circuit. However there are cases in which a fault can occur which does not cause a fault current. In such scenarios a fault may go undiscovered until it is reported by a manual inspection, or by a customer who reports they are without power. The detection time will be longer than if a fault current was generated.

Next the location phases are encountered, beyond a junction which contains the two aforementioned probability values, $p_{loc}$ and $p_{ml}$. If no location phase is needed (with probability $p_{loc}$), the utility can begin the isolation process. The location of a fault when an outage is detected is typically when the occurrence of a fault is reported by a customer or operator of a utility. An example of this could be a customer reporting a broken power line after a vehicle collision. In a situation where the fault location is not known when detected, and is not located manually (with probability $p_{ml}$) the grid must be reconfigured for the fault to be located.

The need for reconfiguration to locate an outage is considered the worst-case scenario for locating a fault. The process is time-consuming and therefore can add significantly to the recovery process time. The method involves energising different sections of the grid using previously planned strategies for each contingency. The utility does this to identify sections of the grid which are not separable from the fault. If a re-energised section of grid trips protection, then the search area can be narrowed down to that section. If reconfiguration is needed to locate a fault, the fault isolation phase is partially completed when the fault is located. Therefore, the duration of this isolation phase is shorter than the other scenario, and this is reflected in the flow chart.

After the fault is isolated to the smallest possible section of grid and all of the reconfiguration is complete, the repair process begins. The actual process of the repair phase depends largely on the asset and the cause of the fault. Typically, the repair process is not influenced by sensors or remote switching, and as such, is not a major focus for this model. Finally, the failed asset is reconnected and all of the reconfiguration is undone, restoring the grid to its default state. Again, the duration of the reconnect

[1] Fuses are passive components which are designed to simply heat up and break when they are exposed to a fault current for some pre-defined amount of time. They don't actively 'observe' a fault current, but their operation can be considered the same as if they did.

phase is unaffected by previous values.

### 5.3.3 Phased Recovery Model

The phased recovery process has been developed into a state-transition model. This was adapted from the flowchart in Figure 5.1. The repair and connect phases have a dashed outline because they are omitted in later analysis. This model is shown in Figure 5.2. Each of the previous phases in the recovery process can be assigned a mean time value. The notation $G(D_x)$ represents the expected duration of phase $x$, where the function $G()$ denotes a generalised distribution.

The model gives the ability to calculate a steady-state MTTR value by creating a closed-form solution. This closed-form solution is a holistic representation of the recovery process, and incorporates all the phases which were discussed in Section 5.3.1. The model is also useful as it enables further analysis. In particular, the model will later be used for sensitivity analysis. The sensitivity analysis will be used to identify key parameters which influence the MTTR value. This is made possibly by the recovery process being separated into distinct phases or phases.

The definitions and mean values for the expected durations are shown in Table 5.1. The probabilities are defined in Table 5.2. These values have been chosen based on experience and discussions with industry experts. The combination of these values make up the Mean Time To Recovery (MTTR) calculated in Chapter 2. This is acceptable for this example application, as the purpose of defining these values is to demonstrate how they affect the recovery process. For analysis of an actual distribution grid, additional measurements and data collection would be required.

Based on the model in Figure 5.2, a closed-form equation has been constructed. This is presented in Equation 5.1.

$$\begin{aligned} &MTTR = \\ &D_{de} + (1 - p_{loc})p_{cl}(D_{ml} + D_{rfi}) + p_{loc}(D_{rfi}) + (1 - p_{loc})(1 - p_{cl})(D_{rl} + D_{rfi,rl}) \\ &+D_{rp} + D_{co} \end{aligned} \tag{5.1}$$

## 5.4 SENSITIVITY ANALYSIS

This section conducts sensitivity analysis using the developed recovery model. The main goal of this analysis is to obtain knowledge of how each of the phases of recovery affect the location and recovery process, and system metrics as a whole. The sensitivity will be analysed by first perturbing the values of each phase duration over a range of percentage values. It will then be performed for each of the probability values in the

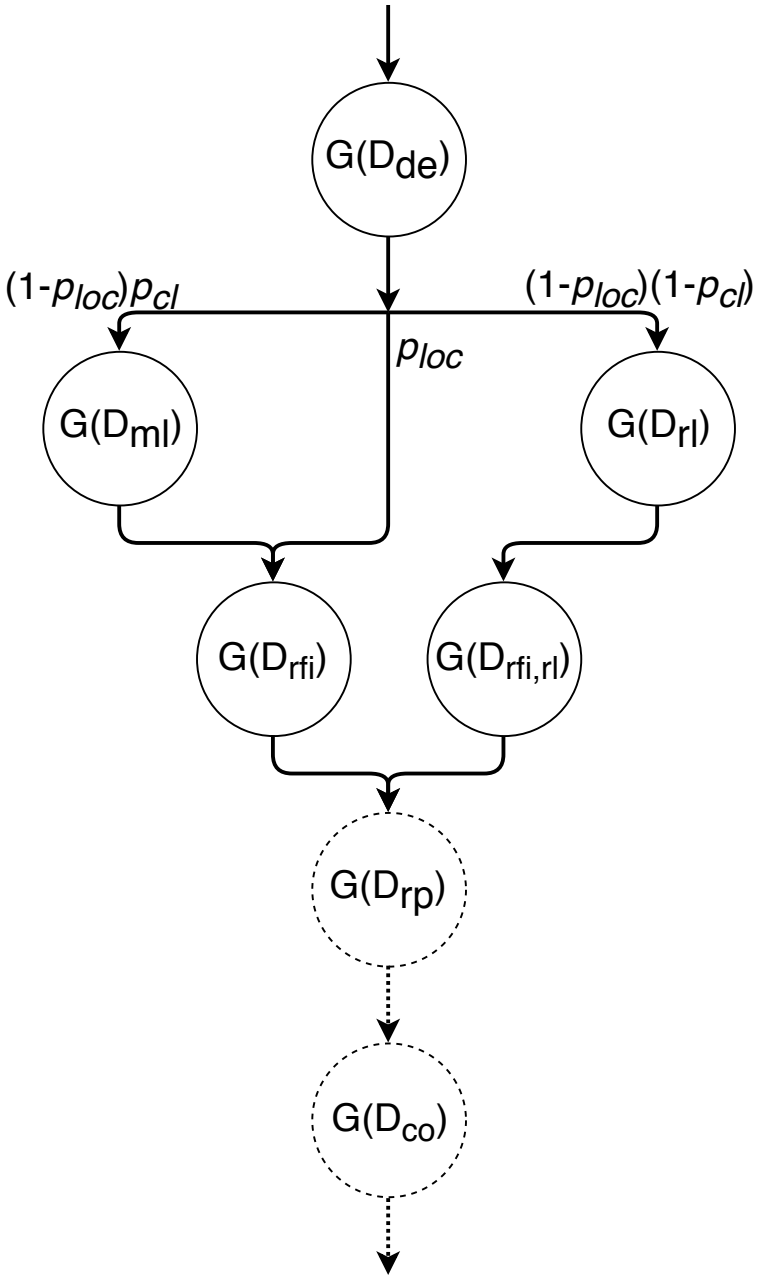


**Figure 5.2** Distribution of outage isolation process model. Phases with dashed outlines represent phases which are omitted in later analysis.

| Duration Name | Symbol | Value (min) | Value (hr) |
|---|---|---|---|
| Detection | $D_{de}$ | 6 $min$ | 0.1 $hr$ |
| Manual Location | $D_{ml}$ | 18 $min$ | 0.3 $hr$ |
| Location with Reconfiguration | $D_{rl}$ | 36 $min$ | 0.6 $hr$ |
| Reconfiguration for Isolation | $D_{rfi}$ | 24 $min$ | 0.7 $hr$ |
| Isolation after Locating with Reconfiguration | $D_{rfi,rl}$ | 24 $min$ | 0.4 $hr$ |
| Repair | $D_{rp}$ | 180 $min$ | 3 $hr$ |
| Reconnection | $D_{co}$ | 60 $min$ | 1 $hr$ |

**Table 5.1** Phase duration definitions and values for recovery model.

| Duration Name | Symbol | Value |
|---|---|---|
| Location Known with Detection | $p_{loc}$ | 0.2 |
| Located Manually | $p_{ml}$ | 0.4 |

**Table 5.2** Recovery probability parameter definitions and values for recovery model.

recovery model. A focus of this analysis is to determine the phases which are the most influential from a recovery perspective. It will demonstrate what impact variation of the duration and probability values have on the overall result.

First, the sensitivity of the system metrics to the phase duration values will be evaluated. Following this, analysis of the model's probability values will be conducted.

### 5.4.1 Recovery Model Sensitivity to Phase Durations

There are two results for the sensitivity analysis of the phase durations, given in Figure 5.3. Figure 5.3 (a) shows the perturbation of each of the phase durations over a range of percentage values, [±50%], along the x-axis, and percentage change to MTTR on the y-axis. For both Figure 5.3 (a) and 5.3 (b), the durations have a linear influence on the MTTR. Figure 5.3 (a) shows that $D_{rl}$ is the most influential phase duration value in the model. This is due to it being the longest duration phase. It should be noted that the probability parameters will affect the slopes of these phase durations.

Figure 5.3 (b) presents the percentage change to MTTR on the y-axis, for each phase duration being set between the range of 0 to 1hr. The point on the x-axis where each duration crosses 0 on the y-axis is the default value for each phase. Conducting this analysis demonstrates the amount of reduction in the MTTR that is achievable by reducing each phase duration. Despite having the biggest slope in the figure, reducing the duration of the detection phases will give the smallest absolute reduction in overall MTTR, because the duration is already short. Reducing $D_{rl}$ will provide the greatest reduction of MTTR, compared to other phase durations. This is because the location phase requiring reconfiguration has the longest duration due to multiple switches requiring operation.

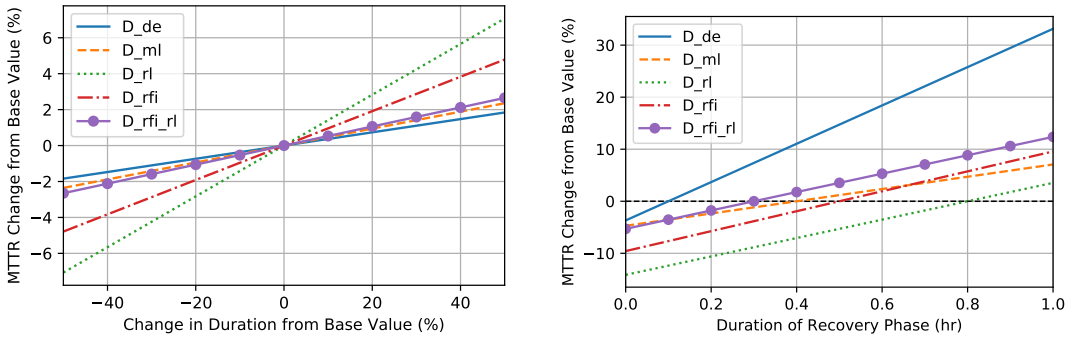


(a) Sensitivity to percentage changes in each phase duration.

(b) Sensitivity to each phase duration set between 0-1 hr.

**Figure 5.3** Sensitivity analysis of recovery model to each phase duration.

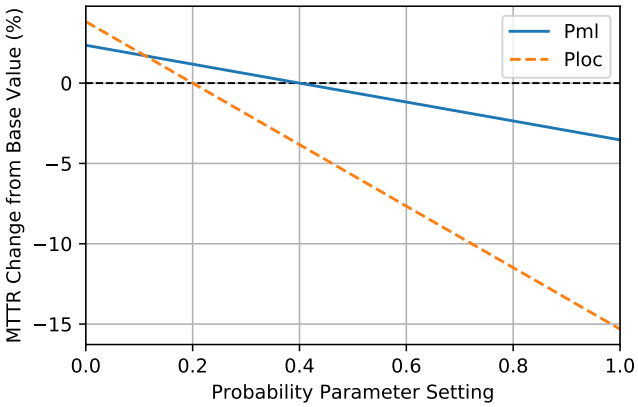


**Figure 5.4** Sensitivity analysis of recovery model to each probability parameter.

### 5.4.2 Recovery Model Sensitivity to Probability Parameters

Sensitivity analysis of the recovery model probability parameters is given in Figure 5.4. As is the case with Figure 5.3 (b), the point on the x-axis where each duration crosses 0 on the y-axis is the default value for each phase duration. $p_{loc}$ has a larger influence on the MTTR than $p_{ml}$. This is expected, as a larger $p_{loc}$ allows the location phase to be bypassed more often. Increased $p_{ml}$ allows for a location phase with reduced duration. Because there is still a location phase, this parameter is less influential.

### 5.4.3 Discussion of Results

This subsection will discuss the results of the sensitivity analysis and their relevance. Of the two results in Section 5.4.1, Figure 5.3 (b) provides the most insight. Figure 5.3 (a) demonstrates that the magnitude of the phase duration has been the dominating reason for the sensitivity. This is due to the percentage change of the large duration phases result in a bigger system change, compared to shorter phase durations. Comparing this

to Figure 5.4 (b), the slope in this result shows the absolute value and thus the actual influence of each phase duration. For example, the slope of the detection phase is the highest. If its duration was increased to the (arbitrary) value of 0.4 $hr$, this would have the largest influence on the MTTR compared to other values, because of its relative magnitude. It should also be made clear that the slope of the phase durations reflect the sensitivity to them. This is slope is a result of the probability of that phase being part of recovery process. The magnitude limits the achievable gains.

The specific phase durations have been chosen based on experience, and to make the MTTR of the model match that of the MTTR observed from the outage data in Chapter 2. If the model's phase durations changed, the sensitivity to them would also change. Hence, the output of a recovery model is different; both for other distribution grids, and also other environments within a single grid.

For example, it would be expected that the parameter $p_{ml}$ would be higher for an urban environment, as the outage is likely to occur in a smaller search area. Similarly, in a rural environment, it would be expected that both $D_{ml}$ and $D_{rl}$ would be longer, as there is likely to be a larger search area. It is important to consider the environment of a feeder or asset when their recovery model parameters are chosen.

This analysis showed that the magnitude of the durations had a large influence on the sensitivity of the system to the probability values. The sensitivity of both the phase durations, and the models' probability parameters, will be different for each system which is modelled. Nonetheless, this method is able to provide useful insight of a systems' recovery process. It can highlight both the significance of each phase duration on the overall MTTR.

## 5.5 SRN BASE MODEL EXTENSION

This section will discuss how the recovery model is utilised by the SRN model introduced in Section 4.3. The model from the previous chapter was referred to as the Base Model, but with the augmentation of the recovery model, it shall henceforth be known as the augmented SRN Model. Recall that this model represented each feeder line as a four-place subsystem. The four places; $\mathrm{P_{ok}}$, $\mathrm{P_{is}}$, $\mathrm{P_{fa}}$, $\mathrm{P_{rp}}$ represent the main states of the feeder line which affect the availability. These are sufficient for analysing asset interaction with feeders, as was shown in Chapter 4. However the focus of this chapter is how the recovery process after a fault can affect a LP or feeder, and so this SRN will be augmented with the phased recovery model developed in Section 5.3.

The task of augmenting the SRN model with the recovery model requires equating each part of the two models. Both models have a repair and reconnection phase, and these two are equivalent. The remaining majority of the recovery model is used to replace the isolation transition of the SRN subsystem. This is illustrated in Figure 5.5. The SRN model assumes all transition rates are exponentially distributed, and thus

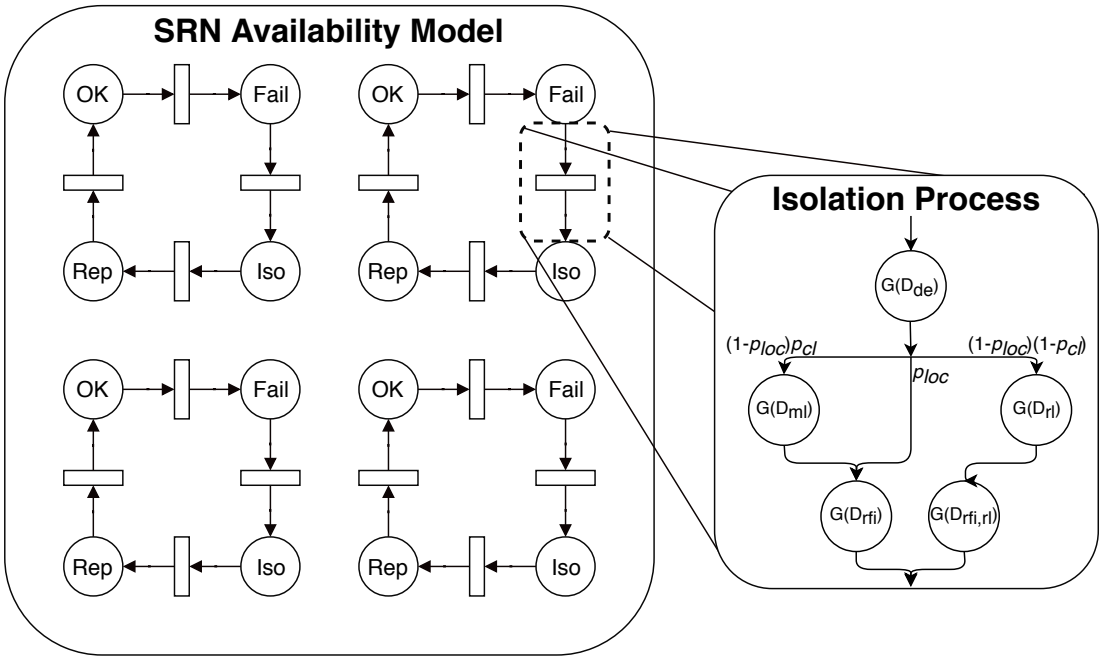


**Figure 5.5** An illustration of the augmented SRN model.

the mean sojourn time of each of the places is the reciprocal of the transition rate. Therefore, the rate at which the transition $T_{is}$ fires, $\sigma = 1/\text{MTTI}$. Mean Time To Isolation (MTTI) makes up a portion of the MTTR output from the recovery model in Equation 5.1. Therefore, MTTI can be derived with the recovery model, and used to define the firing rate of $T_{is}$, $\sigma$. Thus, the equation for $\sigma$ is,

$$\begin{aligned}\sigma &= 1/\text{MTTI} \\ &= 1/(D_{de} + (1-p_{loc})p_{cl}(D_{ml} + D_{rfi}) + p_{loc}(D_{rfi}) + (1-p_{loc})(1-p_{cl})(D_{rl} + D_{rfi,rl}))\end{aligned} \tag{5.2}$$

This model can now be used to investigate the effect of each of the phase durations on an actual system. Observing the sensitivity analysis of reconfiguration rate in Figure 4.4, it was stated that each assets transition rate has the same effect on LP availability and down time (DT). Due to this, the results from the sensitivity analysis in Section 5.4 for the phased recovery model are the same for the LP. This augmented SRN model is now capable of evaluating the effect of adjusting individual recovery phases of an asset, and calculating the effect at LP and system level.

## 5.6 FAULT INDICATING SENSOR PLACEMENT AND RESILIENCY ANALYSIS

### 5.6.1 Introduction

Section 5.5 decribes a SRN model, augmented with the recovery model developed in this chapter. This is capable of analysing the recovery process of individual assets, from the perspective of their feeder. This section will apply the augmented SRN model to evaluate the placement of sensors, specifically FIs, on a distribution grid feeder. Similar to Section 4.6, this analysis will be first done to assess the contribution of different locations of FIs to the reduction of DT, and then for the enhancement of resilience.

Two separate approaches will be taken for this analysis. The first approach will be to identify switches to deploy FI on, with the purpose of maximising the improvement to availability and DT. The second approach will be to identify switches where deployment of FIs will maximise the resilience. The enhancement enabled by the introduction of FIs is simulated by introducing a reduction in the expected time of the fault location phase of the recovery model at each candidate location.

For this analysis, the possible locations for placing FIs will be the junctions between each feeder line, namely the switches. The example system used will be the same used in previous analysis, displayed in Figure 3.1. Possible locations specific to this system are SW1, SW2 and SW3.

The analysis in Section 4.4 revealed that the isolation rate of each asset affects both the LP and feeder as much as any other that is connected to the asset. The best placement to reduce the location time, and thus overall MTTI, will therefore will be the best placement for both the LP DT and the feeder System Average Interruption Duration Index (SAIDI). Because of this, only analysis for DT will be shown. This is not the case for resilience however. Because resilience analysis introduces an additional parametric change, the results differ for LP and feeder.

This section is structured as follows. Firstly FIs will be deployed in to different locations. The locations which produce the greatest improvement to feeder SAIDI will be identified. This will be done by evaluating placement of FIs using the augmented SRN model from Section 5.5. After improvements to availability have been determined, the focus will switch to resilience analysis. The locations of FIs which provide the greatest contribution to resilience will be identified. Finally, the section will conclude by comparing the results of the two analyses.

### 5.6.2 Evaluating the Contribution of Fault Indicators

FIs reduce the location time by diminishing the search area. With the assumption that the *expected* location time along a feeder line is uniform, then the FI will reduce the


**Figure 5.6** Resulting split in fault location time, after the applications of an FI to a $1km$ line.

search time based on the size of the resulting sections. An example $1km$ feeder line is shown in Figure 5.6 with expected fault location time $T_L$. If the FI is placed at $0.33km$ from the base, then the two resulting sections will have location times

$$T_{L,a} = 0.33T_L$$

and

$$T_{L,b} = 0.66T_L.$$

Typically, applying $n$ FIs to a feeder line of length $L$ will result in the line being split into $n+1$ sections. If the expected location time for the feeder line without any FIs is $T_L$; then the location time, $T_{L,i}$ of any section, $i$, can be calculated as;

$$T_{L,i} = T_L \left( \frac{L_i}{\sum_{j=1}^{n+1} L_j} \right) = T_L \left( \frac{L_i}{L} \right). \tag{5.3}$$

This methodology provides a straightforward means of weighting location time, based on the placement of new FIs. There are two phase durations associated with the location time of an outage on a line with length $L$. These are $D_r l$, the time required to locate using reconfiguration, and $D_m l$, the time required to manually locate a fault. Both of these will be reduced using the method of Equation 5.3.

### 5.6.3 Fault Indicator Placement

This section will evaluate the placement of FIs on the test system, with regards to the improvement gained in LP6 DT, and for feeder F1 SAIDI. Analysis will be conducted by inserting different combinations of FIs into the test system, and evaluating the resulting DT or SAIDI. Results will be presented as was done in Section 4.6. The charts will present the percentage of reduction obtained by deployment of FIs to the specified location(s).

#### 5.6.3.1 LP6 Availability Analysis

The contribution of FIs to the enhancement of LP availability is evaluated first. As with previous analysis, demonstrating a change in availability is not intuitive, so reduction in DT will be the measure presented. The upgrade has been modelled by reducing the

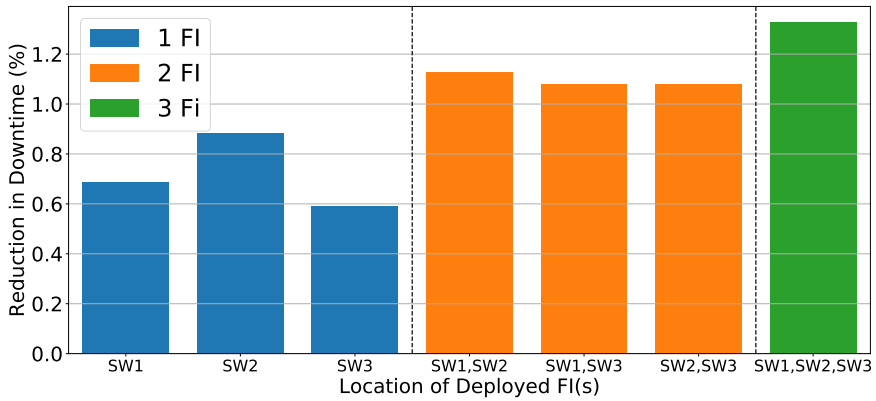


**Figure 5.7** Reduction in LP6 DT obtained by deploying FIs to various locations.

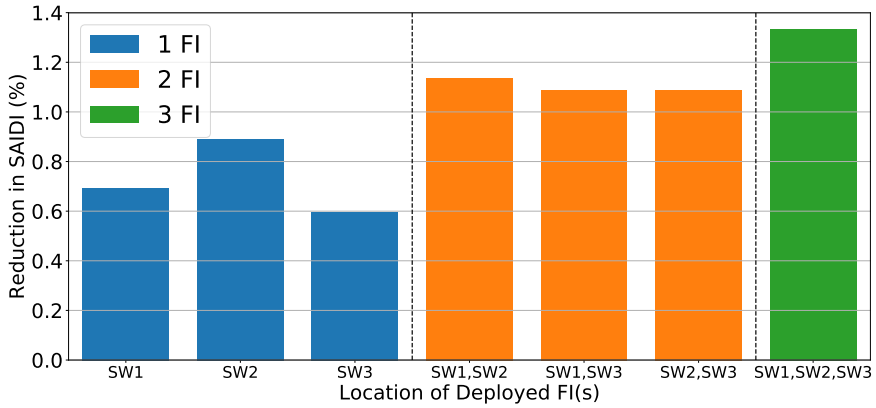


**Figure 5.8** Reduction in F1 SAIDI obtained by deploying FIs to various locations.

location phase durations of the model, according to the method described in Equation 5.3. The result of this analysis can be seen in Figure 5.7.

The results of this analysis show the achievable reduction in DT obtainable by deploying FIs to the locations specified by the switch names. If a single FI is deployed, the best contribution can be obtained by deploying the FI to the location of SW2. For two FIs, the best reduction will be to deploy FIs at the locations of SW1 and SW2.

#### 5.6.3.2 Feeder SAIDI Analysis

Figure 5.8 shows the contribution of FIs to the enhancement of feeder F1 SAIDI. The upgrade has been modelled by reducing the location phase durations, using the method described in Equation 5.3.

The results show the achievable reductions in SAIDI are identical to those of the previous section. This is because reducing a specific asset's isolation time by reducing location time affects all LPs equally. All LPs are forced offline before isolation occurs. Therefore, all LPs will benefit equally, regardless of the location of the asset which has its location time enhanced.

### 5.6.4 Fault Indicator Placement for Resilience

This section will evaluate different combinations of locations to place FIs, for the purpose of enhancing the resilience of LP DT and for feeder SAIDI. The resiliency analysis deployed in Chapter 3 and again in Chapter 4 will be deployed here. Similar methodology used here has been used in Section 4.6.4 for the deployment of AEC for switches. The comparison of resilience will be made for all possible combinations of locations of deployment, for up to three FIs.

The results in this section are presented differently to those in Section 4.6.4. This is because the difference in DT between the no-FI case and all other cases is not as significant, so the results are not as obvious. To conduct the analysis in this section, the results will show the difference (as a percentage) of the DT resulting from an introduced parametric change, compared to that of the system with no FIs deployed. An increase in resilience is represented by the magnitude of the reduction in DT that the location of FIs provide. The reduction is a comparison between that specific combination and the system with no FIs.

Each figure contains seven combinations of FIs, and five results for each combination. The first of the five results is the reduction in DT which the FI(s) provide, before a parametric change is introduced. These percentage values are the same as in Figure 5.7 and Figure 5.8, for LP and SAIDI results, respectively. The other four results for each combination are the amount of difference between the DT of the system with the specified FI location, and the system with no FIs. Both systems have the parametric change introduced.

#### 5.6.4.1 LP6 Resiliency Analysis

Figure 5.9 demonstrates the resiliency analysis of LP6. There are several results in this figure, corresponding to the different possible combinations of locations, where up to three FIs are deployed. The key interest here is the relative magnitude of reduction in DT of each result, when compared to the result of a system with no FIs deployed. The 'base' case represents comparison to the DT of the system when no parametric changes are introduced.

First the cases where a single FI is deployed are analysed. The largest general improvement to resilience is obtained by placing the FI at the location of SW2. This provides a large increase in resilience to failures in lines L1, L4 and L10; and also an increase in resilience to failures in line L7, though not as significant. However, placement at the location of SW1, provides the largest increase in resilience to failures in L1, but less resilience to failures in the remaining three feeder lines. Placement at SW3 provides a similar result, but the increase in resilience is to failures in L10.

Next, the cases where two FIs are deployed are analysed. There are no clear

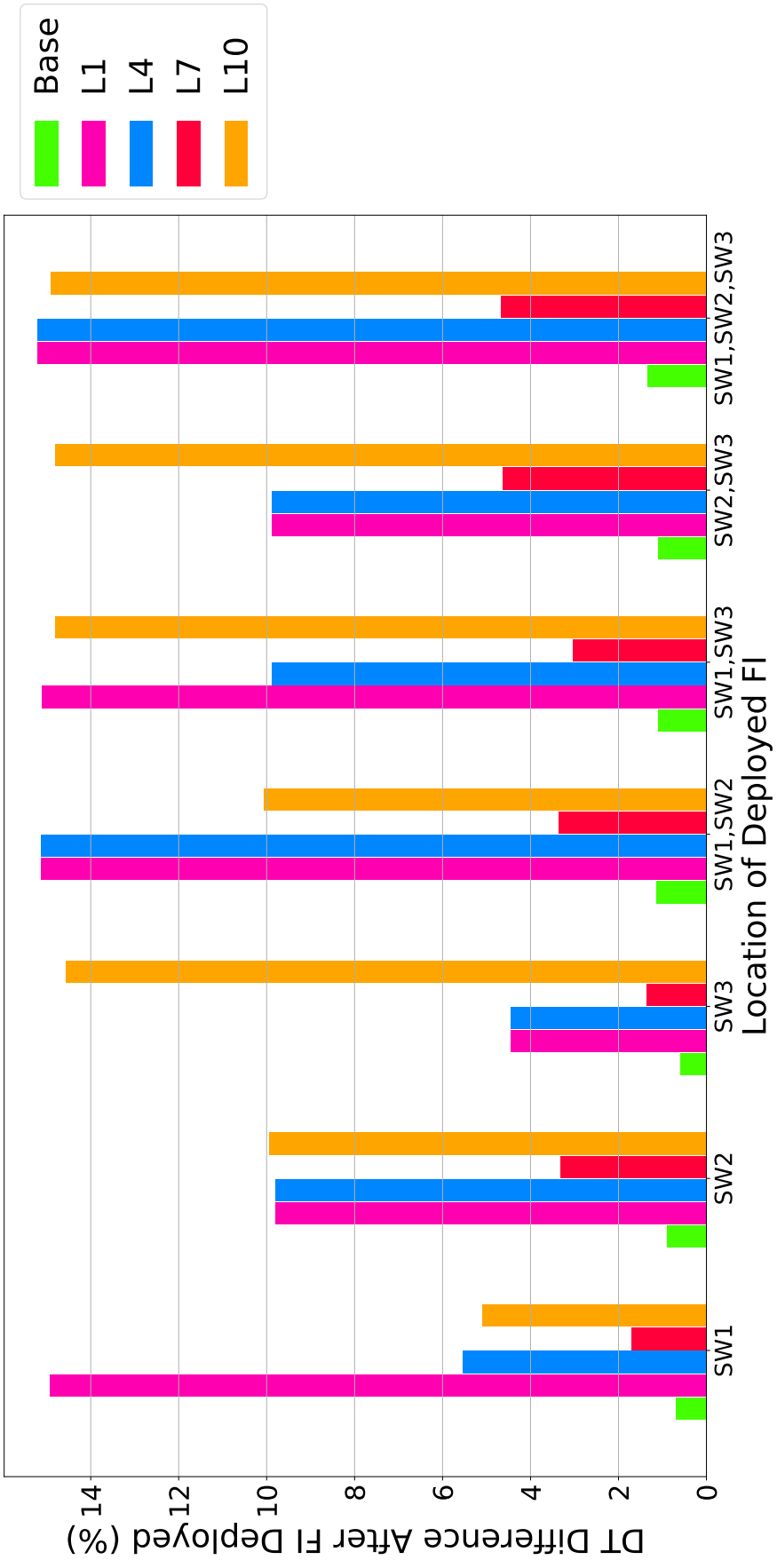


**Figure 5.9** Bar chart of effect of introducing parametric changes to different feeder lines, for different combinations of different locations of placed FIs, on LP6. The results shown are of the reduction in DT, compared to the case where no FIs are deployed.

outstanding results for these combinations, as each provides enhancement in resilience to different lines. Deploying at the locations of SW1 and SW2 provides a significant increase in resilience to failures in lines L1 and L4, and a reasonable increase to L10. Deploying at SW1 and SW3 provides a large increase to the resilience of LP6 to lines L1 and L10, and a reasonable increase to L4. Deploying FIs at SW2 and SW3 provides a significant increase in resilience to failures of L10 and a reasonable increase in resilience to L1 and L4 failures, but less so than other combinations. However, it provides the largest increase in resilience to failures of L7. Finally; as expected, deploying an FI to all three locations provides the largest increase in resilience of all other combinations.

As was stated in Section 4.6.4 the decision of which combination to choose should be made with consideration of the priorities of the utility, and the nature of the grid in regards to environmental factors. For the cases where a single FI is deployed, the greatest enhancement in resilience to all lines could be when an FI is placed at SW2. However, if L1 or L10 are prone to failure in some cases, including during storms, then these might be considered alternative options. For the cases where two FIs are deployed, there is no clear contender, and any of the options are valid, depending on the effects on each line.

#### 5.6.4.2 Feeder Resiliency Analysis

Figure 5.10 shows the resiliency analysis results for feeder F1. As with the LP analysis in Section 5.6.4.1, there are seven sets of results presented, one for each of the possible combinations of locations where FIs can be deployed. Each feeder line has had a significant parametric change to its failure rate. The reduction in the resulting feeder SAIDI will be analysed to identify the increase in resilience of the feeder to each of the feeder lines.

First to be analysed are the single-FI cases. Of the three results, placing the FI at SW2 is the most favourable. It provides the largest increase to resilience to failures in lines L4 and L7, and an equally significant increase in resilience to failures in line L10. Placing at SW1 provides a slightly larger increase to resilience to failures in L1, but overall is the least favourable result due to its relatively small enhancement to resilience to the other lines. Placing at SW3 provides a significant increase to the resilience to failures of line L10, but there is very little resilience gained to failures in the remaining lines.

There is combination of locations with two FIs which is clearly best. Placing FIs at the locations of SW1 and SW2 provides a reasonable increase in resilience to failures on all lines. Deploying at SW1 and SW3 provides the same contribution of resilience to failures in L1, and slightly less resilience gained to failures on L4 or L7, but a significant increase to the resilience to failures on L10. Finally, deploying FIs at the locations of SW2 and SW3 contributes a large amount of resilience to failures in L7 and L10, but a

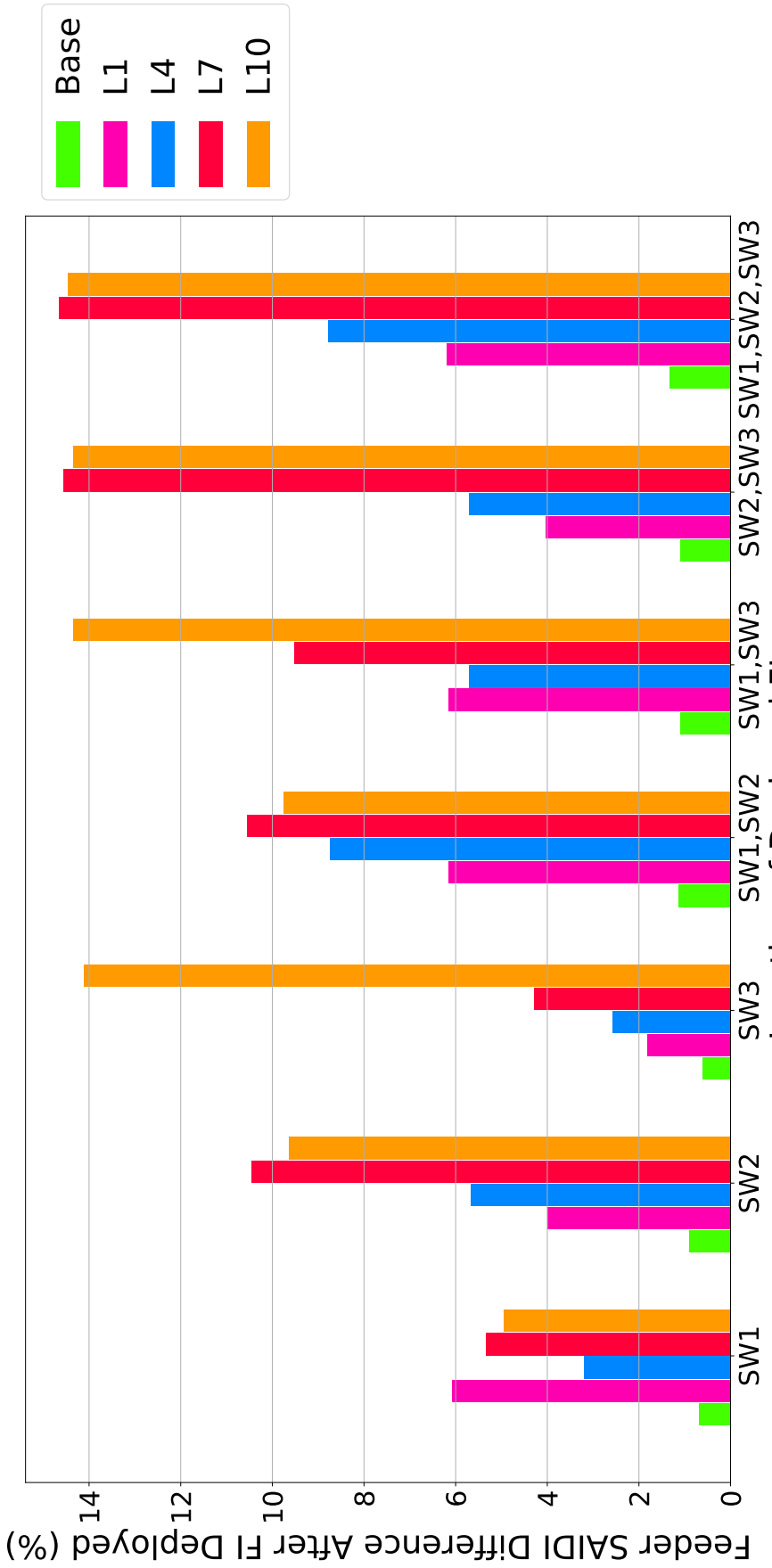


**Figure 5.10** Bar chart of effect of introducing parametric changes to different feeder lines, for different combinations of different locations of placed FIs, on the feeder. The results shown are of the reduction in SAIDI, compared to the case where no FIs are deployed.

smaller amount of resilience to failures on L1 and L4. Finally, deploying an FI to all three locations provides the largest increase in resilience of all other combinations, as expected

### 5.6.5 Discussion of Results

A notable factor of both results is that due to the way that FIs reduce location time, there is little additional benefit gained from the case of deploying three FIs, compared to that of deploying two. This is an important observation from an optimisation perspective, as the actual gain from deploying a third FI may not be worth the financial cost.

Placement of FIs to enhance the availability and SAIDI clearly indicated the key contributions. Regarding resilience, the best locations are less obvious. Placement of FIs in different locations enhanced the system's resilience to failures in different sections of the feeder, both for the LP case and for the feeder case. This was a finding of the analysis of the switch placement model of Section 4.6, which concluded that the utility must decide which lines to prioritise, based on their policy and the environment in which their grid operates. This analysis however, provides a means of evaluating possible locations which meet these requirements. This is related to the prior planning and retrospective analysis phases of resilience, which have been discussed in Section 1.2.

Overall, this section has demonstrated that the recovery model is capable of evaluating the contribution of individually placed FIs on the total availability of an LP or feeder.

## 5.7 DISCUSSION

The purpose of this Chapter is to develop a model for the complex recovery process which takes place when there is a failure on a distribution grid feeder. The specific contributions are listed below.

- Develop a phased recovery model which describes the recovery process with the purpose of evaluating how DA can contribute to different phases.
- Evaluating the influence of the duration of different phases of the recovery process, by conducting a sensitivity analysis on the recovery model.
- Augment the SRN LP model of Chapter 4 with the developed recovery model.
- Evaluate the placement of FIs on distribution grid feeders, using the augmented SRN recovery model.

The phased recovery model which has been developed has a number of benefits which enhance its usability. Firstly, the MTTR is based on the mean durations of each

phase of the recovery process, and the probability that each phase occurs. Its output is distribution-less, and thus straightforward to calculate. A second benefit is that although it can be inserted into state-based models, the model itself is not state-based. Therefore, it can be described by a single equation without evaluating a steady-state solution. Finally the model is a linear combination of each of the expected phase durations. When evaluating the contribution of technology such as DA, it does not require exact knowledge of the phase durations. This is because the contribution can be evaluated by assessing proportional difference made when the technology is deployed.

In the context of this thesis, this model provides the final link that enables evaluation of the recovery process. It allows for the effect of distribution automation to be evaluated at a system level. This enables the placement of technology which reduces the duration of each phase of the recovery process to be evaluated at a system level. The impact of small-scale decisions, such as the placement of an individual FI, are able to be evaluated in the context of the system as a whole.

In summary, this chapter has developed a phased recovery model representing the complex phases of the recovery process. This model was used to evaluate how each phase duration influences the system DT and resilience.. The phased recovery model was then used to augment the SRN model from Chapter 4. This was then used to evaluate the placement of sensors, specifically fault indicators in terms of day-to-day reliability, and in terms of resilience.

# Chapter 6

# DISCUSSION AND CONCLUSION

## 6.1 SUMMARY OF CONTRIBUTIONS

This thesis presents a novel method of evaluating Distribution Automation (DA) and its application to a distribution grid. Several modelling approaches have been developed to assess the performance enhancement that is provided by DA to reliability, availability, down time (DT) and also to overall system resilience. The following is a summary of the contributions made:

- First, Chapter 2 conducts an analysis of real outage data from an operational distribution grid. A proportional breakdown analysis was used to investigate the key contributors to outages on a distribution grid. Following this, statistical inference was used to estimate parameters for recovery and failure rates. Through this analysis, important insights about the distribution grid were discovered, which emphasised points made in later analysis. It was shown that the recovery time has significant variance, corresponding to the range of different phases required in the recovery process. It was also shown that the parameters of recovery time for High-Impact Low-Probability (HILP) events is different for those of standard day-to-day outages, corresponding to the difficulties of recovery which come from wide-spread outages.

- Chapter 3 then develops a computationally efficient method of analysing distribution grid availability and DT, based on the interconnections between assets with a hierarchical model. It utilises Reliability Graphs (RGs) to assess a system with Fully Automated Reconfiguration (FAR), in order to discover the impact to the performance and sensitivity of the system and individual assets when ideal DA is deployed. It then applies an analytical resiliency analysis methodology, an approach novel to distribution grids. This analysis demonstrated the contribution of FAR to the resilience of a distribution grid. It was shown that a state-based model was required to analyse the reconfiguration and recovery process.

- Next, Chapter 4 develops an Stochastic Reward Net (SRN) model which captures

the dependencies of different assets and protection equipment during the recovery process. This enabled modelling of the reconfiguration process, and contains measures to reduce state-explosion through logical functions which prohibit unneeded states. The model was used to evaluate the availability, sensitivity and resilience of a distribution grid. The model was also extended to assess the influence of each individual switch in a system. This extension was able to evaluate the placement of automation onto exisiting switches, and assess their effect on the DT and resilience. It was shown that further detail of the recovery process was needed in order to model the complexities of the reconfiguration process, a requirement for the evaluation of placement of distributed sensing equipment such as Fault Indicator (FI).

- Finally, Chapter 5 constructs a model of the recovery process which occurs after an outage. This is used to augment the SRN from the previous chapter and demonstrate the effects which the the different recovery phases and parameters have on the recovery time, and resulting system uptime by performing a sensitivity analysis. The final contribution of this chapter was a demonstration of using the developed augmented recovery model to place FIs for both improving DT and resilience. The analytical resiliency analysis method provided an effective means of evaluating the contribution of each FI to load point (LP) and feeder resilience.

Collectively, these works provide the methodology to holistically model the operation of distribution grids to calculate the availability and downtime, as well as the sensitivity and the resilience of distribution grid LPs and feeders. The developed tools have enhanced the field of distribution automation placement, through several contributions. The following novel contributions have come from this thesis:

- Application of an analytical resiliency analysis methodology to distribution grids is used to analyse the resilience of the system to failures of specific assets. This methodology is capable of evaluating the resilience contribution of DA.

- A novel three-tier hierarchical model using RGs is developed. This can be used to evaluate the potential performance of distribution grids with best case DA. It can be used to identify the assets of which failure causes the biggest impact on availability, DT and resilience, and how DA can reduce the impact of these failures.

- A novel SRN feeder model has been developed. This is able to model the dependence of LPs on assets and accompanying protection equipment. It allows for multiple failures to affect the model, which is important for resiliency analysis and the modelling of HILP events.

- A phased recovery model was constructed to represent the phase durations of the distribution grid outage recovery process. This can augment the developed SRN model and make it capable of supporting analysis of the reduction which sensors such as FIs make to fault location time.

## 6.2 FUTURE WORK

There are a number of Smart Grid technologies such as microgrids and distributed generation which can further enhance system resilience. A microgrid is a section of feeder which is intentionally islanded. In the case of an outage, the post-fault reconfiguration can construct a microgrid, supplied by distributed generation. The SRN model developed in Section 4.3 can be adapted to model this behaviour. It was shown that the availability of each LP is modelled by a reward function. This reward function could be redefined to allow for the case of a microgrid being constructed and supplied with distributed generation.

A second means of enhancing the contributions of this thesis would be to utilise the established methodology to optimally place distribution automation technology. It was demonstrated in Sections 4.6 and 5.6 that the developed methodology is able to assess the impact of placement of switch communications and FIs onto distribution grids. These methods can be used as part of an optimisation algorithm. By utilising the output of the developed SRN model as the function to minimise in an optimisation methodology, it is possible to optimally place distribution automation technology.

The data analysis of Chapter 2 focused solely on estimating the recovery and failure rates. These were the only available parameters which could be estimated due to the nature of the data which was recorded. If additional outage data was recorded, such as the method of outage localisation, and a breakdown of specific phase durations, then the recovery model phase durations could be more accurately modelled for a system.

The recovery process model could be improved to incorporate the fault localisation in more detail. Utilities develop and maintain contingency plans for the recovery of feeders on their grid. These plans detail a series of operational steps to locate and isolate a fault in the case of an outage. These are designed prior to a fault, and are followed in the cases where there is no knowledge of the location of an outage. When the plan is implemented, and as more information becomes known, steps of the plan are removed, thus reducing total time. It is possible to utilise these plans to better estimate the location and reconfiguration phase durations. By doing so, a more accurate analysis could be conducted.

The model could be further enhanced by adding the capability to utilise other sensors for analysis of the reduction in fault location time. FIs were placed using the SRN augmented with the recovery model in Section 5.6. These are used in this thesis because there exists a well-established method of calculating the impact FIs have on

the location time of an outage. If other methods were developed for other distribution grid sensors such as Phasor Measurement Units (PMUs), these could be placed using a similar methodology.

Government and community resiliency and recovery planning must consider all affected stakeholders [19]. Conducting a wide-scale resilience analysis from a community perspective would therefore consider customers who can self-supply using off-grid options such as generators or renewable energy. The methods developed within this thesis could be applied to such wide-level planning.

## 6.3 CONCLUSION

Modern distribution grids utilities are quickly employing distribution automation technology in order to enhance their grid. One motivation for this is the increasing need to ensure that distribution grids are resilient to HILP events. This thesis developed a model which can holistically model the complex recovery process which distribution automation contributes to. Further, it implemented a methodology to analyse the resilience contribution of this technology. Overall, these methods provide tools for system designers which can be used to evaluate and optimally place DA on existing and future grids, in order to enhance availability and resilience.

## REFERENCES


[1] M. Panteli, P. Mancarella, D. Trakas, E. Kyriakides, and N. Hatziargyriou, "Metrics and quantification of operational and infrastructure resilience in power systems," *IEEE Transactions on Power Systems*, vol. 32, no. 6, pp. 4732–4742, 2017.

[2] E. Hossain, Z. Han, and H. V. Poor, *Smart Grid Communications and Networking*. New York: Cambridge University Press, 2012.

[3] A. Escalera, B. Hayes, and M. Prodanović, "A survey of reliability assessment techniques for modern distribution networks," *Renewable and Sustainable Energy Reviews*, vol. 91, pp. 344–357, 2018.

[4] C. Ji, Y. Wei, H. Mei, J. Calzada, M. Carey, S. Church, T. Hayes, B. Nugent, G. Stella, M. Wallace, J. White, and R. Wilcox, "Large-scale data analysis of power grid resilience across multiple us service regions," *Nature Energy*, vol. 1, p. 16052, 2016.

[5] A. Massie and N. R. Watson, "Impact of the christchurch earthquakes on the electrical power system infrastructure," *Bulletin of the New Zealand Society for Earthquake Engineering*, vol. 44, no. 4, pp. 425–430, 2011.

[6] F. Longo, R. Ghosh, V. K. Naik, A. J. Rindos, and K. S. Trivedi, "An approach for resiliency quantification of large scale systems," *ACM SIGMETRICS Performance Evaluation Review*, vol. 44, no. 4, pp. 37–48, 2017.

[7] M. Panteli and P. Mancarella, "The grid: Stronger, bigger, smarter?: Presenting a conceptual framework of power system resilience," *IEEE Power and Energy Magazine*, vol. 13, no. 3, pp. 58–66, 2015.

[8] Y. Wang, C. Chen, J. Wang, and R. Baldick, "Research on resilience of power systems under natural disasters - a review," *IEEE Trans. Power Syst*, vol. 31, no. 2, pp. 1604–1613, 2016.

[9] H. Falaghi, M.-R. Haghifam, and M. O. Tabrizi, "Fault indicators effects on distribution reliability indices," in *Electricity Distribution, 2005. CIRED 2005. 18th International Conference and Exhibition on*, pp. 1–4, IET.

[10] C.-Y. Ho, T.-E. Lee, and C.-H. Lin, "Optimal placement of fault indicators using the immune algorithm," *IEEE Transactions on Power Systems*, vol. 26, no. 1, pp. 38–45, 2011.

[11] H. O. Cruz and F. B. Leão, "Optimal placement of fault indicators using adaptive genetic algorithm," in *Power & Energy Society General Meeting, 2017 IEEE*, pp. 1–5, IEEE.

[12] W. F. Usida, D. V. Coury, R. A. Flauzino, and I. N. da Silva, "Efficient placement of fault indicators in an actual distribution system using evolutionary computing," *IEEE Transactions on Power Systems*, vol. 27, no. 4, pp. 1841–1849, 2012.

[13] O. K. Siirto, A. Safdarian, M. Lehtonen, and M. Fotuhi-Firuzabad, "Optimal distribution network automation considering earth faults," *Smart Grid, IEEE Transactions on*, vol. 6, no. 2, pp. 1010–1018, 2015.

[14] A. Heidari, Z. Y. Dong, D. Zhang, P. Siano, and J. Aghaei, "Mixed-integer nonlinear programming formulation for distribution networks reliability optimization," *IEEE Transactions on Industrial Informatics*, vol. 14, no. 5, pp. 1952–1961, 2018.

[15] Z. Popovic, S. Knezevic, and D. Popovic, "Risk-based allocation of automation devices in distribution networks with performance-based regulation of continuity of supply," *IEEE Transactions on Power Systems*, 2018.

[16] A. Huda and R. Živanović, "Improving distribution system reliability calculation efficiency using multilevel Monte Carlo method," *International Transactions on Electrical Energy Systems*, vol. 27, no. 7, p. e2333, 2017.

[17] M. Panteli, C. Pickering, S. Wilkinson, R. Dawson, and P. Mancarella, "Power system resilience to extreme weather: Fragility modelling, probabilistic impact assessment, and adaptation measures," *IEEE Transactions on Power Systems*, 2016.

[18] D. D. Woods, "Essential characteristics of resilience," in *Resilience engineering*, pp. 33–46, CRC Press, 2017.

[19] P. R. Berke and T. J. Campanella, "Planning for postdisaster resiliency," *The Annals of the American Academy of Political and Social Science*, vol. 604, no. 1, pp. 192–207, 2006.

[20] D. T. Ton and W. P. Wang, "A more resilient grid: The u.s. department of energy joins with stakeholders in an r amp;amp;d plan," *IEEE Power and Energy Magazine*, vol. 13, pp. 26–34, May 2015.

[21] M. Panteli and P. Mancarella, "Modeling and evaluating the resilience of critical electrical power infrastructure to extreme weather events," *IEEE Systems Journal*, 2015.

[22] M. Panteli, D. N. Trakas, P. Mancarella, and N. D. Hatziargyriou, "Power systems resilience assessment: hardening and smart operational enhancement strategies," *Proceedings of the IEEE*, vol. 105, no. 7, pp. 1202–1213, 2017.

[23] R. Arghandeh, A. von Meier, L. Mehrmanesh, and L. Mili, "On the definition of cyber-physical resilience in power systems," *Renewable and Sustainable Energy Reviews*, vol. 58, pp. 1060–1069, 2016.

[24] N.-K. C. Nair, D. K. Maina, and L. Y. Liu, "How do you assess and quantify resilience for distribution networks?," in *EEA Annual Conference, 2018*.

[25] D. S. Menasché, A. Avritzer, S. Suresh, R. M. Leão, E. de Souza e Silva, M. Diniz, K. Trivedi, L. Happe, and A. Koziolek, "Assessing survivability of smart grid

distribution network designs accounting for multiple failures," *Concurrency and Computation: Practice and Experience*, vol. 26, no. 12, pp. 1949–1974, 2014.

[26] S. Keshav and C. Rosenberg, "How internet concepts and technologies can help green and smarten the electrical grid," pp. 35–40, ACM, 2010.

[27] R. Ghosh, D. S. Kim, and K. S. Trivedi, "System resiliency quantification using non-state-space and state-space analytical models," *Reliability Engineering and System Safety*, vol. 116, pp. 109–125, 2013.

[28] J.-C. Laprie, "From dependability to resilience," in *38th IEEE/IFIP Int. Conf. On Dependable Systems and Networks*, pp. G8–G9, 2008.

[29] K. S. Trivedi, *Probability & statistics with reliability, queuing and computer science applications.* John Wiley & Sons Inc., 2002.

[30] R. E. Brown, *Electric Power Distribution Reliability.* Power Engineering, CRC Press, 2nd ed., 2009.

[31] R. Billinton and R. N. Allan, *Reliability Evaluation of Power Systems.* Plenum Press, New York, 2nd ed., 1996.

[32] T. A. Short, *Electric power distribution handbook.* CRC press, 2014.

[33] R. E. Brown, S. Gupta, R. D. Christie, S. S. Venkata, and R. Fletcher, "Distribution system reliability assessment using hierarchical markov modeling," *Power Delivery, IEEE Transactions on*, vol. 11, no. 4, pp. 1929–1934, 1996.

[34] F. Famoye, *Continuous Univariate Distributions, Volume 1*, vol. 37. 1995.

[35] L. M. Leemis, *Reliability: Probabilistic models and statistical methods.* Englewood Cliffs, N.J: Prentice Hall, 2nd ed., 2009.

[36] T. Gönen, *Electric Power Distribution System Engineering.* CRC Press, 2nd ed., 2008.

[37] R. A. Sahner, K. Trivedi, and A. Puliafito, *Performance and Reliability Analysis of Computer Systems.* Kluwer Academic Publishers, 1996.

[38] J. R. Norris, *Markov Chains.* Cambridge University Press, 1998.

[39] D. Poole, *Linear Algebra: A Modern Introduction.* Cengage Learning, 2014.

[40] B. Falahati, F. Yong, and M. J. Mousavi, "Reliability modelling and evaluation of power systems with smart monitoring," *Smart Grid, IEEE Transactions on*, vol. 4, no. 2, pp. 1087–1095, 2013.

[41] K. S. Trivedi and R. Sahner, "SHARPE at the age of twenty two," *SIGMETRICS Perform. Eval. Rev.*, vol. 36, no. 4, pp. 52–57, 2009.

[42] G. Ciardo, J. Muppala, and K. Trivedi, "SPNP: Stochastic Petri net package," in *Petri Nets and Performance Models, 1989. PNPM89., Proceedings of the Third International Workshop on*, pp. 142–151, IEEE, 1989.

[43] K. Morris, D. S. Kim, A. Wood, and G. Woodward, "Availability and resiliency analysis of modern distribution grids using stochastic reward nets," in *Innovative Smart Grid Technologies-Asia (ISGT-Asia), 2017 IEEE*, IEEE, 2017.

[44] K. Morris, D. S. Kim, A. Wood, and G. Woodward, "Reliability and resiliency analysis of modern distribution grids using reliability graphs," in *IEEE International Conference on Communications (ICC) Workshop 2018*, IEEE, 2018.

[45] R. E. Brown and J. R. Ochoa, "Distribution system reliability: default data and model validation," *Power Systems, IEEE Transactions on*, vol. 13, no. 2, pp. 704–709, 1998.

[46] M. Doostan and B. H. Chowdhury, "A data-driven analysis of outage duration in power distribution systems," in *Power Symposium (NAPS), 2017 North American*, pp. 1–6, IEEE.

[47] M. Bessani, R. Z. Fanucchi, J. A. Achcar, and C. D. Maciel, "A statistical analysis and modeling of repair data from a Brazilian power distribution system," in *Harmonics and Quality of Power (ICHQP), 2016 17th International Conference on*, pp. 473–477, IEEE.

[48] G. Wang, L. Zhang, and W. Xu, "What can we learn from four years of data center hardware failures?," in *2017 47th Annual IEEE/IFIP International Conference on Dependable Systems and Networks (DSN)*, pp. 25–36, IEEE.

[49] M. Lin, H. C. Lucas Jr, and G. Shmueli, "Too big to fail: large samples and the p-value problem," *Information Systems Research*, vol. 24, no. 4, pp. 906–917, 2013.

[50] B. Schroeder and G. Gibson, "A large-scale study of failures in high-performance computing systems," *IEEE Transactions on Dependable and Secure Computing*, vol. 7, no. 4, pp. 337–350, 2010.

[51] P. A. Hoffman, "2014 smart grid report to congress," report, Energy, U.S. Department of, 2014.

[52] D. Gaver, F. Montmeat, and A. Patton, "Power system reliability I - Measures of reliability and methods of calculation," *IEEE Transactions on Power Apparatus and Systems*, vol. 83, no. 7, pp. 727–737, 1964.

[53] R. A. Sahner and K. S. Trivedi, "Reliability modeling using SHARPE," *Reliability, IEEE Transactions on*, vol. 36, no. 2, pp. 186–193, 1987.

[54] R. Billinton, R. R. Ringlee, and A. J. Wood, *Power-System Reliability Calculations*. MIT Press, 1973.

[55] N. Z. C. Commission, "Electricity distribution services default price-quality path determination 2015," report, 2015.

[56] R. N. Allan, R. Billinton, I. Sjarief, L. Goel, and K. S. So, "A reliability test system for educational purposes-basic distribution system data and results," *Power Systems, IEEE Transactions on*, vol. 6, no. 2, pp. 813–820, 1991.

[57] K. Xie, J. Zhou, and R. Billinton, "Fast algorithm for the reliability evaluation of large-scale electrical distribution networks using the section technique," *IET Generation, Transmission & Distribution*, vol. 2, no. 5, pp. 701–707, 2008.

[58] M. Grottke, D. S. Kim, R. Mansharamani, M. Nambiar, R. Natella, and K. S. Trivedi, "Recovery from software failures caused by mandelbugs," *IEEE Transactions on Reliability*, vol. 65, no. 1, pp. 70–87, 2016.

[59] V. B. Mendiratta, "Reliability analysis of clustered computing systems," in *Software Reliability Engineering, 1998. Proceedings. The Ninth International Symposium on*, pp. 268–272, IEEE.

[60] A. Koziolek, A. Avritzer, S. Suresh, D. S. Menasché, M. Diniz, E. de Souza e Silva, R. M. Leão, K. Trivedi, and L. Happe, "Assessing survivability to support power grid investment decisions," *Reliability Engineering & System Safety*, vol. 155, pp. 30–43, 2016.

[61] X. Chang, J. M. Martinez, and K. S. Trivedi, "Transient performance analysis of smart grid with dynamic power distribution," *Information Sciences*, vol. 422, pp. 98–109, 2018.